Understanding the Molecular Basis of HPV-16 Neoplastic Progression Using an Organotypic Raft Model

Thesis

Understanding the molecular basis of HPV-16 neoplastic progression using an organotypic raft model

Erin Isaacson

Division of Virology
National Institute for Medical Research
The Ridgeway
Mill Hill
London UK

Thesis submitted to the Open University for the degree of Doctor of Philosophy
September 30th, 2009

DATE OF SUBMISSION: 30 SEPT 2009
DATE OF AWARD: 11 DEC 2009

ProQuest LLC.
789 East Eisenhower Parkway
P.O. Box 1346
Ann Arbor, MI 48106 – 1346

Acknowledgments

I would first like to acknowledge my supervisor John Doorbar for allowing me to conduct an ever evolving, yet interesting project throughout my PhD.
I would also like to thank my second supervisor Ken Raj for all of the long discussions and for always enforcing a positive vision towards this work.

With much gratitude and appreciation I would also like to thank my fellow students for getting me through an uphill battle. Thank you Gareth for always making me laugh and for being so helpful. Thank you Jameela for being such a delightful and free spirited person. No one has ever told me an Isaac Asimov story (and by memory) as well as you. I would also like to thank all of the strong ladies around: Thanks Pauline and Clare for all of your discussions and advice. A big "Thank You" to Clare for trudging through my results and always setting a high standard.
I would also like to give a special "Thank you" to Deborah Jackson for always being so helpful and for being the one and only lab manager.

My time here in London and making it through two degree programs would not have been possible without my family and friends. I am so lucky to have four wonderful parents who have always been a stronghold and wonderful role models.

I would also like to thank my ever so talented sister Loryn for always being my best friend (who also makes me fantastic clothing). I would also like to thank her wonderful husband Mark, who is the best brother-in-law in the world.
I also want to thank my brother Erik for always being such a nice person.
Thank You to Grandma and Auntie Arlene for always being so supportive.

Thank you also to my good friends Sheri and Rob for always being so positive.

I have also met so many wonderful people in London and I am so happy to have met my good friend Taron.-Thank you to Taron for your friendship and I know we will always be close.

Last but not least I would like to thank my wonderful fiancé Thomas. Everything seems possible when by his side and I am so grateful for all of his support and friendship. Now we are on to bigger and better adventures together!

This Thesis is dedicated to Bapa Joe--"*For I suspect he held in him so much to wonder*"

Abstract

High-risk Human Papillomavirus (HPV) types such as HPV-16 cause a spectrum of pre-cancerous neoplastic changes in epithelial sites including that of the cervix. HPV-induced cervical lesions that display low to moderate neoplastic changes are graded as low-grade squamous intraepithelial neoplasia (LSIL). HPV-induced lesions that display high levels of neoplasia are graded as high-grade squamous intraepithelial neoplasia (HSIL).

The previous analyses of cervical lesions of LSIL and HSIL grades have shown that the timing of early and late viral gene expression changes, as the lesion becomes more neoplastic. In HSIL lesions, the HPV-16 E7 surrogate marker MCM-7 persists throughout the epithelium, which coincides with a delay in late gene expression including L1 capsid expression. HSIL lesions often do not support a complete virus life cycle.

The work in this thesis has shown that the Normal Immortalized Human Keratinocyte (NIKS) organotypic raft culture system, which is commonly used to study the HPV-16 life cycle, surprisingly recapitulates the spectrum of gene expression patterns identified in both LSIL and HSIL lesions. In addition, this model also demonstrates pathological changes, which correlate with both LSIL and HSIL phenotypes. This has rendered this system a potential model of episomal HPV-16 induced neoplasia. This auspicious finding led us to make use of this system to explore viral characteristics that potentially underlie HSIL-like gene expression patterns and neoplastic changes. Monolayer LSIL-like and HSIL-like HPV-16 cell lines were subsequently used to evaluate viral copy number, early oncogene expression and growth potential.

In these experiments we have found that episomal HSIL-like HPV-16 cell lines bypass density-dependent growth arrest, which coincides with a rise in E6 and E7 oncogene levels. Finally, we have found that high E6 and E7 expression levels and growth potential at cell-cell contact correlate with MCM-7 persistence in the HPV-16 raft epithelium.

Table of Figures

Table of Abbreviations

AJ	Adherin Junction
APC	Adenomatous polyposis coli
Bp	Base pairs
BSA	Bovine serum albumin
C-myc	Avian myelocytomatosis virus oncogene cellular homolog
C8:O	N 1,2-dioctanoyl-sn-glycerol
CDK	Cyclin dependent kinase
CIN	Cervical Intraepithelial Neoplasia
CL	Cornified layer
ct	Cycle threshold
DAB	3,3'-Diaminobenzidine
DAPI	4'-6' diamidino-2-phenylindol
DC	Dysplastic cell
DH2O	Distilled water
DIG	Digoxygenin
DNA	Deoxyribonucleic acid
E2BS	E2 binding site
EGF	Epidermal Growth Factor
FC	F Media Complete
fg	Femtogram
FI	F Media Incomplete
g	Gram
GAPDH	Glyceraldehyde 3-phosphate dehydrogenase
GRE	Gluccocorticoid Responsive Element
Gy	Gray unit
H&E	Haematoxylin and Eosin
hDlg	Human discs large
HPV	Human Papillomavirus
HRP	Horseradish Peroxidase
hScrib	Human Scribble
HSIL	High-grade Squamous Intraepithelial Lesions
L	Liter
LB	Luria-Bertani
LCR	Long control region
LEF	Lymphoid enhancing factor
LSIL	Low-grade Squamous Intraepithelial Lesions
mg	Milligram
mL	Milliliter
mRNA	Messenger ribonucleic acid
MS	Mature squame
NGS	Normal goat serum
NIKS	Normal Immortalised Human Keratinocytes
NP40	Nonyl phenoxylpolyethoxylethanol
PBS	Phosphate buffered saline
PCNA	Proliferating cell nuclear antigen

PCR	Polymerase Chain Reaction
pg	Picogram
PV	Papillomavirus
QPCR	Quantitative Polymerase Chain Reaction
RNA	Ribonucleic acid
rpm	Rotations per minute
RT	Real-Time
rt	Room temperature
SDS	Sodium dodecyl sulfate
TAE	Tris-acetate EDTA
TCF	T-cell factor
TGF	Transforming growth factor
tL	Lower limit
v/v	volume/volume
w/v	weight/volume
wt	Wild-type

1.0 Introduction

1.1 Classification of Papillomaviruses

Papillomaviruses (PVs) are non-enveloped double-stranded DNA viruses. PVs are a member of the family Papillomaviridae, which is comprised of 200-300 PV types. The Papillomaviridae are an extremely old family of viruses and it is estimated that the existence of PVs date back beyond the origin of *Homo sapiens* (Ho, Chan et al. 1993; Bernard, Chan et al. 1994). The mutation rate of PVs is estimated to be 0.25% per 10-20,000 years. In relation to the evolutionary time-scale, this rate is thought to be similar to the mutation rate of the host germ line (Chan, Bernard et al. 1997).

It is not surprising that PVs have been part of a long evolutionary trail due to the enormous diversity of animal species that PV infect. Some of these species other than *Homo sapiens* include bovine and other ungulates such as goats and pigs, birds, reptiles and cetaceans, which include whales and dolphins (de Villiers, Fauquet et al. 2004).

To date there is no knowledge of interspecies transmission, which can be partially explained through a divergence in their PV nucleotide sequence identity. PVs are broadly organized into genera based on their highly conserved L1 capsid ORF where greater than a 60% difference in nucleotide sequence identity constitutes a new PV genus (Bernard, Chan et al. 1994). Most host species appear to be infected by PVs within their own genera. PV genera can be further broken down into PV species, which are based on a 40% difference in L1 nucleotide sequence

identity and then to PV types where only a 10% difference in L1 nucleotide sequence identity distinguishes these types (Bernard, 1994)

Amongst a genetic divergence a common fundamental biological feature of all PV genera is demonstrated by their complex and unique requirement of infecting epithelial cells and utilizing the entire epithelium to complete their life cycle. It is widely established however that within the epithelium PV types also diverge to create a clinical spectrum of PV disease. These pathological differences have formed a large basis for the study of different HPV types.

1.2 Human Papillomaviruses

The first genital and laryngeal HPV isolates were discovered over thirty years ago (Gissmann, Pfister et al. 1977; zur Hausen 1977; Gissmann, Wolnik et al. 1983). To date over 100 different HPV types have been isolated from various tissues (Bernard 2005)

HPVs infect a range of tissues including the skin and mucous membranes of conjunctiva, oral cavity, larynx, tracheobronchial tree, esophagus and areas of the anogenital tract including the anus, vulva and cervix. HPVs are also tissue and site specific. HPV-1 infects stratified squamous epithelium of the sole and foot producing plantar warts. HPV-2 and 4 infect skin of fingers to produce common warts. HPV-6 and 11 almost exclusively infect mucosal surfaces of oral cavity and anogenital tract. (de Villiers, Fauquet et al. 2004)

HPVs can be divided into five genera including Alpha, Beta, Gamma Mu and Nu (reviewed in (Doorbar 2006) . Beta HPVs such as HPV 5 and 8 infect cutaneous

tissue and are usually associated with mild skin lesions. The exception is for some individuals who suffer from the inherited disease epidermodysplasia verruciformis. This hereditary skin disorder predisposes these patients to non-melanoma skin cancers (Harwood and Proby 2002; Pfister 2003). The Gamma, Mu and Nu such as HPV-65, 63 and 41 respectively mostly infect cutaneous sites and primarily cause benign cutaneous lesions such as verrucas (Pfister 1992).

The largest genera the Alpha Papillomaviruses infect cutaneous tissue such as the hands (e.g. HPV-2) and mucosal tissue, including the cervix (e.g. HPV-16, 18). As just mentioned, the Alpha Papillomaviruses in particular infect various sites of the anogenital tract such as the cervix and vulva.

Some of the Alpha Papillomaviruses have the ability to cause both pre-cancerous neoplastic changes and cancers in the tissues such as the cervix (de Villiers, Fauquet et al. 2004). These types are known as high-risk types, which comprise approximately 20 of the Alpha Papillomaviruses. The remaining 15 Alpha Papillomaviruses that infect areas of the anogenital tract are referred to as low-risk viruses as these types mostly lead to benign disease. Low-risk HPV types are more equally prevalent in infected tissues compared to high-risk HPV types. The high risk types HPV-16 and 18 appear to be the most prevalent, together causing 60% of all cervical cancers (Munoz, Bosch et al. 2003). The ability of high-risk HPV types to cause both benign and malignant disease has rendered them as interesting candidates towards the understanding of HPV oncogenesis.

1.3 HPV-16 related disease

High-risk HPV types such as HPV-16 can cause a clinical spectrum of disease in cutaneous and mucosal tissues. The most studied of these is HPV-16 disease of the cervix. HPV-16 is associated with both precancerous low-grade and pre-cancerous high-grade lesions, which develop in the ectocervix (Wright 2002). However a rare event, persistent HPV-16 infections also have the potential to develop into cancer. Within the cervix, precancerous HPV-16 lesions and HPV-16 associated cancers commonly form in the transformation zone where cells undergo metaplastic changes (Wright 2002).

HPV has been established as the main causative agent of cervical cancer. Approximately 99.8% of cervical cancers are caused by infections with HPV and approximately 50% of these cancers are caused by HPV-16 (Walboomers, Jacobs et al. 1999; Munoz, Bosch et al. 2003). HPV-16 is also thought to be associated with cancers in other places of the anogenital tract including the anus, vulva and penis (Rubin, Kleter et al. 2001; Bosch and de Sanjose 2003). In 2006 2,873 women in the UK were diagnosed with cervical cancer, which caused 941 deaths in 2007 (quoted from the Health Protection Agency, UK). HPV related cancers are more prominent in developing countries where HPV screening programs are less available (Cohen 2005).

1.4 Pathological grading system for HPV associated lesions

It is widely established that HPV-16 can cause a range of pre-cancerous neoplastic changes in the cervix in addition to its ability to cause cancer. As these neoplastic changes precede cancer formation, their diagnosis is crucial for the prevention of cancer.

Pathologists use a diagnostic grading scale to quantify non-invasive cervical squamous epithelial abnormalities associated with HPV infection. In 1988 the Bethesda system of pathological grading was created and is now used in many countries to treat HPV disease. The Bethesda system specifically divides the severity of pre-cancerous neoplastic changes in the cervix into two categories (Diane Solomon 2004) HPV lesions that display mild dysplasia in the first third of the epithelium are categorized as a low-grade squamous intraepithelial lesion (LSIL). HPV lesions that display moderate to severe dysplasia through the middle and final third of the epithelium are categorized as a high-grade intraepithelial squamous lesion (HSIL). An alternative grading scale has also been used which divides the grading scale into three categories. HPV lesions that display mild dysplasia in the first third of the epithelium are categorized as cervical intraepithelial neoplasia 1 (CIN-1) (Ivan Damjanov 2007). The grade of CIN-1 and LSIL are recognized as being equivalent. HPV lesions that display moderate to severe dysplasia in the middle and final third of the epithelium are categorized as CIN-2 and CIN-3, respectively. Both CIN-2 and CIN-3 fall under the Bethesda grade, HSIL(Ivan Damjanov 2007).

1.5 Pathology of high-risk HPV types in cervical lesions

The diagnosis of LSIL and HSIL is based on a set of uniform criteria, which is used to identify the severity of pathological changes in the epithelium. Figure 1.1 contains an example of an H&E stained cervical epithelium with no pathological changes, a cervical lesion graded with LSIL/CIN-1, and two cervical lesions grades with HSIL (CIN-2 and CIN-3, respectively). In cervical tissue that exhibits no pathological changes, the basal cells are small and uniform in size. The cells in the

basal layer are aligned and maintain their normal polarity. Normal stratification or squamous maturation occurs above the basal layer.

In cervical lesions graded with LSIL, hyperplasia is evident in the lower third of the epithelium (Figure 1.1). The nuclei starting in the basal layer are pleomorphic, meaning that they vary in size and shape. The lower third of the epithelium is more disorganized and the cells lack polarity. The lesion also exhibits mild dysplasia or lack of squamous maturation, which persist until the middle-third of the epithelium. Another feature of HPV induced LSIL is the presence of koilocytes, which can be seen in the upper two thirds of the epithelium. This perinuclear clearing is a cytopathic effect from the virus. Pathologists can distinguish koilocytes from the vacuolar glyocogenation seen in normal cervical tissue above (Wright 2002; Ivan Damjanov 2007).

In lesions with HSIL/CIN-2 nuclear pleomorphisms extend throughout the bottom and middle-third of the epithelium (Figure 1.1). The nuclei appear more crowded within this region and most of the cells also exhibit a loss in polarity. There is a further delay in squamous maturation where the cells remain dysplastic until the final-third of the epithelium. In the lesion with HSIL/CIN-3 the cells remain dysplastic throughout the entire epithelium. The nuclei are highly pleomorphic throughout and cellular polarity is not maintained in the majority of the cells. Koilocytes are usually not present in HSIL lesions (Wright 2002; Ivan Damjanov 2007).

The equivalent lesions of LSIL and HSIL grades can be found in other sites of the anogential tract including the vulva and more rarely the penis. (Demeter, Stoler et al. 1993; Hillemanns and Wang 2006)

HSIL is thought to be a prerequisite for cancer development. However, the majority of LSIL and HSIL lesions regress back to asymptomatic phenotypes with the aid of the host immune system (Stanley 2008). The stages of HPV induced neoplasia (i.e. LSIL to HSIL) are also thought to be a progressive disease as a consequence of viral persistence, however recent statistics suggest that HSIL might develop more acutely (Koutsky, Holmes et al. 1992; Woodman, Collins et al. 2001).

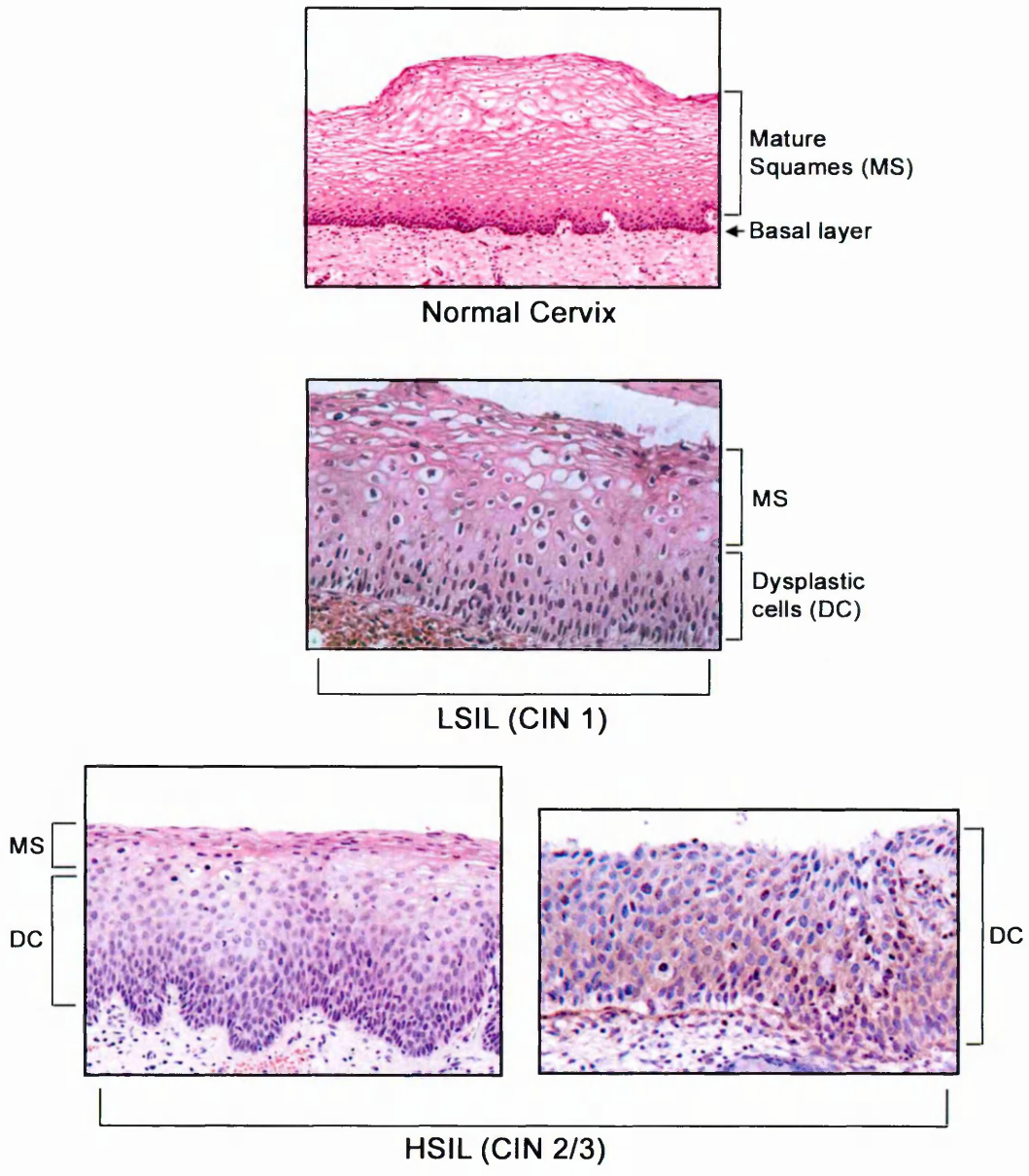

Image taken from (Branca, Ciotti et al. 2004)

Figure 1.1 Pathological changes in cervical lesions with LSIL and HSIL

In the normal cervix basal cells are small and uniform in size. Squamous maturation begins two to three layers above the basal layer. The noticeable vacuolation in the mature squamous cells is caused by the presence of glycogen. In the lesion graded with LSIL, dysplastic cells persist until the middle of the epithelium. The nuclei in the first third of the epithelium are pleomorphic and the cells exhibit a loss of polarity. Squamous maturation is not evident until the middle-and final-third of the epithelium. Koilocytes, recognized as a cytopathic affect of the virus, persist in the middle and final third of the epithelium. In the lesion with HSIL (CIN-2) dysplastic cells are evident until the final third of the epithelium. The nuclei are pleomorphic and most of these cells have lost their normal polarity. Squamous maturation does not occur until the last several layers. In the lesion with HSIL (CIN-3) the cells remain dysplastic throughout the entire epithelium. All of the nuclei are pleomorphic and a loss in cellular polarity is detected throughout the epithelium

1.6 Terminal differentiation of the epithelium

As stated earlier a common biological feature of PVs is their ability to infect keratinocytes of the basal epithelium and use the entire differentiating epithelium to carry out their life cycles. It is therefore important to recognize that the virus will encounter three to four very distinct host cell environments as it completes its life cycle in the differentiating epithelium.

Keratinocytes are named from their high levels of keratin filaments, which compose up to 90% of the total epithelial mass (Candi, Schmidt et al. 2005). Keratins or keratin intermediate filaments (KIFS) form the cytoskeleton of all keratinocytes, which also supply a structure to the epithelium.

The epithelium of cutaneous and mucosal tissues has primarily evolved to protect the underlying tissue by supplying a structural and physical barrier. Keratinocytes create this barrier through the process of terminal differentiation where in this process cells are pushed up to the surface to create several layers of stratified squamous cells. Mucosal and cutaneous epithelia follow a similar program of terminal differentiation first beginning with the basal layer, which is composed of pre-differentiated cells. Directly in contact with the basal lamina or dermis the first layer of cells called the basal layer contain the only cells that have the capacity for DNA synthesis and mitosis. Basal cells are also distinguished by their composition of two distinct keratins, K5 and K14 (Nelson and Sun 1983) (Figure 1.2). During basal cell division, transit-amplifying cells are pushed to the layer above and it is at this point that cells commit to the terminal differentiation program. The process of terminal differentiation can be broken down into early and late stages.

The differentiating cells immediately above the basal layer begin the early phase of terminal differentiation. In these cells a new set of keratins are expressed. One of the most abundant keratins expressed during early differentiation is K10, in cutaneous epithelia and K13, in mucosal tissue. During early differentiation the keratins in this layer such as K10 aggregate into bundles to create spinous-like cells (Eichner, Sun et al. 1986). Several layers of these cells that express K10 form the spinous layer in cutaneous epithelia, which is referred to as the intermediate layer in mucosal tissue. It has been previously suggested that the expression of K10 prevents cellular proliferation above the basal layer (Paramio, Casanova et al. 1999). Spinous cells that express K10 are post-mitotic but are still metabolically active (Fuchs 1990).

The second distinct layers of cells compose the granular layer, which marks the start of late terminal differentiation. The granular layer, which is more predominant in cutaneous epithelia than mucosal epithelia, is smaller than the spinous layer, however it involves more destructive and physical changes to the cells. Within this layer new keratins are no longer made and the structural breakdown of the cells begins. This is accompanied by the start of nuclear degeneration and the end of metabolic functions. The structural breakdown begins with the creation of pro-filaggrin, which is contained in keratohyalin bundles, thus giving this layer a granular appearance (Dale, Salonen et al. 1990; Manabe and O'Guin 1994). Pro-filaggrin is then is cleaved by several proteases such as calpain to create filaggrin (Presland, Kimball et al. 1997). Filaggrin plays an important role in the aggregation of keratins, which leads to the collapse of the entire keratin network. The collapse of the keratin network contributes to the formation of the cornified layer. Filaggrin itself has a very short half-life of 6 hours and is eventually broken down into single

amino acids to form a component of the cornified envelope (Candi, Schmidt et al. 2005).

The cornified layer in cutaneous epithelium, and the superficial layer in mucosal epithelium is the final end-point of terminal differentiation. This is a highly impermeable and protective layer that consists of "cellular skeletons" with cross-linked proteins and keratin filaments (Fuchs 1990).

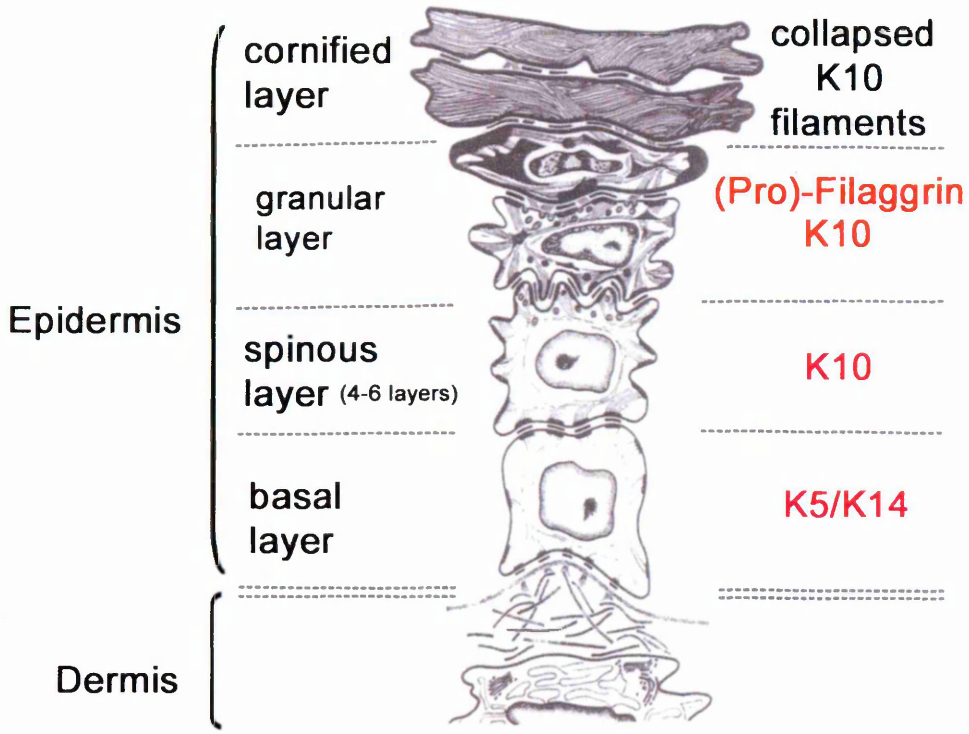

Modified from (Eckert, Crish et al. 1997)

Figure 1.2 Cutaneous Epithelium

Viral life cycle begins in infected cells within the basal compartment. The virus will then encounter three distinct layers during the terminal differentiation process. In normal epithelium, basal cells are the only cells with the ability to proliferate. As these cells proliferate cells are pushed into the spinous layer. This layer consists of four to six layers of cells that have lost the ability to proliferate but still maintain metabolic activity. In the spinous layer, which marks the start of early terminal differentiation, differentiation specific keratins such as K10 are actively expressed. As the cells migrate up through the epithelium they undergo late terminal differentiation. The granular layer specifically marks the site of late terminal differentiation. In this layer pro-filaggrin is contained in keratohyalin bundles, which demonstrate a granular appearance. In this layer pro-filaggrin is also processed into filaggrin. The specific role of filaggrin is to aggregate the keratin network, which will form the cornified layer above. In the granular layer active keratin expression also ends and nuclear degeneration begins. Terminal differentiation ends in the cornifed layer, which is an impermeable and insoluble layer. The cornifed layer is mainly filled with cellular skeletons with collapsed keratin filaments.

1.7 The HPV-16 genome

HPV-16 contains eight functional genes within its 8kb double stranded circular genome (Figure 1.3). As with all PVs, the HPV-16 genome can be divided into three major regions. These regions are separated by two polyadenylation poly (A) sites, which are designated as early poly (A) and late poly (A). The third region contains the long control region (LCR) or upstream regulation region (URR), which lies upstream of both the early poly (A) and late poly (A) regions. The early poly (A) region encodes the majority of the HPV-16 ORFs including that of E1, E2, E4, E5, E6 and E7. E4 and E2 are encoded within the same ORF. The late poly (A) region encodes the ORF for the capsid proteins L1 and L2.

Two main promoters control viral gene expression in the epithelium. The early p97 promoter, which only controls early gene expression (e.g. E1, E2, E4, E5, E6 and E7) is contained within the LCR, whereas the differentiation dependent late promoter, p670, is contained downstream within the E7 ORF (Smotkin and Wettstein 1986; Grassmann, Rapp et al. 1996). Due to its location in the genome several early genes (e.g. E1, E2, E4 and E5) as well as the late L1/L2 capsid genes can be expressed from the late promoter. Transcription from the late promoter must bypass the early poly (A) site to allow gene expression from the late region (Zheng and Baker 2006).

The regulatory region of the virus or the LCR lies just upstream of the E6 ORF. As just mentioned this region houses the early p97 promoter and also contains cis-acting regulatory sequences upstream of the p97 promoter, which are necessary for both replication and viral transcription. The binding sites for several cellular

transcription factors have been identified in this region. Some of these cellular transcription factors that bind to designated sites within the LCR include: Sp-1, AP-1, Oct-1 and YY1. Transcription factors have been shown to both positively and negatively regulate transcription (Morris, Dent et al. 1993; Lace, Yamakawa et al. 2009). Amongst the transcription factor binding sites the LCR also contain gluccocorticoid responsive elements (GRE). The binding of gluccocorticoid to GREs results in an increase in replication (Piccini, Storey et al. 1997).

The LCR also contains four HPV-16 E2 binding sites (E2BS (1-4)) that are situated close to cellular transcription factor sites (Androphy, Lowy et al. 1987). The binding of E2 can consequently make these regions in the LCR inaccessible to cellular transcription factors. It has been further shown that when E2 binds to specifically E2BS-2 and -4, viral transcription from the p97 promoter is repressed (Sousa, Dostatni et al. 1990; Tan, Leong et al. 1994).The E2 protein has therefore been established as regulator of early transcription. In addition, E2BS-3 within the LCR is also located next to the viral origin of replication. E2 binds to this site as it recruits the HPV-16 E1 helicase to the origin of replication to begin the viral replication process (Desaintes and Demeret 1996). It has been shown that both E1 and E2 are necessary to carry out viral replication (Berg and Stenlund 1997).

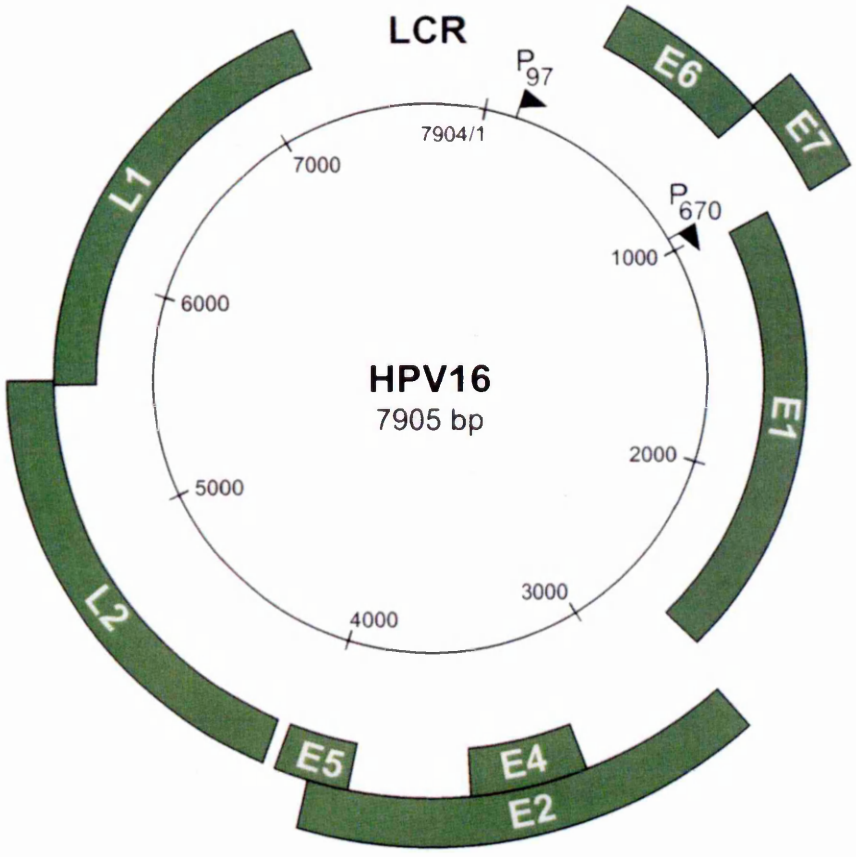

Figure 1.3 HPV-16 8kb double-stranded circular genome

The HPV-16 genome consists of six early genes (E1, E2, E4, E5, E6 and E7) and two late genes (L1 and L2) which are situated upstream of the early poly(A) and late poly (A) sites respectively. Early genes are expressed from the early p97 promoter whereas a subset of early as well as the late genes are expressed from the differentiation dependent late promoter, p670. The LCR is situated upstream of the early region and contains cis-acting regulatory regions which are necessary for both viral replication and transcription.

1.8 HPV-16 transcription

The mapping of HPV-16 RNA transcripts and the identification of post-transcriptionally modified early and late mRNA products have been mostly carried out in HPV-16 W12 cells (Doorbar, Parton et al. 1990; Milligan, Veerapraditsin et al. 2007). HPV-16 W12 cells were previously isolated from a patient with low-grade cervical neoplasia and it has been shown that these cells contain the episomal form of the HPV-16 genome (Stanley, Browne et al. 1989). All of the HPV-16 genes are transcribed as polycistronic messages from either the early p97 or late p640 promoters. Several other putative promoters have also been identified within the LCR and within the E4 ORF (Doorbar, Parton et al. 1990; Milligan, Veerapraditsin et al. 2007).

Polycistronic messages undergo extensive post-transcriptional alternate splicing from the early poly(A) and late poly(A) sites, to create early and late viral mRNAs. mRNA products of the early p97 promoter have been indentified in mixed pools of undifferentiated and differentiated cells, which suggest that these gene products are contained in both the basal layer and in the differentiating suprabasal layers. Early mRNA splice products include different combinations of E1, E2, E4 E5, E6 and E7 polycistronic or bicistronic messages. (Doorbar, Parton et al. 1990) (Figure 1.4). The E4 protein is also referred to as E1^E4 as it is translated from a spliced mRNA, with the first five amino acids being encoded from the E1 ORF. Interestingly three distinct splice products of the E6 gene have also been identified which include E6-full length, and two truncated species, E6*I and E6*II. E6*I has been found to be the most abundant E6 transcript product in cervical cancer cell lines (Cornelissen, Smits et al. 1990). Previous studies have also identified E6*I as

a translated product and it also thought to have functional components in the HPV-16 life cycle (Pim, Tomaic et al. 2009).

mRNA products from the differentiation dependent late promoter, p640, have been mostly identified in differentiated cells. These mRNA products include different combinations of E1, E2, E5 E1^E4, L1 and L2 (Doorbar, Parton et al. 1990) (Milligan, Veerapraditsin et al. 2007). The bicistronic E1^E4 and L1 transcript has been identified as one of the main late transcript products. The E1^E4 and L1 capsid protein have been subsequently identified in the differentiating cells of the suprabasal layers (Doorbar, Foo et al. 1997; Middleton, Peh et al. 2003; Peh and Doorbar 2005).

More recently L1 transcript products have also been found in undifferentiated cells, however these L1 transcripts did not contain a poly (A) site. L1 transcripts, including a poly (A) site, were subsequently detected in differentiated cells (Milligan, Veerapraditsin et al. 2007). It is therefore thought that late genes can also be transcribed early on in the life cycle, however the post-transcriptional regulation of late genes are carried out in the differentiating layers above.

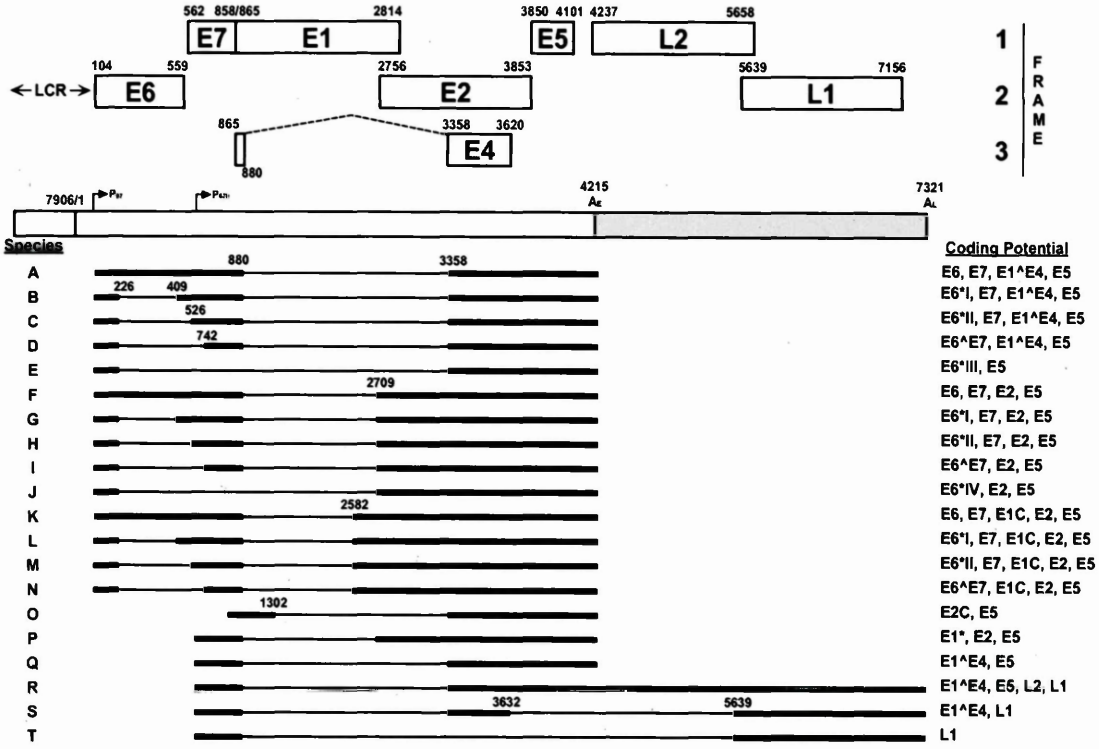

Image taken from (Zheng and Baker 2006)

Figure 1.4 HPV-16 transcription map

HPV 16 ORFs are designated in the boxes at the top of the figure. Nucleotide boundaries of each ORF are indicated above each box. The positions of the early p97 promoter and the p640 promoter are indicated below the boxed ORFs. The early poly (A) site and late poly (A) site are identified at nucleotides 4215 and 7321 respectively. The different early and late mRNA species are indicated in rows A-T. The heavy lines indicate all exons, and the thin lines indicate introns. Early transcript products mapped to the p97 promoter are indicated in rows (A-N, #266). Late transcript products mapped to the differentiation-dependent late promoter, p640, are indicated in rows (O-T)

1.9 The HPV-16 life cycle in the epithelium

1.9.1 Early events in the HPV-16 life cycle

It is thought that initial infection of HPV occurs in basal cells, which are the only mitotically active cells in the epithelium. More recently it has been shown that in order for viral transcription to commence, the virus must establish itself in cells that can undergo mitosis (Pyeon, Pearce et al. 2009). Following viral capsid uncoating the virus establishes itself as a stable episome in the host nucleus. Here the virus maintains itself at a low copy number which is estimated to be between 10-200 copies (De Geest, Turyk et al. 1993). The low level replication of the virus in basal cells is facilitated by two viral early genes E1 and E2, which are expressed from the early p97 promoter. E1 serves as the viral helicase, which is transported to the origin of replication by the E2 protein (Hughes and Romanos 1993; Masterson, Stanley et al. 1998). In order to maintain viral genomes during cell division E2 also anchors the viral episomes to mitotic chromosomes, which leads to correct viral genome segregation (You, Croyle et al. 2004).

During basal cell division cells that contain the HPV genome are pushed up to the suprabasal layer immediately above (Figure 1.5). In uninfected epithelium these cells would normally exit the cell cycle however doing so would likely prevent further replication of the virus, due to the absence of host replication machinery. To overcome the process of cell cycle exit the virus expresses its two viral oncogenes E6 and E7 from the early p97 promoter, which result in an extended S-phase compartment in the epithelium (Cheng, Schmidt-Grimminger et al. 1995) (Middleton, Peh et al. 2003). The most well established function of E7 is its ability to bind and degrade hypophosphorylated forms of Rb, which allows the E2F transcription factor to remain in a free state (Dyson, Howley et al. 1989; Boyer,

Wazer et al. 1996). The active form of E2F transactivates several genes that are required for S-phase which include MCM-7 and PCNA (Black and Azizkhan-Clifford 1999). The E6 oncogene circumvents G1 cell cycle checkpoints by down regulating the tumor suppressor gene p53, which prevents apoptosis of the cell (Scheffner, Huibregtse et al. 1993) In addition E6 expression is thought to be necessary for viral episomal maintenance through it's binding of several cellular PDZ domain proteins (Lee and Laimins 2004) .

Viral episomes are maintained in an extended S-phase compartment above the basal layer, however these cells coincidently enter into the terminal differentiation program (Cheng, Schmidt-Grimminger et al. 1995). Terminal differentiation is required for the upregulation of the differentiation dependent late promoter, p640, and late viral gene expression (Grassmann, Rapp et al. 1996) (Figure 1.5).

1.9.2 Late events in the HPV-16 life cycle

As the cells migrate up the differentiating epithelium viral genes which include E1, E2 E5 E1^E4 and L1 and L2, are expressed from the differentiation dependent promoter. This promoter is also referred to as the late promoter, which is why the E1^E4 protein is sometimes referred to as a late gene. There is still uncertainty as to where in the differentiating layers the different dependent promoter is upregulated. The E1^E4 and L1 proteins which are translated from a highly abundant late bicistronic transcript have been detected in the spinous and granular layers of the epithelium (Doorbar, Foo et al. 1997; Middleton, Peh et al. 2003; Peh and Doorbar 2005). The identification of these late proteins might therefore be coincidental with late promoter upregulation.

It is estimated that the E1^E4 protein accounts for 90% of the total viral protein mass in the upper layers of the epithelium. E1^E4 is typically first detected in the last layer of the extended E7/S-phase compartment (Peh, Middleton et al. 2002; Middleton, Peh et al. 2003; Peh and Doorbar 2005) (Figure 1.5). The overlap of E1^E4 and E7 is thought to mark the switch from early gene expression to late gene expression. The cells that contain both E7 and E1^E4 are also thought to contain the first amplified viral genomes (Doorbar, Foo et al. 1997; Middleton, Peh et al. 2003; Peh and Doorbar 2005). Past work has shown that in addition to the E1 and E2 viral replication proteins, E7 and E1^E4 expression is necessary for viral DNA amplification to occur. It is thought that E7 aids in viral DNA amplification by extending host replication machinery above in the suprabasal layers (Flores, Allen-Hoffmann et al. 2000). It has also been shown that in the absence of full-length E1^E4 proteins, viral amplification is reduced in the upper layers of the epithelium (Nakahara, Peh et al. 2005). The specific mechanism that E1^E4 carries out to aid in viral DNA amplification is currently not known. One possible way that E1^E4 aids in amplification is through its ability to arrest cells in the G2 phase of the cell cycle (Davy, Jackson et al. 2002). Arresting cells in G2 would potentially prevent the cell from proceeding through mitosis and would therefore allow viruses to amplify their genomes, following normal cellular replication

1.9.2.1 Viral DNA amplification

During viral amplification the genome is amplified up to 1000 fold in order to create new genomes for packaging (Bedell, Hudson et al. 1991). There is also speculation that viral amplification itself is required for further expression of late E1^E4, L1 and L2 genes in the upper layers (Chow, Duffy et al. 2009).

Amplified genomes are then carried throughout the remaining upper layers of the epithelium for virus packaging (Figure 1.5). Interestingly it is has also been shown that the virus changes to a different mode of replication in the upper layers which differs from the mode of replication used during low-level replication, in the early part of the life cycle. During low-level replication such as in the basal layer it has been show that the virus replicates it genome through theta structures, which requires that the viral E1 helicase, are recruited to the origin of replication by E2, with every round of replication (Flores and Lambert 1997). In addition, host cell replication machinery, such as DNA polymerases, are also needed for every round of replication. It was further shown that when the virus amplifies its genome in the upper layers, the virus switches to rolling circle replication (Flores and Lambert 1997). Rolling circle replication requires only one initiation event that subsequently leads to abundant levels of replicated DNA. This mode of replication might be more efficient for the virus when cellular replication machinery is not available beyond the E1^E4/E7 overlapping region.

1.9.2.2 HPV-16 virus assembly and release

The final productive stage of the HPV-16 life cycle involves encapsidation of amplified viral genomes and the subsequent release of new viruses from the epithelium. HPV capsids are composed of the major L1 capsid and the minor L2 capsid. The L1 protein and L2 protein are organized into a 72-capsomere icosohedral capsid shell (Chen, Garcea et al. 2000; Modis, Trus et al. 2002). It has been suggested that the L1 and L2 cased proteins accumulate at nuclear structures known as PML bodies to facilitate virus packaging (Day, Baker et al. 2004).

L1 and L2 proteins are expressed as late proteins and are typically detected in E1^E4 positive cells of the cornified and superficial layers of the epithelium (Figure 1.5) (Peh, Middleton et al. 2002; Middleton, Peh et al. 2003). A temporal gap between the onset of the first detection E1^E4 and the first detection of L1/L2 proteins occur in the upper layers of HPV-16 induced lesions.

Mature virus particles are not released until reaching the uppermost layer of the epithelium. As PVs are non-lytic viruses, it is thought that virus progeny are released from the epithelium within cornified squames that are shed from the top layer. It has been suggested similar to the case of HPV-11, the HPV-16 E1^E4 protein might increase cellular fragility in the cornfield layer to facilitate virus release (Bryan and Brown 2000).

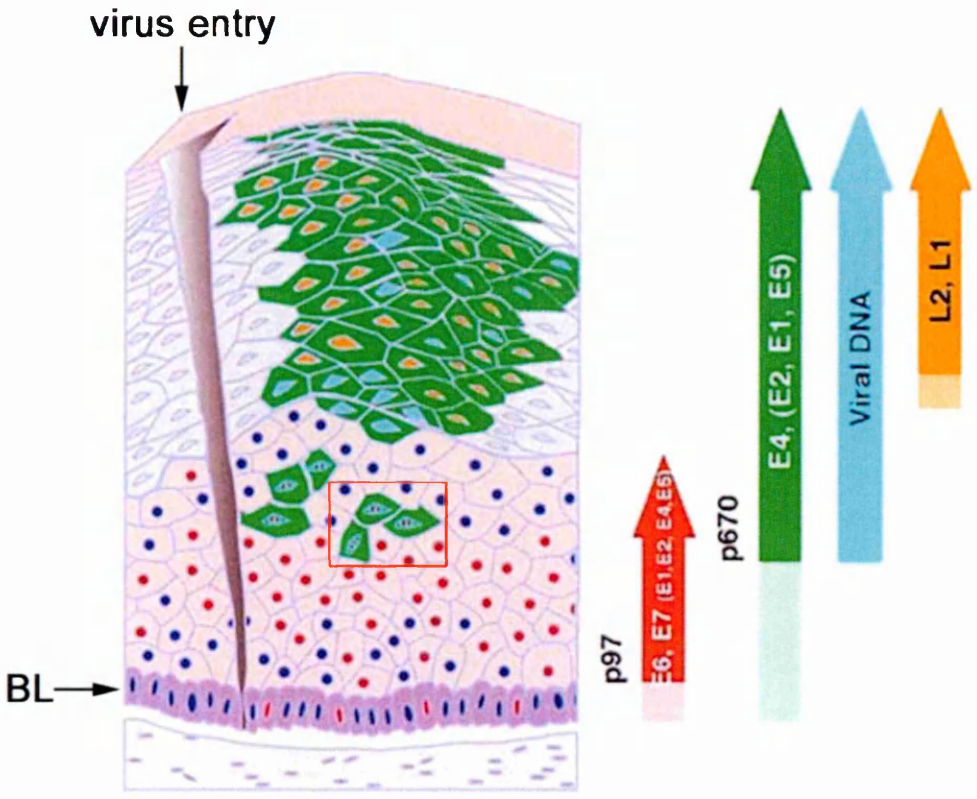

Figure 1.5 HPV-16 expression patterns in the differentiating epithelium Image taken from (Doorbar 2006)

Viruses enter the epithelium likely through a micro-wound. HPV-16 infects S-phase competent cells within the basal layer (BL). In these cells viral episomes are maintained at low levels. As these HPV infected cells divide they are pushed up into the suprabasal layers where the terminal differentiation program begins. At this point the HPV-16 p97 early promoter is active which results in the expression of the E1 and E2 replication proteins as well as the E6 and E7 oncognes (red cells). The E7 oncogene is necessary for S-phase entry. In addition to E1 and E2, E6 and E7 are necessary for episomal replication. As the cells proceed through the differentiation program, the differentiation dependent (late) promoter p670 is upregulated. This leads to increased levels of E1, E2, E5 and E4 (green cells). The start of late gene expression also coincides with a brief overlap of early genes and late genes (these cells can be identified within the red square). Cells that contain both (early) E7 and (late) E4 are thought to be the site of viral DNA amplification. Above this overlap the early genes are no longer expressed and high levels of E4 are expressed from the late promoter. A large number of E4 positive cells also contain amplified genomes (blue and green cells) and later L1/L2 capsid proteins (green and orange cells). Mature capsids that contain amplified genomes are released as cells are shed from the top layers.

1.10 The use of cellular and viral markers to detect HPV-16 gene expression patterns in cutaneous and cervical mucosal epithelium

Due to extensive mapping of HPV-16 transcripts from the early and late promoters, the boundaries of early and late gene expression have been identifiable in the HPV infected epithelium through the use of three specific antibodies. In the early part of the life cycle the E6 and E7 oncogenes are expressed from the early promoter. Due to the lack of good antibodies it has been difficult to detect E6 and E7 proteins in paraffin embedded tissues. More recently, MCM-7 has been used to detect the presence of E7 and has been further established as a surrogate marker for E7 (Williams, Romanowski et al. 1998; Middleton, Peh et al. 2003).

MCM (2-7) complexes are highly expressed throughout the cell cycle and specifically perform the function of a DNA helicase during cellular S-phase (Maiorano, Lutzmann et al. 2006). During the early stages of infection HPV E7 can induce cellular S-phase through its binding to the hypo-phosphorylated form of Rb and additionally Rb family pocket proteins (e.g. p107 and p130) (Munger, Werness et al. 1989; Boyer, Wazer et al. 1996). The binding of E7 to Rb family proteins, which lead to their degradation, allows the E2F transcription factor to remain in an active state. In its active state E2F transactivates several cellular genes such as MCM-7, which are necessary to proceed through S-phase.

In cervical lesions MCM-7 protein expression overlaps with several other E2F activated genes such as PCNA and Cyclin B, and Cyclin D. However MCM-7 is a more reliable surrogate marker of E7 S-phase induction, as it appears to be more

highly expressed in cervical lesions, when compared to other E2F activated genes (Williams, Romanowski et al. 1998; Freeman, Morris et al. 1999; Peh, Middleton et al. 2002). To date there are no sufficient antibodies to detect the E6 protein, however it is assumed that E6 and E7 are expressed in the same cells as they are both translated from the same bicistronic message.

The expression of HPV genes from the differentiation dependent late promoter has been easier to analyze in paraffin embedded tissues. This is due the availability of good antibodies targeted to the E4 gene and L1 capsid protein. DNA *in-situ* methods are also available for the detection of viral DNA amplification.

1.11 HPV-16 gene expression patterns in low- and high-grade cervical lesions

As mentioned earlier HPV-16 infections can cause both low-and high-grade neoplasias, which are pathologically diagnosed as LSIL and HSIL respectively. The diagnosis of LSIL and HSIL has been primarily based on cellular pathology. Recent studies have also shown that HPV-16 gene expression patterns change in the epithelium, as the lesions become more neoplastic (Middleton, Peh et al. 2003) (Figure 1.6).

HPV-16 lesions of LSIL grade mostly contain gene expression patterns of a complete HPV life cycle. In lesions of LSIL grade MCM-7 expression is confined to the lower third of the epithelium, where late E4 expression is typically detected in the last layer of MCM-7 positive cells. E4 is also abundantly expressed throughout the upper layers of the epithelium. Late L1 capsid protein is also

detected in E4 positive cells in the upper layers (Peh, Middleton et al. 2002; Middleton, Peh et al. 2003). By comparison in lesions with HSIL, MCM-7 positive cells persist throughout the middle third and final third of the epithelium (Figure 1.6). The high persistence of MCM-7, correlates with a delay in late E4 and L1 capsid expression. In many cases L1 capsid proteins are not detected in lesions with HSIL, which demonstrates that the epithelium is unable to support a complete life cycle (Middleton, Peh et al. 2003). These analyses have shown that the order of HPV gene expression is conserved in low and high-grade lesions, however, early gene expression persists higher up in the epithelium as the lesion becomes more neoplastic. The level of MCM-7 persistence seems to also identify when late viral gene expression begins. This has emphasized important aspects of early and late gene regulation. Furthermore it has been proposed that MCM-7 and E4 could be potential biomarkers for neoplastic progression (Middleton, Peh et al. 2003).

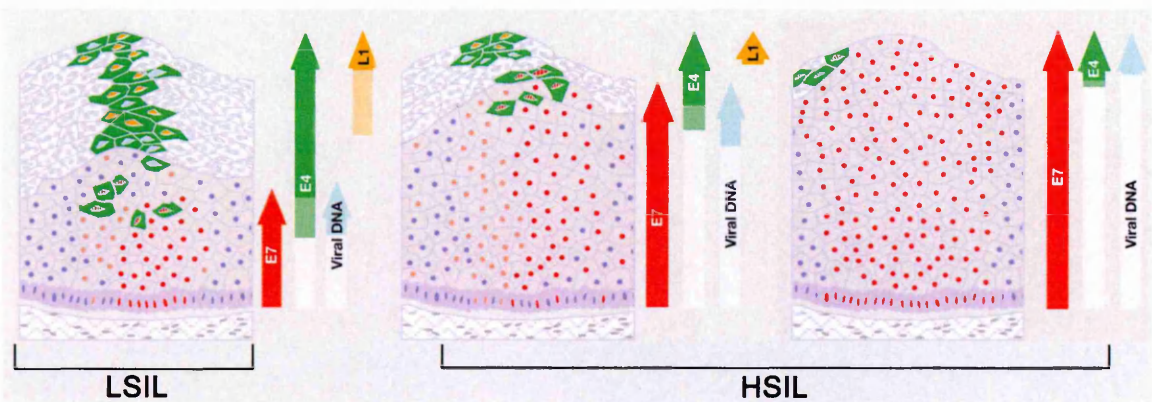

Image taken from (Doorbar 2006)

Figure 1.6 HPV-16 gene expression patterns during neoplastic progression

During neoplastic progression the order of early and late viral gene expression is conserved in the epithelium, however early genes persist in the upper layers in lesions with high-level neoplasia (i.e. HSIL) Early oncogene persistence coincides with a delay in late events (e.g. viral amplification) and late gene expression (e.g. E4 and L1). Lesions of HSIL grade typically do not support a complete life cycle.

1.12 HPV-16 Viral oncogene regulation

Viral gene expression patterns of low and high-grade neoplastic lesions also highlight important aspects of HPV gene regulation. Early viral gene regulation associated with neoplasia and cervical cancer is not completely understood. Past studies have correlated HSIL and cancer with E6 and E7 integration. (Klaes, Woerner et al. 1999; Fujii, Masumoto et al. 2005). Viral Integration typically involves the insertion of E6 and E7 into host chromosomes, which over time can lead to genomic instability and the accumulation of cellular genetic mutations (McLaughlin-Drubin and Munger 2009). The integration of E6 and E7 has been shown to coincide with the loss of several other viral transcriptional regulatory genes such E2 (Baker, Phelps et al. 1987). When E2 is present at high levels as with expression from viral episomes it has been show to act as a transcriptional repressor of E6 and E7 (Steger and Corbach 1997). Past work has shown that E6 and E7 integration coincides with an increase in E6 and E7 mRNA stability and an increase in E7 oncogene levels (Jeon and Lambert 1995; Alazawi, Pett et al. 2002) These cells also maintain a selective growth advantage over cell lines that maintain episomal forms of the virus (Jeon and Lambert 1995). The actual integration of the genome can occur near fragile sites in the host genome sites however integration is not linked to any common regions in the host chromosome (Thorland, Myers et al. 2003; Ziegert, Wentzensen et al. 2003).

More recently it has been suggested that integration is not however important for precancerous stages of HPV induced neoplasia (i.e. LSIL and HSIL). In a recent study the authors found that E7 was only expressed from episomal forms of the virus, in 85% of lesions of HSIL grade (Klaes, Woerner et al. 1999). By comparison E7 was expressed from integrated forms of the genome in the majority

of carcinomas *in-situ*. These results suggest that Integration of the genome occurs later in the disease process and that integration is more likely important for the final stages of HPV associated cancer rather than LSIL and HSIL.

It is therefore possible that the deregulation of E6 and E7 expression during neoplasia, leading to S-phase persistence, could therefore be due to differences in the episomal replication or transcription capacities.

1.13 The molecular basis of neoplastic progression and cancer with respect to the E6 and E7 oncogenes.

E6 and E7 expression is necessary to carry out a complete HPV life cycle however the persistent expression of the HPV oncogenes can lead to abnormal proliferation, cell survival and cellular genomic instability. E6 and E7 are both potent inducers of keratinocyte immortality. However, the viral molecular basis of HPV carcinogenesis and the exact mechanisms of E6 and E7 required to bring about pre-cancerous and cancerous stages of HPV disease, still form a large basis of research. Presented below are several mechanisms that are thought to be important for neoplastic progression and cancer development.

1.13.1 E7 and the cell cycle

The E7 oncogene is a small protein with a predicted molecular weight of 11kDA. Following infection with high risk HPVs E7 binds to over 20 cellular proteins. Most of these interactions take place in the cell nucleus and consequently allow the cell to progress from G1 to S phase of the cell cycle. It has also been shown that E7

can induce S-phase in differentiated cells that have already exited the cell cycle (Banerjee, Genovese et al. 2006).

The most established cellular interaction partner of E7 is the Rb protein (Dyson, Howley et al. 1989). In quiescent HPV negative cells hypophosphorylated forms of Rb prevent progression through cellular G1 through its binding to the cellular transcription factor E2F. To begin G1 cell cycle progression Rb is phosphorylated by Cyclin D/Cyclin dependent kinase (CDK4) which allows for its dissociation from E2F (Buchkovich, Duffy et al. 1989). Active or unbound E2F can then transactivate several cellular proteins that allow the cells to proceed through S-phase and proliferation. Several of these proteins that are necessary for S-phase include MCM (2-7) complexes, PCNA and Cyclin E.

A similar mechanism involved in the release of E2F from Rb is established through the binding of E7 to Rb, which also leads to Rb degradation (munger 2001,Band 1996). Similar to its hyperphosphorylated form, degraded Rb leads to E2F transactivation of S-phase proteins, which then allows for cell cycle progression. E2F activation is necessary for life cycle maintenance however, persistent inactivation of Rb leads to genomic instability, hyperplasia and disruption of the terminal differentiation program. (Balsitis, Sage et al. 2003). Mutations in the Rb gene are frequently detected in many types of cancers such as prostate and bladder cancers. (Gallie 1994; Kubota, Fujinami et al. 1995; Miyamoto, Shuin et al. 1995).

It has also been shown in mouse models that the absence of Rb without the presence of E7 was not sufficient for tumors to form. It is therefore likely that

additional cellular protein interactions of E7 are important for cancer progression (Balsitis, Dick et al. 2006).

E7 also binds to and degrades a similar set of proteins within the Rb family, which are the pocket proteins, p130 and p107 (Munger, Werness et al. 1989). These proteins have a similar role in the cell cycle where the phosphorylation of p130 and p107 leads to the transactivation of E2F transcription factors. The binding of E7 to the pocket proteins have been shown to be important for the productive life cycle and likely serves a similar function in the life cycle as Rb degradation (Collins, Nakahara et al. 2005). It has also been suggested that Rb degradation is confined to the basal layer where E7 interacts with and degrades p130 and p107 more-so in the suprabasal layers (Collins, Nakahara et al. 2005).

E7 also binds to histone deacetylases (HDACs) (Brehm, Nielsen et al. 1999). HDACs normally lead to the formation of compact and repressive chromatin. HDACs therefore function as transcriptional co-repressor and can also associate with hypophosphorylated forms of Rb. The binding of E7 to HDACs is however independent of its interactions with Rb but can also lead to increased transcription of E2F transactivated genes (Longworth, Wilson et al. 2005).

E7 has also developed mechanism to prevent the inhibition of cell cycle progression. E7 has been shown to bind to CDK inhibitors p21 and p27 (Zerfass-Thome, Zwerschke et al. 1996; Funk, Waga et al. 1997). The CDK 2/ CDK 4 inhibitor, p21 is usually upregualted during times of cellular stress and also serves as part of the p53 mediated G1 checkpoint pathway. The binding of E7 to p21 thus prevents the inhibition of G1 cell cycle progression. It has been previously shown

that the inactivation of both Rb and p21 is necessary to inhibit G1 cell cycle arrest. (Helt, Funk et al. 2002)

1.13.2 E6 and E7 related genomic instability

As stated previously it has been shown that E7 expression is sufficient to immortalize cells but expression on its own is not sufficient to cause cancer (Brake and Lambert 2005). It is widely established that additional host mutations or chromosomal abnormalities are needed for cancer development. It has been shown that both E6 and E7 can lead to the accumulation of chromosomal abnormalities in the host cell (Plug-Demaggio and McDougall 2002; McLaughlin-Drubin and Munger 2009). E6 and E7 associated chromosomal abnormalities have been identified in pre-cancerous stages of HPV neoplasia as well as in cancers (Duensing, Duensing et al. 2001). Cellular aneuploidy is a common chromosomal abnormality identified in HPV associated disease. Aneuploidy is specially the gain or loss of chromosomes in the cell and is subsequently caused by abnormal centrosomal duplications.

Centrosomal duplication is normally linked to the cell cycle and is controlled by hyper-phosphorylated forms of Rb. Correct centrosomal duplication ensures that equal segregation of the chromosomes occurs. It was originally thought that Rb degradation by E7 uncouples centrosomal duplication form the cell cycle, which would increase the centrosome number, thus leading to leading to aneuploidy and multipolar mitoses. However more recent evidence suggests that the abrogation of centrosome replication by E7 is independent of Rb degradation.(Duensing and Munger 2003)

Recent work has also suggested that centrosomal abnormalities caused by E7 are more likely to occur in the presence of integrated vs. episomal forms of the virus. As stated earlier, during E6 and E7 integration, E2 is typically lost from the genome. When E2 is present, as during episomal maintenance, it has been shown to interact with E7 and consequently sequester E7 to an insoluble compartment in the cell (Gammoh, Grm et al. 2006). This interaction has shown to inhibit E7 related Rb degradation and also centrosomal abnormalities (Gammoh, Isaacson et al. 2009). By comparison centrosomal abnormalities were not inhibited in the absence of E2, which would be in the case of viral integration. In addition centrosomal abnormalities were not inhibited when both E2 and E6 were expressed together (Gammoh, Isaacson et al. 2009). It is therefore thought that E6 rather than E7 is likely to cause centrosomal abnormities when viral episomes are maintained. However following the integration of E6 and E7, it is likely that the expression of both oncogenes lead to centrosomal abnormalities.

1.13.3 E6 and cell survival

The E6 proteins are approximately 150aa in size and contain four conserved Cys-X-X-Cys motifs that give rise to two zinc fingers. Unlike the E7 gene that directly activates cellular proliferation, the mechanisms of E6 enhance cell survival and prevent density dependent growth arrest, that both contribute to malignancy. The induction of abnormal cellular and viral DNA replication by E7 leads to a host defense response termed as the trophic sentinel response (Eichten, Rud et al. 2004). The expression of E7 alone has been correlated with elevated levels of p53 and cellular apoptosis (Demers, Halbert et al. 1994). In response to heightened

levels of p53 by E7, the E6 proteins partly eliminate the trophic sentinel response by through inactivating p53. E6 inactivates p53, through its interaction with the cellular ubiquitin ligase E6AP (E6-associated protein) (Scheffner, Huibregtse et al. 1993). This interaction subsequently leads to the proteosome-mediated degradation of p53.

Expression of high-risk E6 also enhances cell survival by inducing human telomerase reverse transcriptase (hTERT) (Klingelhutz, Foster et al. 1996). Expression of hTERT leads to the prevention of telomere shortening. hTERT is normally present in cell types such as stem cells that undergo high numbers of cell division. Somatic cells however do not normally express hTERT, which is a strategy to restrict their proliferation capacity. HPV-16 E6 however contributes to cellular immortalization through inducing hTERT expression in these cells.

1.13.4 E6 and E7 interaction with adherin junction proteins

E6 and E7 can also induce transformation through interactions with adherin junction (AJ) related proteins. AJs are linked to the cytoskeleton network and serve as the main epithelial adhesive junctions. AJs contain receptors for several proteins that are important for cell-cell contact signaling pathways, which regulate proliferation, differentiation and cell polarity.

E-cadherin, one of the most studied AJ proteins is regarded as a tumor suppressor gene. When cell-cell contact is established, E-cadherin sequesters Beta-catenin from the nucleus to the cell membrane (Balda and Matter 2003). When Beta-catenin is active in the nucleus it forms a complex with LEF/TCF transcription

factors. This complex transactivates proteins such as Cyclin D and C-myc that activate the cell cycle (Huelsken and Behrens 2002). It is therefore thought that E-cadherin can by one way, regulate the cell cycle by sequestering Beta-catenin away from the nucleus to sites of cell-cell adhesion.

Recent work has shown that E-cadherin is delocalized away from the cell membrane in the presence of E6 and E7, thus potentially removing it's ability to sequester Beta-catenin to the membrane (Wilding, Vousden et al. 1996). Additional work has also shown that E7 suppresses cadherin mediated cell adhesion (Yuan, Ito et al. 2009). A reduction in E-cadherin expression has been correlated with increasing grades of neoplasia (Vessey, Wilding et al. 1995). Furthermore, increased nuclear Beta-catenin has been associated with many types of cancers including cervical cancer (Morin 1999).

The HPV-16 E6 protein has also been shown to interact with, degrade or delocalize AJ-related proteins, which include several cellular PDZ domain proteins. Cellular PDZ domains proteins are thought to be critical for maintaining cell polarity and regulating the cell cycle. PDZ proteins consist of different cellular pools however they mostly interact with specific transmembrane domains at the cellular basolateral wall. PDZ proteins are also highly expressed at cell membranes when cell-cell contact is established (Thomas, Narayan et al. 2008).

Human Dlg (hDLG) and human Scribble (hScrib) protein are two specific PDZ domain proteins that are degraded by HPV-16 E6 (Thomas, Narayan et al. 2008). In the absence of E6 hScrib and hDlg are recruited to cell junctions and likely transduce extracellular signals towards the cytoplasm, which prevent G1 to S-

phase progression. hDlg and hScrib are also thought to interact with the tumor suppressor gene, adenomatosis polyposis coli (APC) (Matsumine, Ogai et al. 1996; Takizawa, Nagasaka et al. 2006). APC is a primary regulator protein in the Wnt pathway, which controls Beta-catenin activity. APC interacts with cytoplasmic Beta-catenin, which leads to the ubiquitination and degradation of Beta-catenin (Huelsken and Behrens 2002). It is thought that hScrib and hDlg facilitate the interaction between APC and Beta-catenin, which then prevents cell cycle entry (Nagasaka, Nakagawa et al. 2006). High or persistent E6 expression would therefore abolish this interaction.

It has also been shown that hScrib expression is reduced in neoplastic epithelium. (Nakagawa, Yano et al. 2004). The degradation of PDZ cellular proteins by E6 is also thought to lead to an increase in tumor size and enhance malignant progression (Shai, Brake et al. 2007).

1.14 The organotypic raft culture system: A laboratory system for HPV life cycle studies

Studying the HPV life cycle is somewhat arduous, as the virus requires a fully differentiated epithelium to complete its life cycle. In the past ten years organotypic raft cultures have provided a laboratory model to study the HPV life cycle (Lambert, Ozbun et al. 2005; Nakahara, Peh et al. 2005; Wilson and Laimins 2005). Organotypic raft cultures consist of a three-dimensional epidermis, which can successfully support a complete HPV virus life cycle. To create organotypic raft cultures keratinocyte cell lines that carry viral episomes, are first seeded on to dermal equivalents. The dermis in normal epithelium consists of collagen, which gives structural support to the skin and fibroblasts that secrete collagen and other

growth factors to the skin. In addition the dermis contains blood vessels and lymph nodes that allow for the infiltration of lymphocytes and other cells involved in cellular immunity. "Dermal equivalents" in raft cultures primarily consist of collagen and human fibroblasts. More recently it has also been possible to integrate lymphocytes, dendritic cells and various cytokines into raft culture experiments.

To begin the differentiation process episomal cell lines are fed with high calcium media to induce desmosomal formation and differentiation. After several days the dermal equivalents are lifted on several cotton pads and are exposed to the air. Exposure to the air allows for cornification to begin and is necessary to conserve the epithelial architecture of the raft culture. Following a 14–day differentiation regimen several layers of stratified epithelium, that contain the virus are fixed and paraffin imbedded in wax. Similar to cervical biopsy tissue, raft cultures can be subsequently sectioned on to slides to carry out immunohistochemical analysis. Through this method viral gene expression patterns can be detected throughout the raft epithelial layers.

Additional uses of raft culture include: the harvesting of mature virions form raft culture epithelia for use in viral infectivity assays; biomarker development and immunotherapeutic approaches for neoplastic disease (Delvenne, Hubert et al. 2001; Meyers, Bromberg-White et al. 2002).

1.15 Aims of the Thesis

The organotypic raft culture system has been previously established as a reliable model to study the HPV life cycle. In our studies, the immunohistochemical analysis of HPV-16 raft cultures led to the discovery that this system could also recapitulate gene expression patterns that were previously identified in both low- and high-grade HPV induced lesions. This auspiciously led to the characterization of a newly established HPV-16 raft culture model of HPV induced neoplasia.

1) To establish NIKS HPV-31 and HPV-16 episomal cell lines for organotypic raft culture experiments.

NIKS HPV16 episomal cell lines were established in collaboration with several colleagues.

2) To establish a NIKS HPV-16 organotypic raft culture model that supports a complete HPV-16 life cycle.

HPV-16 cell lines were propagated in organotypic raft cell culture to allow epithelial cell differentiation Immunohistochemically stained NIKS organotypic raft cultures were compared alongside previously stained HPV-16 cervical lesions. The aim was to show that early gene expression and the productive phase of the life cycle, including genome amplification and virus cased expression, was conserved in the NIKS HPV-16 raft model system.

3) To present a NIKS organotypic model of episomal HPV-16 induced neoplasia.

Immunohistochemically stained NIKS organotypic raft cultures were compared alongside low and high-grade HPV-16 cervical lesions. The aim was to show that HPV-16 episomal cell lines recapitulate the spectrum of viral gene expression patterns previously identified in low- and high-grade cervical lesions.

4) To characterize NIKS HPV-16 monolayer episomal cell lines in order to understand the molecular basis of HPV induced neoplasia.

The molecular basis leading to HSIL phenotypes is not completely understood. The current theory rests on that high-grade gene expression patterns are due to a deregulation of viral E6/E7 gene expression. Using monolayer HPV-16 cell lines we sought to determine if cellular growth potential, E6 and E7 expression level and viral copy number were important factors for a HSIL phenotype.

Chapter 2: Materials and Methods

2.1 Commonly used buffers and reagents

All chemicals unless otherwise stated were purchased from Sigma-Aldrich Company Ltd. (UK), BDH Laboratory Supplies (UK), Fisher Scientific (UK) and VWR (UK).

2.1.1 Buffers and reagents prepared by the NIMR cell culture facility:

Commonly used buffers were prepared according to Table 2.1.

Table 2.1 Buffers and Reagents

Name	Components
Luria-Bertani (LB) medium	1 % tryptone, 0.5 % yeast extract, 1 % NaCl
LB Agar	LB medium plus 2 % Bacto agar
50x Tris acetate EDTA (TAE)	242 g Tris base, 57.1 mL glacial acetic acid, 18.6 g EDTA
Trypsin-versene	0.8 % NaCl, 0.02 % KCl, 0.12 % Na_2HPO_4, 0.02 % KH_2PO_4, 0.01% EDTA, 0.13 % trypsin, 0.001% phenol red.
1x Phosphate buffered saline (PBS)	1 % NaCl, 0.025 % KCl, 0.14 % Na_2HPO, 0.025 % KH_2PO_4
SDS electrophoresis buffer	25 mM Tris base, 192 mM glycine, 0.1 % sodium dodecyl sulfate (SDS)
Transfer buffer	30 mM Tris base, 192 mM glycine, 20 % methanol
Penicillin/ Streptomycin (cell culture)	0.6 % (v/v) penicillin, 1 % (v/v) streptomycin

2.2 Keratinocyte and fibroblast monolayer cell culture

2.2.1 Cell lines

2.2.1.1 Normal Immortalized Human Keratinocytes (NIKS)

NIKS, a cutaneous foreskin keratinocyte cell line, were used as a host cell and as negative control with all HPV-16 experiments. NIKS were originally recovered as an HPV-negative spontaneously immortalized cell line after successive passages of their parental BCI-EP/SL cell line (Allen-Hoffmann, Schlosser et al. 2000).

2.2.1.2 NIKS wild-type (wt, #53)-HPV-16 (W12) and HPV-31 cell lines

Ten clonal wt-HPV-16 cell lines were established from two separate transfections (courtesy of Kenneth Raj; NIMR, London, UK and Qian Wang; NIMR, London UK). All wt-HPV-16 (W12) cell lines were established following cotransfections with recircularized replication competent W12-HPV-16 genomes and a pCDNA6 vector that contained a Blasticidin resistance gene. All wt-HPV-31 cell lines were established following co-transfections with recircularized replication competent HPV-31 genomes and a pCDNA6 vector that contained a Blasticidin resistant gene. HPV-31 and HPV-16 clonal cell lines were recovered after several days of Blasticidin drug (6 µg/mL) selection and were individually expanded into 6-well plates after the individual colonies became visible.

2.2.1.3 J2-3T3 mouse fibroblast cells

J2-3T3 cells, an immortalized fibroblast cell line, were originally isolated from Swiss albino mouse embryos (Todaro and Green 1963). The J2 clone has been

widely used as a feeder layer to support the growth of human keratinocyte cell lines.

2.2.1.4 EF-IF human foreskin fibroblast cells

EF-IF fibroblasts were originally isolated from human foreskin tissues and have been maintained as a primary fibroblast cell line. EF-IF cells have been previously used for the creation of dermal equivalents.

2.2.2 Media supplements and recipes

2.2.2.1 Supplements

The following media supplements were prepared and filter sterilized, using a 2 µm membrane filter unit. All supplements were stored as 5 mL aliquots at -20°C.

100x Hydrocortisone- 25 mg of hydrocortisone (Calbiochem) was dissolved into 5mL of cold ethanol to make a 5 mg/mL solution. 0.8 mL of this solution was added to 100mL HBES and 5 % (v/v) Fetal Bovine Serum (FBS) (Hyclone; UK).

100x Cholera Toxin- 1 mg of cholera toxin (Sigma; UK) was dissolved into 1.2 mL of sterile water to make a 10 µM solution. 50 µl of this working stock was added to 50mL HBES that contained 0.1 % (w/v) bovine serum albumin (BSA).

100x Insulin- 12.5 mg of insulin (Sigma; UK) was dissolved into 25 mL of 0.005 M HCL (247.5 µl concentrated HCL in 500 mL water). 2 mL of FBS was passed through the 2 µm syringe filter prior to adding the insulin stock.

100x Adenine- 121 mg of adenine (Sigma; UK) was dissolved into 50 mL of 0.05M HCL (24.7 mL concentrated HCL into 476 mL water)

2.2.2.2 Cell culture media

The following medias in Table 2.2 were used to grow and maintain monolayer cultures of keratinocytes and fibroblasts.

Table 2.2 Monolayer cell culture media

Cell type	Media name	Media components
J2-3T3	3T3 media	500 mL DMEM (Sigma), 10 % (v/v/) FBS and 5 mL pen/strep
NIKS and wt-HPV-16 cell lines	F-Media Incomplete (FI)	375 mL F12-Hams (Gibco; UK), 125 mL high glucose DMEM (Gibco; UK). Supplements: 5 mL (100x stocks) of adenine, cholera toxin, hydrocortisone, insulin and pen/strep, 5 % (v/v) FBS
NIKS and wt-HPV-16 cell lines	F-Media Complete (FC)	500 mL FI media with 500 µl 1000x EGF
EF-IF	Human Fibroblast Media	500 mL F12-Hams, 5 mL pen/strep and 10 % (v/v) FBS
J2-3T3 and NIKS	Freeze Media	45 mL FBS and 10 % (v/v) DMSO
EF-IF	Freeze Media	22.5 mL FI media, 22.5 mL FBS, 10 % (v/v) DMSO

2.2.3 Maintenance of monolayer cells

2.2.3.1 J2-3T3

J2-3T3 fibroblasts were cultured in 10 mL of 3T3 media in 75 cm flasks (Corning; UK) at 37°C and 5 % CO_2. The fibroblasts were grown until they were 80 % confluent and were then split 1:20-1:50 to another 75 cm flask. To harvest the fibroblasts, the cells were washed with 5-10 mL PBS followed by the addition of 1mL trypsin versene. The fibroblasts, along with the trypsin, were incubated at 37°C for 1 minute followed by the addition of 9 mL of 3T3 media. An aliquot of the suspended cells was then added to a new flask for culturing. Cultures of J2-3T3

were not used for experimental purposes above passage 20, where early passage stocks were frozen down (-70°C overnight then into liquid nitrogen indefinitely) in 1 mL of 3T3 freeze media to maintain the line.

2.2.3.2 NIKS and wt HPV-16 cell lines

NIKS and HPV-16 cell lines were cultured on a bed of ∂-irradiated J2-3T3 cells in 75 cm flasks at 37°C, 5 % CO_2. Prior to culturing the NIKS, J2-3T3 cells were irradiated at a dosage of 60Gy. Approximately $2x10^6$ of these irradiated fibroblasts were seeded into the flask and were allowed to attach for 2 hours at 37°C. Following their attachment, a minimum of $5x10^6$ NIKS or HPV-16 clones were added to the flask along with 10 mL of FI media. After 24 hours the media was changed and 10 mL of FC media was added every other day thereafter. All keratinocyte cell lines were cultured until they were 80-90 % confluent. To harvest the cells the media was removed and 10 mL of PBS was added and removed to wash the cells. To follow, 1mL of trypsin versene was added to the flask and the cells were incubated at 37°C for 1 minute. The flask was tapped several times to completely dislodge the feeder layer from the keratinocytes, which were then aspirated away. 2 mL of fresh trypsin versene was added to the remaining keratinocytes and the cells were incubated at 37°C for up to 15 minutes. After the cells were completely dislodged, 8 mL of FI media was added to the trypsin and a counted resuspension of the cells was added to a fresh flask of irradiated feeders or were frozen down in 1 mL freeze media for later use. All keratinocyte cell lines were never left in culture for more than 2-3 passages.

2.2.3.4 Cell counts of NIKS and HPV-16 cell lines

For all experiments and the culturing of NIKS and HPV-16 cell lines, all cells were counted using a Beckman Z1 coulter particle counter. In order to get an accurate count, the coulter counter carried out an initial sizing of the keratinocytes, which consisted of increasing 2 µm increments. To do this, 1 mL of an 80 % confluent flask was resuspended in 9 mL of isotone solution (Beckman; UK) (1:10 dilution) and 1 mL of this suspension was then counted. To establish a more precise range of cell size for accurate counting the readout was plotted out on a graph as the total number cells/mL vs. cell size in µm. The majority of the cells fell within a peak range of 11-20 µm. In order to account for cells that were slightly larger due to differentiation, the coulter counter parameters were set to count all cells above the lower limit tL=11 µm.

2.2.3.5 EF-IF human foreskin fibroblasts

Fresh stocks of early passage (passage 5-10) EF-IF fibroblasts were grown in T-25 flasks (NUNC; UK) in 5-6 mL of human fibroblast media until they were 90% confluent. To harvest the cells 5 mL of PBS was added and removed to wash the cells and the cells were then incubated at 37°C, 5 % CO_2 with 1 mL of trypsin, in order to dislodge the cells. Following this incubation 4 mL of human fibroblast media was added to the cells and the entire suspension was transferred to a 75 cm flask for expansion. The cells were harvested when they were 90 % confluent and were passaged at 1:4 to an additional 75 cm flask. EF-IF fibroblasts were not cultured beyond 2-3 passages before being used for experimental purposes. The maximum passage used for experimental purposes did not exceed passage 12.

2.3 Organotypic raft cultures of NIKS and HPV-16 wild-type cell lines

Note: The entirety of these raft culture experiments, up until the time of sectioning, were carried out in a level 2 containment cell culture hood.

2.3.1 Media and reagents for raft cultures

Table 2.3 includes the media components and supplements required for the growth of organotypic raft cultures.

Table 2.3 Organotypic raft culture media and supplements

Media name	Components
Human Fibroblast Media	See Table 2.2
Keratinocyte Plating Media	500 mL FI media with 0.5 % (v/v) FBS and 610 µl $CaCl_2$ (Ca^{2+} final concentration 1.88mM)
Cornification Media 1	500mL FI media with 5% (v/v) FBS and 610 µl $CaCl_2$ (Ca^{2+} final concentration 1.88mM). Add fresh N 1,2-dioctanoyl-sn-glycerol (C8:0) (Sigma; UK) to a final concentration of 10 µM

2.3.2 Preparation of dermal equivalents

To prepare dermal equivalents for growing raft cultures 20 mL of collagen (approx. 3.5mg/mL) (BD Scientific; UK) was resuspended on ice with 2.5 mL 10x F12 media (Sigma), 6 µl 10N NaOH, 250 µl 100x Pen/Strep and 2.5mLFBS. 1 mL of this suspension was plated into individual 24mm transwell inserts (Costar; UK) that had been previously placed in a deep 6-well plate (BD Biosciences; UK). The deep well plate containing the collagen suspension was left in the cell culture hood for 5 minutes to allow the collagen mixture to harden. 600 µl of a 7.5 x 10^6 cells/ mL suspension of EF-IF fibroblasts was added to the remaining collagen mixture and an additional 2.6 mL of this mixture was plated out into the individual transwell inserts. The deep well plate was left to incubate for 30 minutes at 37°C, 5% CO_2

until the dermal equivalents had completely solidified. 20 mL of human fibroblast media was added to each transwell and the plate was left to incubate at 37°C, 5 % CO_2 for 5-7 days.

2.3.3 Seeding and differentiation of keratinocytes

NIKS or wt-HPV-16 cell lines that were 90 % confluent were trypsinised, counted and resuspended in FI medium at a concentration of $4.2x10^6$ cells/mL. The human fibroblast medium was removed from the transwell inserts and 100 µl of either NIKS or HPV-16 cell line suspensions were added drop-wise into individual transwell inserts. A gentle rocking of the dish was necessary to allow for the entire volume to cover the insert. The inserts were left to incubate at 37°C 5 % CO_2 for 2 hours to allow for the complete attachment of cells to the dermal equivalents. Following this incubation, 20mL of keratinocyte plating medium was added to each insert and the plate was left at 37°C 5 % CO_2 for 4 days. During this interval, the keratinocytes and dermal equivalents were fed every other day with 20 mL of keratinocyte plating medium. On the fourth day the medium was removed and three sterile cotton pads (2.5 cm x 2.5 cm) (Schleicher and Schwell; Germany) were placed under the transwell inserts in order to lift them towards the air. The raft cultures were fed from underneath with 12.5 mL of cornification media and then 9.5 mL of cornification medium every other day thereafter until the time of harvest. Raft cultures were left to differentiate for a total of 10 days post lifting.

2.3.4 Harvesting and fixation of raft cultures

After 10 days of differentiation, the dermal equivalents and their intact keratinocyte layers were removed from the transwell inserts for fixation. Prior to harvesting the raft cultures a fresh 2 % Bacto Agar, 1 % formalin solution was prepared as a fixation solution. To prepare the fixation solution 2 g of Bacto Agar was added to 90 mL of sterile dH_2O and the entire volume was boiled in the microwave on a low setting for 3 minutes. The dissolved agar was left to cool with constant stirring and was not allowed to cool below 55° C. After the agar cooled to 55°C 10 mL of 10 % formalin was added to it in the fume hood. The fixation solution was then placed in a 50°C water bath during the entire harvesting process to ensure that the agar did not solidify. To fix the raft cultures 3-4 mL per raft culture of the fixation solution was applied to glass plates in a slow circular motion where the surface area was roughly double the circumference of the raft culture. The fixation solution was left to solidify on the glass plates in the cell culture hood (approx. 2 minutes). Following the removal of the cornification media, the raft cultures were removed from the transwell inserts with sterile forceps and were each placed on the solidified layers of fixation solution. An additional 2-3 mL of fixation solution was placed on each raft culture at roughly the same surface area. Each glass plate was wrapped in aluminum foil and was placed at 4°C overnight. The following day, any excess solidified fixation solution around the perimeter of the raft cultures was removed with a sterile blade. The circular raft cultures sandwiched between two layers of fixation solution were cut into two equal halves with sterile scissors and were placed side by side in a tissue-tek cassette. The cassettes were then submerged in a 4 % formalin solution overnight at 4°C. The following day, the 4 %

formalin solution was replaced with 70% ethanol. The cassettes remained in 70 % ethanol at 4° C until the time of sectioning.

2.3.5 Sectioning of raft cultures

All of the raft cultures were paraffin embedded in wax and sectioned by an NIMR histologist. The raft cultures were paraffin embedded and were transversely sectioned (5 µm thick sections) on to Superfrost plus slides. The slides were placed at 37° C overnight prior to immunostaining.

2.4 Immunocytology and Immunohistochemistry

2.4.1 Immunocytology of monolayer NIKS and wt-HPV-16 clones

In order to view monolayer cells for immunocytology purposes, round glass coverslips were added into 60 mm 6-well plates. Irradiated fibroblasts and keratinocytes were seeded on top of the coverslips as described in section 2.6.1.

2.4.1.1 Fixation of coverslips

Unless otherwise stated, all coverslips were fixed with 5 % paraformaldehyde for 5 minutes at RT. To do this the coverslips were washed with 1x PBS and the coverslips were submerged in the 5 % parafomaldehyde. After this incubation the paraformaldehyde was removed and the coverslips were washed again with PBS.

2.4.1.2 Haematoxylin and Eosin (H&E) staining of monolayer cells

Coverslips were fixed and stained with H&E in order to look at the cytological and nuclear morphologies of the keratinocytes. A regressive Haematoxylin method was used for every experiment. To stain the coverslips, Harris's Haematoxylin (Sigma; UK) was applied to the coverslips for 5 minutes at (rt). The Haematoxylin was removed with running tap water and the coverslips were quickly (approx. 10

seconds) differentiated in 1 % acid alcohol (1 % (v/v) concentrated HCL, 95 % (v/v) 100 % ethanol). The acid alcohol was quickly removed with tap water and the coverslips were returned to a more alkaline environment by the addition of Scott's tap water (40 g sodium bicarbonate, 7 g magnesium sulfate per 2 L of dH_2O). The blue stained cells were then washed again in tap water and an eosin solution was applied to the coverslips for 30 seconds. After this incubation the eosin was removed with tap water and then were dehydrated in 70 % ethanol. Prior to mounting the coverslips were cleared with the xylene substitute, Histoclear (National Diagnostics; USA).

2.4.2 Immunohistochemistry of raft culture section

2.4.2.1 Antibodies and chemical reagents

Table 2.4 Primary Antibodies

Target	Species	Clone	Dilution	Incubation	Supplier
K14	Mouse	CKB1	1:100	1 hr. RT	Sigma
K10	Mouse	DE-K10	1:200	1 hr. RT	Neomarkers
Filaggrin	Mouse	N/A	1:50	1 hr. RT	Novacastra
MCM-7*	Mouse	47DC141	1:200	o/n 4°C	Neomarkers
HPV-16 E4	Phage display	B11	1:100	o/n 4°C	In house
HPV-16 L1	Mouse	K1H8	1:50	o/n 4°C	DAKO

Table 2.5 Secondary Antibodies					
Target	**Species raised**	**Conjugate**	**Dilution**	**Incubation**	**Supplier**
Mouse IgG	goat	Alexa 594	1:150	1 hr.	Invitrogen
Mouse IgG	goat	Biotinylated	1:100	1 hr.	Vector Labs
Goat IgG	donkey	Alexa 594	1:150	1 hr.	Invitrogen

Table 2.6 Chemical Reagents			
Reagent	**Dilution/Diluent**	**Incubation**	**Supplier**
DAPI	1:1000 / 5% NGS	1 hr.	
Strep A/B (avidin/biotin) (peroxidase) complex	1:400 50mM Tris/HCL pH 7.6	30 min.	Vector Labs
Tyramide (rhodamine)	1:100 Amplification diluent	8 min.	NEN Life Science

2.4.2.2 De-paraffinization and epitope exposure of raft sections

In order to conduct immunohistochemical analysis on raft culture sections, the paraffin embedded sections underwent, a dewaxing and rehydration process, followed by epitope exposure. To dewax the sections, each slide was submerged into two separate containers of xylene; the first for 10 minutes and the second for 5 minutes. After the wax had been removed the sections were rehydrated in graded alcohols (2 x in 100 % ethanol for 2 minutes and then 1 x 80 %, 50 % and 30 % ethanol, each for 2 minutes). The sections were then submerged in dH_2O for a minimum of 5 minutes. Finally, in order to unmask targeted antigens, the next step included a microwave based epitope exposure. To do this the slides

were placed in a plastic beaker with 500 mL of 0.01M citric acid buffer, pH 6.0 (10N NaOH was used drop-wise to increase the pH of the buffer). The slides were first allowed to equilibrate in the buffer for 10 minutes before they underwent two successive rounds of boiling in the microwave. The microwave method included a boiling step of 7 minutes on high setting, followed by a resting period of 2 minutes at (rt), and finally a second boiling step for 5 minutes on high setting. The sections were allowed to cool at (rt) for 20 minutes before blocking and applying antibodies to the sections.

2.4.2.3 Applying primary and secondary antibodies to raft sections

Directly following the epitope exposure of raft sections, the sections were equilibrated in PBS for 5 minutes. During this time a working stock of 10 % normal goat serum (NGS) (v/v) in PBS was prepared as a blocking solution. All sections were blocked with 10 % NGS in a human chamber at RT for at least one hour. After blocking, primary antibodies were diluted in 5 % NGS and were applied to the sections according to Table 2.4. All primary antibodies were removed by washing each section in PBS/Tween-0.05 % for 3x5 min at (rt). Secondary antibodies were diluted in 5 % NGS and were applied to each section according to Table 2.5. At this time the DAPI nuclear stain was also applied to the sections, according to Table 2.6. Secondary antibodies were removed using the identical wash program. In cases where Alexa conjugated secondary antibodies were applied to the sections, the raft cultures were immediately ready for visualization.

2.4.2.4 Primary antibody signal amplification

In cases where an amplified signal of the primary antibody was needed, secondary biotinylated antibodies were applied to the raft sections, according to Table 2.5. Approximately 30 minutes through this incubation, Strep A/B (avidin/biotin)

complexes were assembled using the ABC (peroxidase) kit according to Table 2.6 and the manufacturer's instructions. The complexes were removed using the same PBS-Tween 0.05 % wash regimen. In order to quench endogenous human peroxidases, 3 % hydrogen peroxide/PBS (v/v) was applied to the section for 15 min. at RT, following the removal of ABC complexes. The hydrogen peroxide was removed by rinsing the sections several times in PBS. To complete the amplification process, the fluorochrome labeled Tyramide (rhodamine) was applied to the sections according to Table 2.6 and the manufacturer's instructions. The rhodamine was removed using the same PBS-Tween 0.05 % wash regimen.

2.4.2.5 H&E staining of raft cultures

In order to examine the cellular pathology of NIKS and wt-HPV-16 raft cultures, raft culture sections were stained with H&E reagents. Prior to this staining, the sections were de-waxed and rehydrated using the identical procedure as described in Section 2.3.4. A regressive H&E staining procedure was then carried out using the same protocol as described in Section 2.4.1.2.

2.4.2.6 Mounting raft culture coverslips for microscopy

Prior to viewing and capturing images of raft culture sections, coverslips were mounted on to the sections using the appropriate mounting reagents. For fluorescently stained raft cultures 10-20 µl of citifluor reagent (Citifluor LTD; UK) was dropped on to the section and a coverslip was laid on top of the section. Slides that contained fluorescently stained raft cultures were kept in the dark at 4°C. For raft culture sections that had been stained with H&E a drop of DPX mountant (Sigma; UK) was placed on to the section and a coverslip was applied

on to the section. The slides were either left to dry at (rt) o/n or were dried using the microwave on a medium setting, for 2 minutes.

2.5 Microscopy and imaging software

All fluorescently stained cells were viewed on a Nikkon EFD-3 microscope equipped with fluorescent filters. Fluorescent images were captured using a SenSytem camera and images were viewed using IPLAB software. All H&E stained cells were viewed on a Zeiss A1 microscope. Color images were captured using a MRc camera and images were viewed using Axiovision software.

2.6 Monolayer growth assays of NIKS and HPV-16 clones

Growth assays were used to assess the level of proliferation for monolayer NIKS and HPV-16 clones. NIKS and all selected clones were counted in triplicate on specific days over a 7-day time period. Unless otherwise specified total cell numbers/mL for each triplicate were assessed on days 1, 3, 4, 5 and 7.

2.6.1 Seeding of fibroblasts and keratinocytes for growth assays

Approximately $1x10^5$ ∂ irradiated fibroblasts were seeded into each required well, of a 60 mm 6-well plate. The cells were allowed to attach for 2 hours in 1-2 mL of FI media at 37°C, 5 % CO_2. $1x10^5$ NIKS or HPV-16 clones were seeded on to the attached fibroblasts and were incubated in FI media overnight at 37°C, 5 % CO_2. Until the end of the experiment all remaining cells were fed with 4 mL FC media every other day thereafter.

2.6.2 Harvesting and counting NIKS and HPV-16 cell lines during growth assays

On each day of harvesting, each well was first washed with 1 mL PBS and then 0.5 mL of trypsin was added to the fibroblast and keratinocyte layers. The cells were incubated at 37° C, 5 % CO_2 for 1 minute followed by a light tapping of plate,

in order to completely dislodge the fibroblasts. Any excess fibroblasts were washed away with PBS. To remove the keratinocytes 1 mL of trypsin was added to each well and the cells were left to incubate at 37°C, 5% CO_2, for at least 15 minutes or until the cells had completely dislodged from the plate. In order to create a single cell suspension, 1 mL of FI media was added to each well and the entire contents were put into individual 15 mL Falcon tubes. To count the cells 0.5 mL of each individual suspension was added to 9.5 mL isotone solution (1:20 dilution) and were counted using a coulter counter as described in section 2.2.3.4. The results were plotted on an x vs.y axis graph (days vs. cell number) using standard deviation error bars. The remaining cells were used for various other experiments, which will be described later.

2.7 Molecular biology techniques

2.7.1 Bacterial transformation

Plasmid DNA was transformed into the XL-1 Blue Supercompetent strain (Stratagene; UK) using the manufacturers protocol. 50-100 µl of the transformed bacterial culture was plated out on to ampicillan (100 µg/mL) LB agar plates. All plates were left to incubate at 37°C overnight.

2.7.2 Extraction of bacterial plasmid DNA

Prior to the extraction of plasmid DNA from transformed bacterial colonies, each colony was picked with a sterile micropipette tip and was placed in 3-5 mL of LB broth with100 µg/mL ampicillin. Tubes were used to allow for optimal shaking. The bacterial cultures were shaken at approximately 300 rpm overnight at 37°C. To extract plasmid DNA, 1.5 mL of the expanded culture was used to perform a mini-prep DNA extraction using the QIAprep spin mini-prep kit (Qiagen; UK). The

DNA was extracted and eluted using the buffers and protocol supplied by Qiagen. In order to grow up larger scale preps for DNA extraction, 250 µl of the remaining mini-prep culture was used in 250 mL (1:1000 dilution) of LB broth with 100 µg/mL ampicillin. The culture was shaken at approximately 300 rpm overnight at 37°C. The entire culture was used to perform a DNA extraction using the EndoFree plasmid maxi kit (Qiagen; UK). (It should be noted that if the mini-prep culture was more than 8 hours old, a fresh colony was picked for a small-scale overnight culture and 250 µl of this culture was then used for the large-scale maxi prep).

2.7.3 Extraction of total genomic DNA from NIKS and wt-HPV-16 cell lines

Prior to extracting the DNA, the cells were washed with PBS and pelleted at a low speed (3000rpm) in a microcentrifuge for 5 minutes. The cells were immediately put on ice and the pellets were prepared for the removal of RNA. In order to remove RNA from the cells, the pellet was resuspended in 140 µl of PBS and 40 µl of (10mg/mL) RNaseA (Invitrogen; UK). The cells were incubated in a 37°C water bath for 20 minutes and the DNA extraction protocol immediately followed. The extraction of total genomic DNA, including HPV genomic DNA, from NIKS or HPV-16 cell lines was performed using the QIAamp DNA Blood Mini kit (protocol for small volumes of blood) (Qiagen; UK). The complete set of buffers and reagents required to extract the DNA were contained in the Qiagen kit.

2.7.4 Quantification of plasmid and genomic DNA

Plasmid and genomic DNA was quantified using a Nano-drop 8000 spectrophotometer.

2.7.5 Agarose gel electrophoresis

The separation of plasmid and genomic DNA was carried out using 0.8%-1% agarose gels (depending on the size of the product). Agarose gels were prepared with 0.8 %-1 % (w/v) agarose in 1x TAE buffer with 5 µl (10 mg/mL) ethidium bromide per 100 mL of gel. The gels were cast into a BioRad electrophoresis gel tank and were run at a constant voltage of 100V.

2.7.6 Quantitative RT-PCR (QPCR)

Quantitative real-time (RT) polymerase chain reaction (PCR) was carried out on NIKS chromosomal and HPV genomic DNA to determine the HPV copy number per cell, within wt-HPV-16 cell lines. Forward and reverse primers (Table 2.7) were designed to detect a 150 bp HPV-16 E4 sequence and a 150bp human GAPDH sequence, which was used as an internal housekeeping gene. It should be noted that the region of GAPDH primer amplification was selected based on the fact that it contained the least amount of homology to that of the mouse GAPDH DNA sequence. This was to ensure that any contamination by mouse J2-3T3 fibroblasts would not be reflected in the readout.

A Sybr Green ROX mix reagent that contained a Thermo Start DNA polymerase was used to amplify the DNA. The samples were run in triplicate wells (per primer set) in 96 well plates (Abgene; UK) using an ABI 7000 sequence detector system.

2.7.6.1 QPCR primer design

Primer sets were designed using Primer Select software

Table 2.7 Primer Sequences

Target	Sequence
HPV-16 E4 (F)	5' GACTATCCAGCGACCAAGATCAG 3'
HPV-16 E4 (R)	5' CTGAGTCTCTGTGCAACAACTTAGTG 3'
GAPDH (F)	5' CCTCCCGCTTCGCTCTCT 3'
GAPDH (R)	5' CTGGCGACGCAAAAGAAGA 3'

2.7.6.2 QPCR reagent cocktails

To amplify HPV-16 and NIKS genomic DNA a fresh cocktail of reagents was prepared for each primer set, (Table 2.8) immediately prior to the PCR analysis. The volume of cocktail was made according to the number of triplicates required for all DNA samples.

Table 2.8 QPCR cocktail		
	Cocktail 1 HPV-16	**Cocktail 2 GAPDH**
	(µl) per reaction (well)	**(µl) per reaction (well)**
*Primer Forward	1.75 µl	1.75 µl
*Primer Reverse	1.75 µl	1.75 µl
Syber Green	12.5 µl	12.5 µl
H_2O	8 µl	8 µl
	x number reactions needed	x number of reactions needed

* Primers were diluted to 1µM working stocks in sterile TE (Tris, EDTA) pH 8.0.

2.7.6.3 QPCR plating scheme and cycle parameters

To be statistically significant each sample was plated into triplicate wells, for both HPV-16 and GAPDH primer sets. 24 µl of the individual cocktail mixtures were

pipetted into each well and 1 µl of 20-40ng/ µl DNA was then pipetted separately into each well. Table 2.9 contains the cycle parameters use to amplify the DNA products. Due to the fact that Sybr Green can bind to non-specific double stranded DNA products, a dissociation program immediately followed the amplification cycles. For each reaction, this determined if single or multiple PCR products had been amplified. Table 2.10 contains the parameters for the dissociation program.

Table 2.9 ABI 7000 PCR parameters

Step	Number of cycles	Time per cycle	Temperature
1	1	2 minutes	50°C
2	1	15 minutes	95°C
3	40	15 seconds	95°C
4	1	1 minute	60°C

Table 2.10 Dissociation parameters

Step	Number of cycles	Time per cycle	Temperature
1	1	15 seconds	95°C
2	1	20 seconds	60°C
3	1	95 seconds	95°C

2.7.6.4 Standard curves for primers

A standard curve and linear equation was generated for each primer set in order to determine their efficiency and sensitivity, within the selected PCR parameters.

To generate an HPV-16-E4 standard curve, a construct (pTZH16-W12) that contained the entire 8kb genome was used as the template. To establish a linear relationship, six 10-fold serial dilutions (10pg, 1pg, 0.1pg, .01pg, 1fg and 0.1fg) of HPV-16 DNA were plated out in triplicate. To generate the standard equation that

would determine the total number of HPV copies in each reaction, the concentrations of DNA were converted into their corresponding copy numbers ($8.3x10^5$, $8.3x10^4$, $8.3x10^3$, $8.3x10^2$, 83 and 8.3 copies respectively). To generate GAPDH standard curves a pDrive construct that contained the 300 bp of the GAPDH ORF was used as the template. To establish a linear relationship six 10-fold serial dilutions (1pg, 0.1pg, .01pg, 1fg, 0.1fg and .01fg) were plated out in triplicate. To generate the standard equation that would determine the total number of GAPDH copies in each reaction the concentrations of DNA were converted into their corresponding copy numbers ($2.5x10^5$, $2.5x10^4$, $2.5x10^3$, $2.5x10^2$, 25 and 2.5 copies respectively). For both HPV-16 and GAPDH, the standard curves were only generated once as the same primer stocks were used for every QPCR experiment.The following are the standard curve equations for HPV-16 and GAPDH primer pairs:

Standard curve equation: HPV-16 $y=-3.33x + 35.78$

Standard curve equation: GAPDH $y=-3.39x + 40.61$

2.7.6.5 Standard curve equations and calculations for copy number determination

The HPV-16 and GAPDH standard curve equations generated in the form of $y=mx+b$, contained two important parameters. The slope (m) referred to the linear relationship or efficiency of the primer pairs where a slope of -3.33 showed a perfect linear relationship between DNA copy number and cycle threshold (ct) value. The y-intercept or (y) determined the primer sensitivity where y= the number of cycles needed to amplify one copy of DNA. In this case, the y

intercepts suggested that there were differences in sensitivity between primer sets, however both fell within the programmed parameter of 40 cycles (Table 2.9).

To use the standard equations to calculate the total number of HPV-16 copies per cell in wt-HPV-16 clones, each set of triplicate (ct) values were averaged. To account for pipetting errors the software also generated a standard deviation for every triplicate where standard deviations over 0.300 indicated excessive variation within the triplicate. Reactions were repeated if standard deviations exceeded 0.300.

Acceptable (ct) averages were used in the standard equations as follows:

If y=mx+b where **(m)**=slope, **(b)**=y intercept and **(y)**=ct value, then solving for $\mathbf{ln}^{-1}$ **x** generated the total copies of HPV-16 or GAPDH in each reaction. In order to establish the total number of cells in each reaction, the GAPDH copy numbers were divided by four. This was due to the fact that initial work with these GAPDH primers had identified two additional GAPDH pseudogene sequences within the NIKS genome. To finally complete the HPV copy number/cell calculation for each cell line, the total number of HPV copies were divided by the total number of cells.

2.7.6.6 Copy number evaluations from growth curve assays

HPV copy numbers/cell of HPV-16 clones were assessed on day four of the monolayer growth assays. On day four of the monolayer growth assays (section 2.6) the triplicate wells of each clone were harvested and counted as described in section 2.6.2 The entire remains of each well within a triplicate were washed with PBS and pelleted separately in micorcentrifuge tubes. Total genomic DNA was extracted as described in section 2.7.3. For each HPV-16 clone, a total of three triplicates or nine samples were harvested on day four, however each triplicate

was harvested on a different day in order to test for the biological reproducibility of episomal maintenance. To quantify the HPV copy numbers/cell for each clone, all nine samples were plated as a single experiment on one 96-well plate. HPV copy numbers were quantified as described in 2.7.6.5.

2.7.6.6.1 Statistical evaluation of HPV copy numbers from growth assays

HPV copy numbers from the 9 samples were averaged and normalized against one DNA sample that had been carried through to each experiment. This sample was used to control for day-to-day variation caused by the PCR machine. Normalized averages of each clone were put through a two-tailed unpaired T test statistical significance was shown at $p<0.05$.

2.7.7 Southern blot analysis

A Southern blot analysis was conducted on each monolayer clone in order to show the physical state of the HPV genome. An entire 75cm flask of monolayer cells were harvested and pelleted. Total genomic DNA was extracted from the pellet as described in 2.7.3.

2.7.7.1 Restriction enzyme digests for Southern blot analysis

5µg of genomic DNA from NIKS and wt-HPV-16 cell lines were digested separately with *Bam* HI (Roche; UK) and *Hind* III (Roche; UK). The DNA samples were digested as follows:

Restriction digest	
5µg DNA	X µL
10x Restriction buffer	5µL
100x BSA	0.5µL
(10mg/mL) Rnase A	0.5µL
(10U/µl) Restriction enzyme	5µL
dH_20	Final Vol. 50µL

The digests were incubated o/n at 37°C

2.7.7.2 The separation of genomic DNA for southern blot analysis

Digested DNA samples were separated on a 0.8% agarose gel that contained 40 µl (10 mg/mL) ethidium bromide. The samples were run for 10 minutes at 100V, then at 20V for 16 hours.

2.7.7.3 Southern blot transfer

Prior to transferring Southern blot gels, the gels were first soaked in denaturing buffer (0.5M NaOH ,1.5M NaCl) for 45 minutes, washed briefly with dH20 and then soaked in a neutralization buffer (0.5M Tris pH 7.4, 1.5M NaCl) for 45 minutes. The gels were briefly washed again with dH20 and then were set up for an

overnight transfer. To transfer the gels each gel was placed face up in a clean transfer apparatus basin. A single hybond N+ (Amersham; UK) membrane cut to fit the exact dimensions of the gel, was pre-wet in dH_20 and then placed on top of the gel. All air bubbles were removed with a clean strippette. One sheet of Whatman filter paper pre-wet in dH_20 was placed on top of the membrane, which was followed by 2 dry sheets of Whatman filer paper. A moderate stack of dry towels was placed on the top layer and a flat book that supported two 500 mL bottles was used on top as a weight. The gel was transferred o/n at RT. After the transfer was complete the membrane was UV cross-linked (30 seconds at $12x10^4 J/cm^2$) to the membrane. The membrane was left in the dark until the probe hybridization.

2.7.7.4 Probe preparation and probe labeling for southern blot analysis

The entire 8kb HPV genome was used as a probe to detect physical forms of the HPV-16 genome. To prepare the probe, the 8kb genome was digested out of the backbone vector and excised from a 0.8% agarose gel. The probe was purified form the gel slice using a Qiamp gel extraction kit (Qiagen; UK). Up to 50 ng of the probe was labeled with 5ul alpha-^{32}P-dCTP using the Ready to Go labeling system (GE ;UK) based on the manufacturer's instructions. Prior to use in hybridization, radioactively labeled probes were cleaned using a G50 Sephadex column (GE; UK) according to the manufacturer's instructions.

2.7.7.5 Pre-hybridization, hybridization and washing of southern blot membranes

Prior to the hybridization of HPV-16 probes, the membrane underwent a pre-hybridization regimen. Membranes were rolled and placed inside tubes and 50mL of pre-hybridization buffer (3X SSC, 0.1 % SDS, 100X Denhardts, 50% Dextran sulphate) was added along with 500 µl of denatured salmon sperm DNA

(Invitrogen; UK). Prior to adding to the pre-hybridization buffer, the salmon sperm DNA was denatured for 5 minutes at 95° C and then was immediately cooled on ice for 5 minutes.) The membrane was incubated for at least one hour at 65° C prior to hybridization. During the pre-hybridization process the probes were labeled and purified as described above. Prior to probe hybridization the purified probes were denatured along with an additional 500 µl of salmon sperm DNA. The denatured DNA was then added directly to the pre-hybridization buffer and the membrane was incubated o/n at 65° C.

2.7.7.6 Exposure of southern blots

All membranes were exposed overnight in a Phosphorimager cassette. Southern blot analysis was conducted using a Storm 860 Phosphorimager scanner.

2.8 Amplification of Papillomavirus Oncogene Transcripts (APOT) analysis

2 x 10^6 sub-confluent HPV-16 cell lines were first harvested for total RNA extraction. Total RNA extraction was carried out using the Qiagen RNAeasy kit (Qiagen; UK) APOT analysis of HPV-16 extracted RNA was carried out using the exact primers and protocol as described in (Klaes, Woerner et al. 1999).

2.9 Protein Analysis

2.9.1 Cell lysis for western blot analysis

Monolayer HPV-16 cell lines were grown in 60cm dishes. Approximately 2x10 ^{6} NIKS or HPV-16 cell lines were harvested and pelleted for lysis. Pellets were washed with 1 X PBS and were then were resuspended in 100 µl lysis buffer (50 mM Tris [pH 7.4], 150 ml NaCl, 1 mM EDTA + 4µl of 1x complete protease inhibitor solution (Roche; UK)), The lysates were held on ice for 30 minutes and then were spun at 14000 rpm for 30 minutes. The soluble supernatant was

removed and stored separately at -70°C until further analysis. The insoluble pellet was then resuspended in 100 µl 3x Laemelli buffer (New England Biolabs; UK) and was spun at 14000 rpm for 15 minutes at room temperature.

2.9.2 Protein quantification

The protein quantification of soluble lysates was carried out using the Bio-Rad RCDC kit (Bio-Rad; UK). Quantification was carried out according to the manufacturers instructions

2.9.3 SDS PAGE

2.9.3.1 Gel electrophoresis for E6 and E7 protein analysis

The separation of E6 and E7 proteins was carried out using 15 % Tris/ Glycine polyacrylamide gels. Table 2.7 contains the gel composition for both the stack and resolving gel. 7.5 mL of the resolving gel mixture was first poured and set at room temperature for 30 minutes. 2 mL of the stack gel was overlaid on top of the resolving gel and was left to polymerize for 30 minutes. 40 µg of soluble lysate was loaded into each well. Each gel was submerged in 500 mL of SDS running buffer (25mM Tris pH 8.3, 200mM glycine, 0.1% SDS) in Bio-Rad gel tanks. The separation of E6 and E7 proteins was carried out at 80 V for 30 minutes and then at 160 V for 1 hour.

Table 2.7 15% Tris / Glycine polyacrylamide gel composition (resolving gel) 10 mL total	
H_2O	3.3 mL
30 % Acrylamide	4.0 mL
1.5 M Tris (pH 8.8)	2.5 mL
10 % SDS	0.1 mL
10 % APS	0.1 mL
TEMED	0.004 mL
(stack gel) 2mL total	
H_2O	1.4 mL
30 % Acrylamide	0.33 mL
1.0 M Tris (pH 6.8)	0.25 mL
10 % SDS	0.02 mL
10 % APS	0.02 mL
TEMED	0.002 mL

2.9.3.1 Gel electrophoresis for cellular proteins

The separation of various cellular proteins was carried out using 8 % or 10% Tris/ Glycine polyacrylamide gels. Proteins greater than 80 kDa were separated on a 8% gel. Table 2.8 contains the gel composition for both the stack and resolving gel. 7.5 mL of the resolving gel mixture was first poured and set at room temperature for 30 minutes. 2 mL of the stack gel was overlaid on top of the resolving gel and was left to polymerize for 30 minutes. 20 µg of soluble lysate was loaded into each well. Each gel was submerged in 500 mL of SDS running buffer in Bio-Rad gel tanks. The separation of cellular proteins was carried out at 80 V for 30 minutes and then at 160 V for 30 minutes to 1 hour depending on the protein size.

Table 2.8 (8% or 10%) Tris / Glycine polyacrylamide gel composition (resolving gel) 10 mL total	
H_2O	**4.6 mL or 4.0 mL**
30 % Acrylamide	**2.7 mL or 3.3 mL**
1.5 M Tris (pH 8.8)	**2.5 mL or 2.5 mL**
10 % SDS	**0.1 mL**
10 % APS	**0.1 mL**
TEMED	**0.006 mL or 0.004 mL**
(stack gel) 2mL total	
H_2O	**1.4 mL**
30 % Acrylamide	**0.33 mL**
1.0 M Tris (pH 6.8)	**0.25 mL**
10 % SDS	**0.02 mL**
10 % APS	**0.02 mL**
TEMED	**0.002 mL**

2.9.3.2 Membrane transfer for Western Blot

15 % polyacrylamide gels were transferred on to 0.22 µm nitrocellulose membranes. All other polyacrylamide gels were transferred on to 0.46 µm

nitrocellulose membranes. Prior to transfer each membrane was submerged in methanol. All gels were transferred in 500 mL of transfer buffer (25 mM Tris-HCL pH8.3, 200mM glycine, 20 % methanol (v/v)) in Bio-Rad gel tanks. All transfers were conducted overnight at 50V at 4 °C.

2.9.3.4 Blocking and Primary antibody incubation for Western blot

Following membrane transfer, each membrane was incubated in 5 % milk/PBS Tween-0.01 % (w/v) for 1-2 hours at room temperature or for 4-8 hours at 4 °C. Each membrane was then incubated with a specific primary antibody. Primary antibodies were diluted in 5% milk/PBS Tween-0.01 % (w/v). Table 2.9 contains all primary antibodies used for protein analysis and their respective dilutions. All membranes were incubated overnight with the respective primary antibodies at 4 °C. Each membrane was then washed using the wash regimen stated in 2.9.3.5. Following one round of washing a mouse secondary antibody was incubated with the membrane at 1:4000 (diluted in 5% milk/PBS Tween-0.01%). The identical wash regime described below was used following this incubation.

Table 2. Primary Antibodies for Western Blot

Antibody	Clone	Dilution	Supplier
E7*	**ED17 and 8C9**	**1:300 / 1:300**	**Santa Cruz/ Invitrogen (Zymed)**
E6	**2E-3F8**	**1:1000**	**Euromedex**
GAPDH	**MAB374**	**1:4000**	**Chemicon**
Rb	**G3-245**	**1:1000**	**Pharmingen**
P53	**D0-1**	**1:1000**	**Santa Cruz**
P16	**G175-405**	**1:1000**	**Pharmingen**

* Two E7 antibodies were used together as a cocktail

2.9.3.5 Membrane washing for Western blot

Following the incubation with primary antibodies all membranes were washed in PBS/Tween 0.01 % at room temperature. Membranes for E6 and E7 analysis were washed 3 x short, 1 x 15 min. and 3 x 5 min. All other membranes were washed 3 x short and 3 x 5 min.

2.9.3.6 Western blotting detection

To detect E6 and E7 proteins the ECL plus kit (GE Healthcare; UK) was used according to the manufacturers instruction. All other proteins were detected using the standard ECL kit (GE Healthcare; UK) according to the manufacturers instructions

2.10 Beta-catenin activity assay

HPV-16 cell lines and HPV negative NIKS, were transfected with the TopFlash *Photinus* plasmid, which contained the TCF/LEF Beta-catenin binding site. A *Renilla* luciferase plasmid (pRL) was co-transfected with the TopFlash plasmid as a transfection control. Prior to transfection, $4x10^5$ cells of each cell line were seeded on a bed of $1x10^5$ ∂-irradiated feeders. All HPV-16 cell lines were seeded in duplicate in six-well plates. Each cell line was transfected with 0.4µg TopFlash and .04µg of pRL. All transfections were carried out using the appropriate volume of Effectene and media as indicated by Qiagen for the above DNA quantity and plate size. 72-hours post-transfection the feeder cells were first discarded and HPV-16 cell lines were lysed to assay the *Photinus* and *Renialla* activity. The Promega Dual Reporter Luciferase Kit (Promega; UK) was used to lyse the cells and assay the activities of *Photinus* and *Renilla*. The cells were lysed in 100 µl of the supplied lysis buffer at room temperature for 30 minutes. The *Photinus* and

Renilla activities were measured using the supplied regents and standard protocol, according to the manufacturers instructions. *Photinus* and *Renilla* measurements were carried out using a luminometer.

3.0 The NIKS organotypic raft culture model of wild-type-HPV-16 productive infection

3.1 Introduction

The regulation of the HPV life cycle has been broadly studied through the immunohistochemical analysis of various types of HPV-infected tissues. These tissues types can be distinguished as either cutaneous or mucosal epithelium. HPV-induced cutaneous and mucosal lesions have been isolated from common sites on the body that HPV can infect such as the hand (cutaneous) and the cervix (mucosal). Collectively, these studies have shown that a highly conserved order of HPV gene expression exists in both tissue types (Peh, Middleton et al. 2002; Middleton, Peh et al. 2003).

Although these lesions have been valuable for the analysis of viral life cycle regulation, biopsy material can often be hard to obtain. In addition, lesion size may limit the type of analysis. Due to these limitations many questions regarding the virus life cycle remain unanswered.

More recently it has been shown that organotypic raft cultures can support a complete HPV life cycle (Lambert, Ozbun et al. 2005; Wilson and Laimins 2005). In this system foreskin/cutaneous keratinocytes that carry the 8kb viral episome of high-risk HPV types (e.g. HPV-16, HPV-18 and HPV-31), are differentiated to produce stratified epithelial layers. Although this is still considered a quasi *in-vivo* model with regards to the absence of a functional immune system, the raft culture system is superior to current transgenic mouse models, which are only based on the expression of one or two HPV genes (Brake and Lambert 2005). In contrast to

these models the organotypic raft culture system is able to support a productive viral life cycle, which is regulated from all eight HPV genes.

The analysis of this system can be broken down into two parts. The monolayer HPV episomal cell lines of high-risk HPV types mimic the proliferating basal compartment where the early stages of the virus life cycle begin. Early life cycle events such as viral DNA replication and early oncogene expression can be observed in these cells prior to their differentiation. To evaluate HPV gene regulation in the differentiated epithelium, monolayer cells are then differentiated to produce organotypic raft cultures. Immunohistochemical analysis of early and late gene expression can then be carried out on paraffin embedded HPV raft culture sections.

In order to dissect the early and late parts of the HPV-16 life cycle this thesis begins with the establishment of a NIKS (cutaneous) raft culture model of a productive HPV-16 infection. The NIKS HPV-16 raft system has been widely used to study the functions of specific viral genes in the HPV life cycle. However, the viral gene expression patterns in this NIKS (cutaneous) HPV-16 raft model have not been extensively compared to viral gene expression patterns in cervical (mucosal) biopsy material. Therefore, in order to use this model to answer questions about HPV life cycle in both cutaneous and cervical (mucosal) tissues it was first necessary to show that the order and timing of HPV-16 gene expression within the NIKS epithelium was similar to that of cervical epithelium.

3.2 Results

3.2.1 The use of NIKS as a host keratinocyte cell line

First we aimed to establish NIKS clonal cell lines that maintain episomal forms of the HPV-16 and HPV-31 genomes. We chose specifically the high-risk types HPV-16 and HPV-31 with an interest in evaluating the biology of HPV types that have oncogenic potential. In addition HPV-16 and HPV-31 are genetically similar but interestingly have very different oncogenic potentials. HPV-16 alone has been shown to cause over 50% of total cervical cancers. This thesis will first present data on the generation of HPV-31 lines, however HPV-16 lines, which were generated in the same way were used in the remainder of the thesis.

The second aim of this chapter was to establish an organotypic raft culture model of a productive HPV-16 infection through the propagation of early passage NIKS HPV-16 episomal cell lines. By using immunohistochemical techniques we aimed to show that early and late HPV-16 gene expression patterns in our NIKS/cutaneous raft model system were similar to those of HPV-16 induced cervical/mucosal lesions.

We chose Normal Immortalized Human Keratinocytes (NIKS) as a host cell line for our model system due to their known ability to successfully maintain HPV viral episomes. It is also known that NIKS raft culture systems can successfully support the life cycle of several HPV types. NIKS, which are an immortalized cell line, were preferred over the use of primary foreskin keratinocytes, as they were expanded from a single colony (Allen-Hoffmann, Schlosser et al. 2000). By contrast, primary cell lines typically contain a mixture of stem cells and transit amplifying cells and

therefore HPV cell lines could only be established from a heterogeneous population of cells.

Importantly, it was previously shown that NIKS are genetically stable and represent a uniform genetic background. This was crucial for our experiments, as we wanted to avoid genetic variation within our HPV cell lines. Only one abnormality was detected following the karyotyping of NIKS (Allen-Hoffmann, Schlosser et al. 2000). The respective authors found that over time all of the NIKS had acquired an additional copy of chromosome 8. This abnormality however has not affected their ability to produce a fully differentiated epithelium. The NIKS arose as spontaneously immortalized cell line, after 59 passages of their parental neonatal foreskin cell line, BC-1-EP. Despite the fact that foreskin keratinocytes are a natural host cell for HPV viruses, the authors confirmed there were no detectable levels of HPV DNA. In order to confirm that the NIKS maintained normal growth characteristics, they also measured the mRNA levels of autocrine growth factors and markers such as Transforming growth factor (TGF), TGF-ß1 (a keratinocyte growth inhibitor), Epidermal growth factor (EGF), the oncogene c-myc and keratin K14. There were no differences in the expression levels of these growth factors and markers when compared to the parental cell line. NIKS have also been shown to be non-tumorigenic when injected into mice, which suggests that they are not a transformed line.

3.2.2 The generation of NIKS wild-type HPV-16 and 31 episomal cell lines

In order to support a productive virus life cycle using the organotypic raft culture system, the NIKS would have to stably maintain an episomal form of the viral genome and avoid integration into the host chromosome. This has been previously achieved with several high-risk HPV types by the co-transfection of circular HPV genomes and a plasmid carrying a drug resistance gene as selection marker (Nakahara, Peh et al. 2005). To create the circular genomes for transfection, we excised full-length 8kb genomes from a plasmid. Then we religated the ends of the full-length genome to create a double-stranded circular form of the genome. These circular forms are then co-transfected into the keratinocytes together with a plasmid carrying a selection marker. Ideally, this plasmid integrates into a host chromosome whereas the circular genome is maintained in the nucleus but fails to integrate into a host chromosome.

To create HPV-31 cell lines for our system, we co-transfected NIKS cells with circularized wt-HPV-31 and a blasticidin resistance plasmid. The HPV-31 plasmid used for transfection carried a replication competent HPV-31 genome, which was previously cloned from the isolated cervical cell line, CIN 612 (Bedell, Hudson et al. 1991). The transfected cells underwent a positive selection with blasticidin for four days. Following drug selection, the colonies grew for an additional five to seven days. We then picked individual colonies and expanded them as individual cell lines. First we tested these cell lines for the presence of the HPV-31 genome. To do this we amplified a 1.1 kb fragment, contained within the E4 ORF, via conventional PCR methods. Figure 3.1A shows the analysis of a subset of HPV-31 positive clones. Out of the 24 clones tested, 18 clones were positive for the E4 ORF, which accounted for 75 % of the selected clones. This level of efficiency was

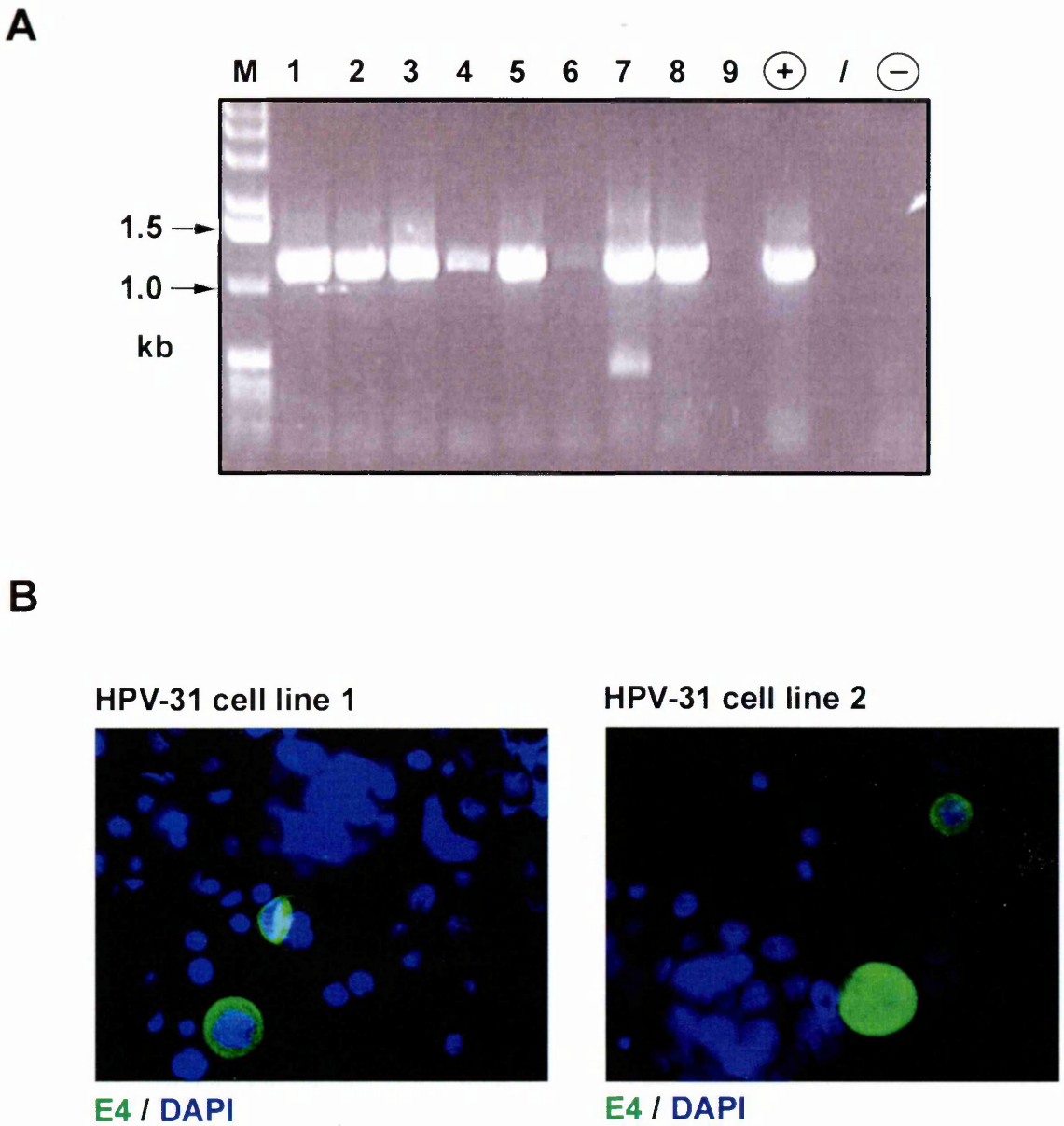

Figure 3.1. Generation of HPV-31 episomal cell lines

Conventional PCR methods were used on total DNA extracts to detect the presence of the HPV-31 genome in HPV-31 positive clonal NIKS cell lines. Primers specific for the E4 ORF amplified a 1.1kb fragment in HPV-31 positive clonal cell lines. (A) The agarose gel shows the presence or absence of the band representing the 1,1 kb PCR product (lanes 1-9). As size standard a 1 kb DNA marker (M) was used. A known positive HPV-31 cell line was used as a positive control (+) and HPV negative NIKS were used as a negative control (-).

(B) Two HPV-31 positive cell lines were differentiated in methylcellulose for 48 hours. To detect late viral protein expression the differentiated HPV-31 cell lines were stained with an E4 antibody (green, #248). DAPI was applied to the cells as a nuclear counterstain (blue).

expected as the genomes of high-risk types are typically very easily maintained in keratinocyte cell lines like the NIKS cells we have used. Next, in order to determine if these clones could express viral proteins from the differentiation-dependent viral promoter, we differentiated two of the HPV-31 cell lines in methylcellulose for 48 hours. Methylcellulose can be specifically used as a semi-solid media for single cell suspensions (Wilson and Laimins 2005). In this environment cell to cell contact is prevented which allows keratinocytes to default into their terminal differentiation program. This experiment was primarily carried out to pre-screen HPV-31 cell lines for their ability to produce late life cycle proteins such as the E4 protein. The HPV-31 cell lines that had this ability could then be used in lengthy raft culture experiments. Our analysis shows that roughly 5-10 % of cells from each line had the ability to express E4 (Figure 3.1B). The 5-10% range of E4 positive cells was somewhat lower than expected, however typical percentages of E4 positive cells using this method of differentiation, do not usually exceed 10-20%. Nevertheless, this percentage was sufficient to proceed with raft culture experiments.

However, for the remainder of our life cycle studies we used NIKS HPV-16 episomal cell lines, which had a similar percentage of E4 positive cells to the HPV-31 cell lines (data not shown). We have chosen HPV-16 cell lines for the remainder of the life cycle studies, as HPV-16 is more highly prevalent in HPV-induced cervical lesions. Two collaborators (Kenneth Raj, National Institute for Medical Research, London, UK; Qian Wang, National Institute for Medical Research, London, UK) established these HPV-16 episomal cells lines by using similar methods to the ones used for HPV-31. A plasmid that contained the replication competent W12 HPV1-16 genome was co-transfected into NIKS with a

plasmid carrying a drug resistance gene to establish the HPV-16 cell lines. After drug selection we have chosen ten individual HPV-16 cell lines to carry out subsequent studies.

3.2.3 The terminal differentiation program is complete in HPV negative NIKS organotypic raft cultures

HPV-16 is highly prevalent in high-grade cervical lesions and we therefore wanted to show that our cutaneous system could also model a productive HPV infection in cervical/mucosal epithelium. Because the activation of the viral late promoter is linked to the terminal differentiation program it was important to show that our cutaneous NIKS model could follow a differentiation program that was similar to the one of cervical/mucosal epithelium. Although some architectural differences exist in cutaneous and mucosal epithelium, the overall process of terminal differentiation is a highly conserved process between these tissue types. We first wanted to show this in HPV-negative NIKS, which would represent a normal cutaneous epithelium

In order to create the NIKS epithelium we differentiated HPV negative NIKS on dermal equivalents for 14 days. To detect the process of terminal differentiation in NIKS/cutaneous raft sections we used antibodies targeted against proteins in early differentiation, Keratin K10, and late differentiation, filaggrin, respectively. We also used an MCM-7 antibody that identified S-phase competent cells, which are typically present in the mitotically active basal layer. This layer immediately precedes the layers of early terminal differentiation. A fellow lab member, Kate Middleton, previously carried out the Immunohistochemistry of cervical(mucosal) sections with stains against MCM-7, filaggrin and Keratin K13, which is the

mucosal equivalent of the cutaneous keratin, K10. These sections were used for a direct comparison with our NIKS HPV-16 raft model.

In cutaneous NIKS raft cultures and cervical(mucosal) tissue, MCM-7 positive cells were sporadically detected within the first layer, which marked the "basal-like" layer (Figure 3.2A). However, cervical epithelium also contained MCM-7 positive transit amplifying cells above the basal layer. In both cutaneous and mucosal epithelial tissues stem cells give rise to daughter cells, which are transit-amplifying cells. These cells of the basal compartment go through subsequent rounds of proliferation and then commit to terminal differentiation in the layers above.
These observations demonstrated that HPV negative NIKS could maintain a proliferative compartment, but were unable to maintain the proliferation levels of a transit-amplifying layer.

In order to identify the start of terminal differentiation within the NIKS epithelium, we used keratin K10, which is the first keratin to be expressed at the start of terminal differentiation. In normal cutaneous tissue K10 is first detected in cells immediately above the basal layer (i.e. spinous layer). Although K10 is actively expressed only in the spinous layer, it can still be detected in its cross-linked forms throughout the granular and cornified layers. The same pattern is typically seen for keratin K13 in HPV-negative cervical (mucosal) epithelium.

In HPV-negative NIKS (cutaneus) raft sections and cervical (mucosal) epithelium both keratins K10 and K13 could be detected immediately above the basal layer and throughout the entire epithelium (Figure 3.2B). However, NIKS epithelium contained some K10 positive cells already within the basal compartment. This

suggested an early onset of terminal differentiation, which was in line with the reduced level of proliferation in NIKS epithelium.

In order to identify the start of late differentiation filaggrin was used as a marker. As explained earlier pro-filaggrin is detected in keratohyalin granules, which constitutes the granular layer. Filaggrin, which represents the processed form of pro-filaggrin, can also be detected as a more filamentous pattern in normal cutaneous tissues. The role of filaggrin is to cross-link keratins to form the cornified layers, which are located immediately above the granular layer. Filaggrin is also more highly abundant in cutaneous versus mucosal tissues. This is due to the extensive cornification process in cutaneous tissue, which does not occur in mucosal tissue. Although extensive cornification is absent in mucosal tissues, keratins are still cross-linked to create the superficial layer in mucosal epithelium. After we stained cutaneous NIKS raft culture sections, a dense layer of pro-filaggrin and filaggrin could be detected in the upper layers (Figure 3.2C). By comparison only a small amount of pro-filaggrin/filaggrin could be seen in the cervical(mucosal) epithelium. In both NIKS(cutaneous) epithelium and cervical(mucosal) epithelium we also noticed a temporal gap between the onset of the respective keratin K10/K13 and filaggrin. These observations suggested that a normal step-wise process of terminal differentiation was occurring in our NIKS raft system. Although the onset of the terminal differentiation process as indicated by K10 was premature in some cells of our NIKS raft epithelium, we concluded that the virus would still encounter the same ordered process of differentiation like in the cervical(mucosal) epithelium and that the NIKS rafts would be a suitable environment for the full HPV life cycle.

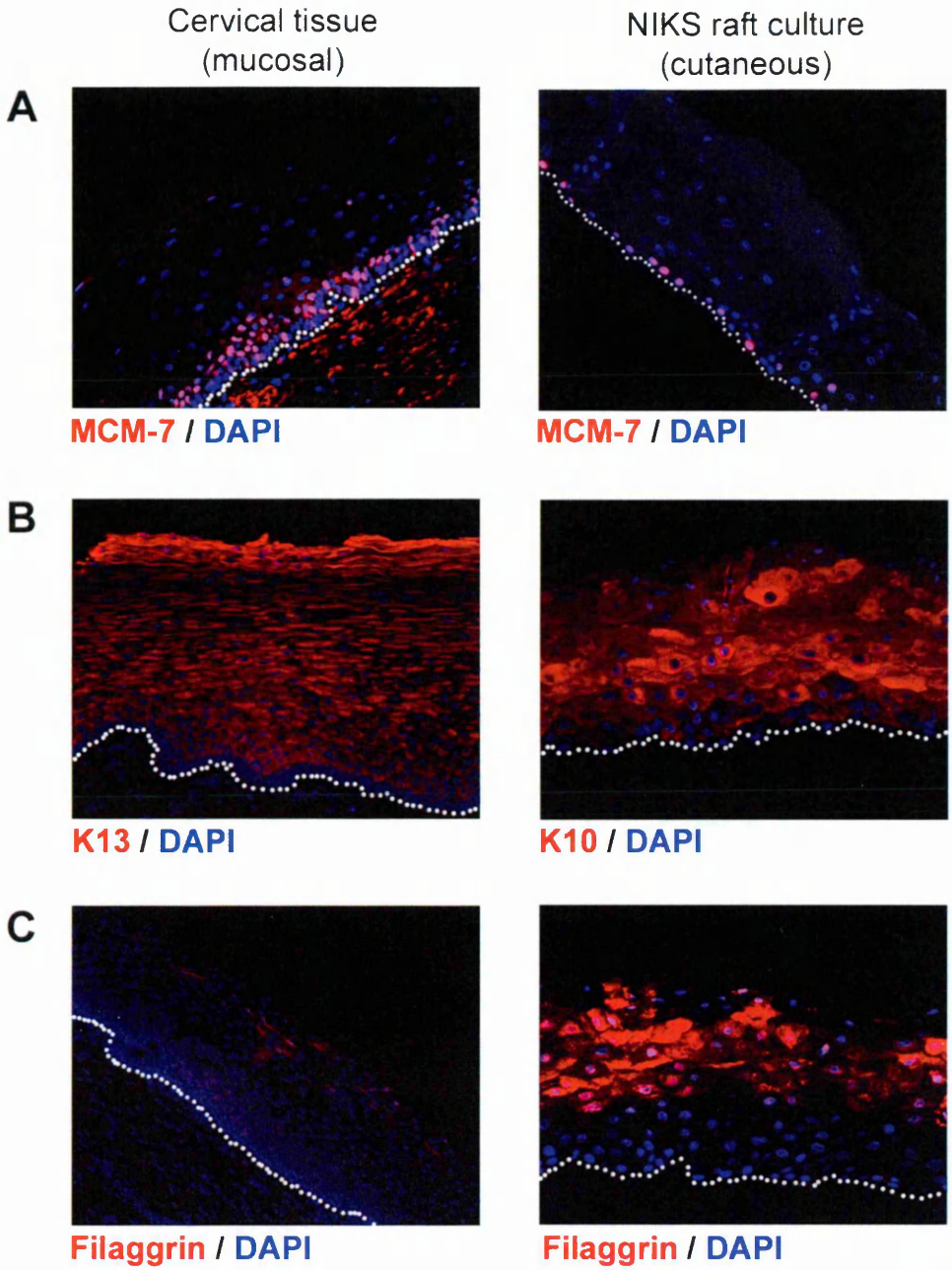

Figure 3.2. Proliferation and terminal differentiation in HPV-negative epithelium

HPV-negative NIKS were differentiated for 14 days to produce organotypic raft cultures. (A) To detect the proliferative compartment of HPV-negative tissues, NIKS raft sections were stained with an antibody against the S-phase marker MCM-7. HPV-negative cervical tissue previously stained with an MCM-7 antibody was used for direct comparison. (B) To detect the start of early differentiation, NIKS raft sections were stained with an antibody against (cutaneous) keratin K10. HPV-negative cervical tissue previously stained with an antibody against (mucosal) keratin K13 was used for direct comparison. (C) To detect the start of late terminal differentiation, NIKS raft cultures were stained with filaggrin antibody. HPV-negative cervical tissue previously stained with filaggrin antibody was used for direct comparison. All sections were counterstained with DAPI (blue) and were photographed at x20 magnification. The broken line on NIKS raft cultures and in cervical tissues indicates the basal layer. The Immunohistochemistry of cervical (mucosal) sections was previously carried out by Kate Middleton (NIMR, London, UK) and used with permission.

3.2.4 NIKS HPV-16 cell lines contain viral episomes and can produce L1 viral capsid upon differentiation

In order to validate our HPV-16 life cycle model we wanted to first establish that all ten HPV-16 cell lines contained characteristics necessary for a productive life cycle. First the cell lines had to maintain the HPV genome in a predominantly episomal and not an integrated state. The episomal form is the productive form of the viral genome. By comparison integration typically leads to the disruption of several viral genes such as the replication gene, E2 (Baker, Phelps et al. 1987). Therefore, integration typically renders the life cycle incomplete. The second criterion was that the differentiated HPV-16 cell lines had to express the late viral gene L1, which encodes the L1 protein, which forms viral capsids. This would demonstrate that we were analyzing the viral gene expression patterns of a complete HPV life cycle.

We first tested for the presence of episomal forms of the viral genome in our HPV-16 cell lines by Southern blot analysis. Only low passage cell lines (passage four to six) were used for rafting and this analysis, as integration events are more likely to occur after long-term culturing (Alazawi, Pett et al. 2002). In order to create a probe, which hybridizes with HPV-16 genomic DNA, a linearized 8 kb viral genome fragment was radioactively labeled with ^{32}P. Then total DNA was first extracted from sub-confluent cultures of each cell line and digested separately with either Bam *H*I or *Hind* III. *Bam H* I, which cuts at the ends of the 8kb genome led to a 8kb linear form of the virus (Figure 3.3). This demonstrated that a full intact undisrupted HPV genome was maintained in all cell lines.

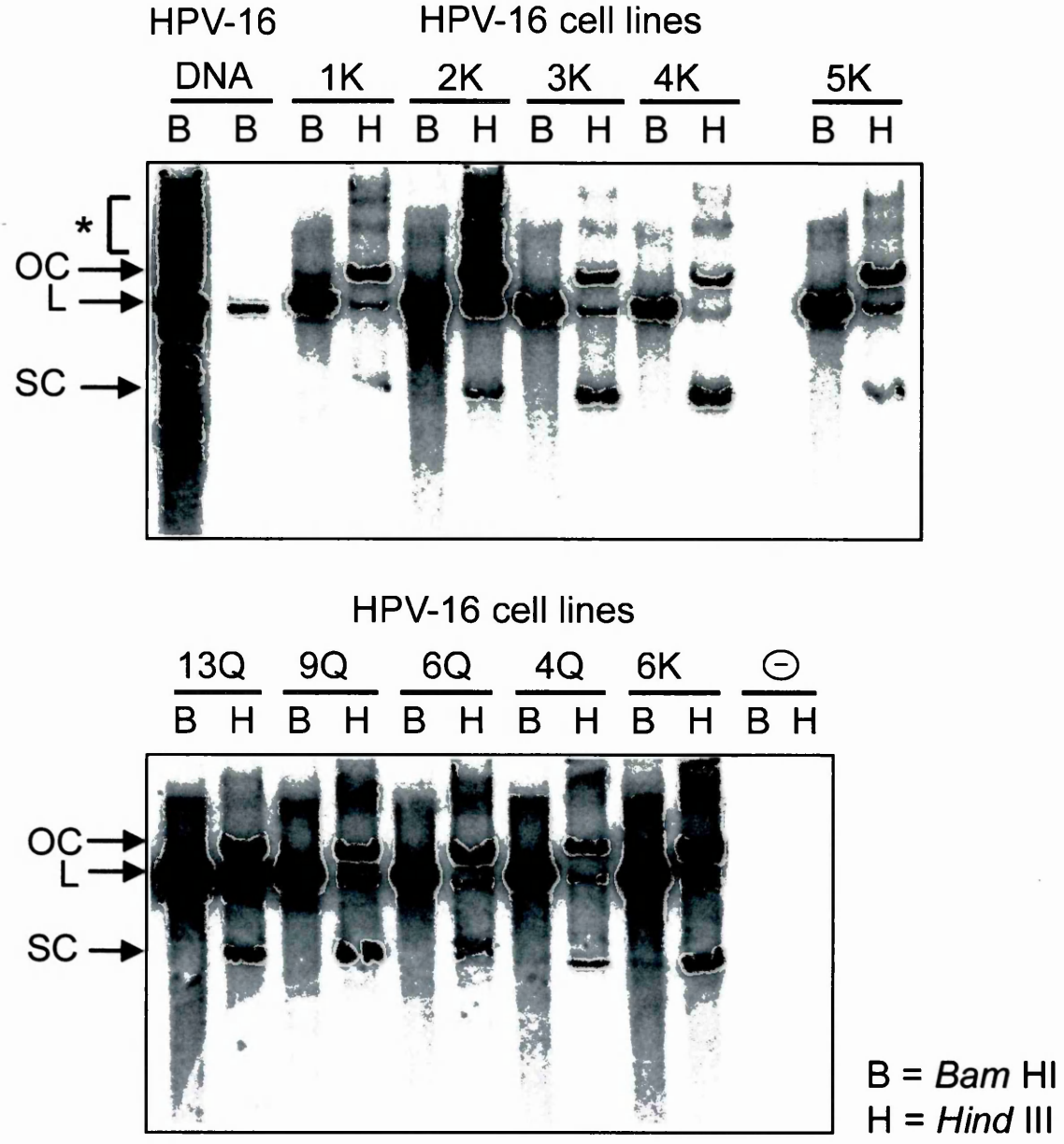

Figure 3.3 Detection of HPV-16 episomes in monolayer cell lines

To test HPV-16 cell lines for their ability to maintain episomal forms of the viral genome, total DNA was extracted from HPV-negative NIKS and HPV-16-positive monolayer cell lines. Southern blot analysis of total DNA extracts digested with *Bam* HI or *Hind* III confirmed the presence of circular and linear forms following hybridization with a ^{32}P radioactively-labelled full-length HPV-16 genome probe. *Hind* III, which does not cut within the genome, resulted in mostly supercoiled (SC) and some open circular (OC) and 8kb linear (L) forms. *Bam* HI, which cuts in the flanking region of the viral genome, resulted in a single 8kb linear band (L). To identify the 8kb linear genome, two dilutions of *Bam* HI-linearized 8kb HPV-16 genomic DNA (HPV-16 DNA) were run alongside the DNA from the cell lines. HPV-negative NIKS were used as negative control (-). The asterix indicates bands, which run uncharacteristically in both the HPV-16 genomic DNA and total DNA from the HPV-16 cell lines

Treatment with the second restriction enzyme, *Hind* III, which does not cut within the HPV-16 genome, retained several circular forms of the virus including the super coiled and open circular forms.

The supercoiled bands, which migrate faster than linear and open circular bands represent the unaltered form of the viral episome. Open circular bands are common as supercoiled structures can become relaxed during spontaneous DNA single-strand breakage. In addition a small amount of linear 8kb genome could be detected probably due to DNA double-strand breakage because of sheering. In addition following *Hind* III digestion, several minor bands were evident at the top of the gel, possibly representing integration events. However, digestion with *Bam H* I completely converts these high molecular bands to exclusively full-length undisrupted viral genome fragments. In contrast, integration events typically only appear as a series of multiple sized bands after *Bam H* I digestion as both the viral and cellular genome contain *Bam H* I. It is possible that the high molecular weight bands represented concatamerised circles of the virus. We therefore conclude that our HPV-16 cell lines predominantly carry episomal forms of the genome. We have conducted additional experiments, which will be presented in a later chapter, to show that viral genes are indeed expressed from episomal forms of the genome.

We next wanted to test if our NIKS HPV-16 cell lines could produce L1 capsid protein. To do so HPV-16 cell lines of identical early passage range were differentiated for 14 days to produce raft cultures. Raft sections of these HPV-16 episomal cell lines were then stained with antibodies against the L1 capsid protein.

We found L1 capsid within the cornified layers of seven out of ten cell lines (Figure 3.4). The remaining three raft cultures that did not produce L1 capsid will be presented in Chapter 4. For our subsequent studies of the viral life cycle we chose to use the seven cell lines that contain predominantly episomal forms of the genome and that show the ability to produce L1 capsid protein.

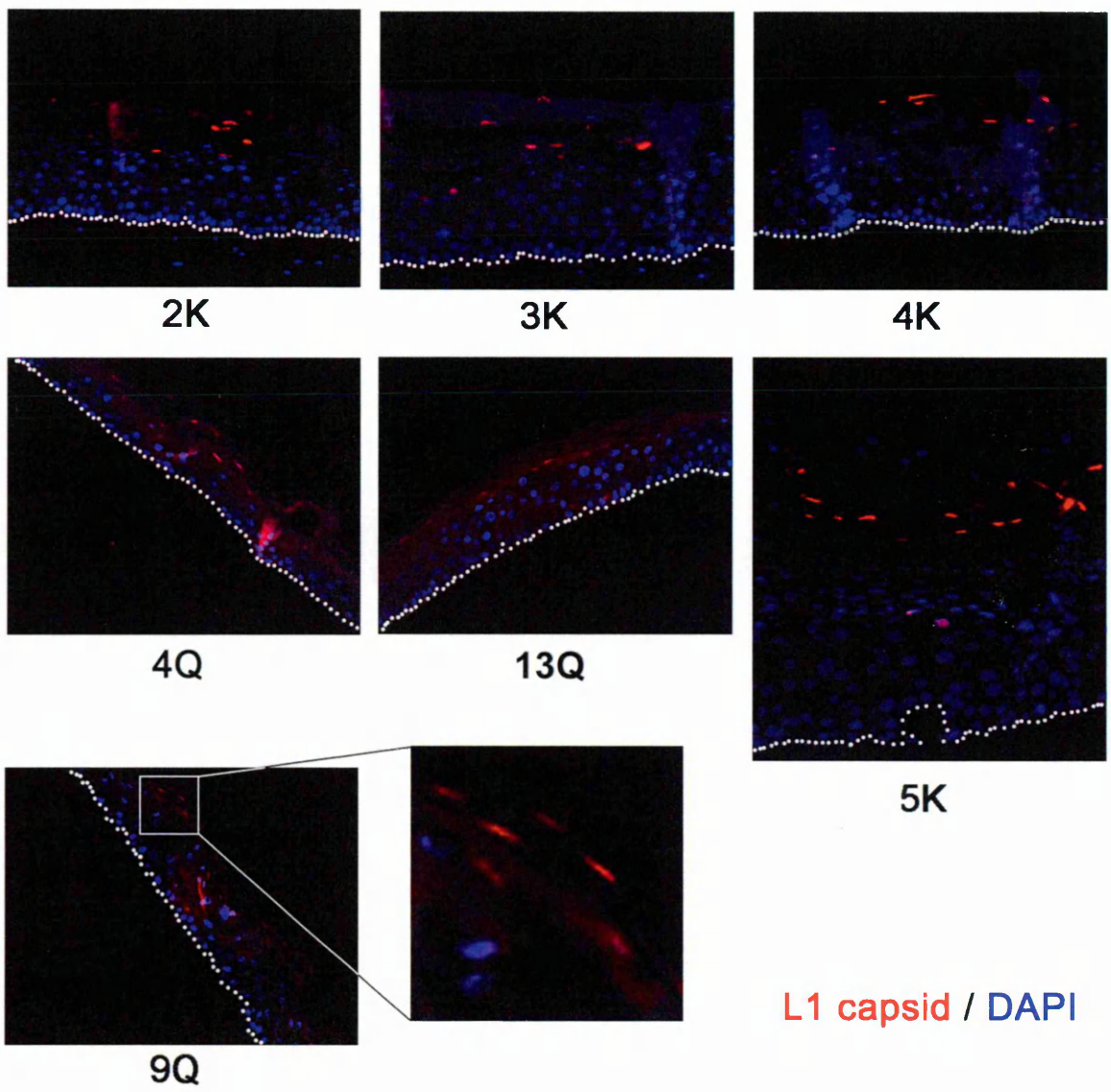

Figure 3.4 L1 capsid expression in HPV-16-positive raft cultures

To assess viral productivity HPV-16-positive monolayer cell lines were differentiated for 14 days to create organotypic raft cultures. Antibodies against L1 capsid protein (red) were applied to formalin fixed raft culture sections. DAPI was used as a nuclear counterstain (blue). The broken line on each raft culture indicates the basal layer. For clone 9Q a magnified section with L1-capsid positive cells is shown to the right.

3.2.5 MCM-7 is a surrogate marker for E7 and S-phase induction in HPV-16 raft cultures

After HPV infects cells in the basal compartment the HPV-16 E6 and E7 oncogenes are expressed from the early p97 promoter (Smotkin and Wettstein 1986). It is widely established that E7 maintains S-phase competent cells above the basal layer, via the E2F pathway, in order to maintain host replication machinery needed for viral DNA replication (Flores, Allen-Hoffmann et al. 2000). It is currently very difficult to detect E7 expression in the epithelium due to a lack of good antibodies. MCM-7, which is highly expressed during S-phase, has been established as a surrogate marker for E7 expression in the suprabasal cells (Freeman, Morris et al. 1999; Middleton, Peh et al. 2003). We therefore wanted to confirm that MCM-7 was indeed a surrogate marker of E7 in the NIKS raft system. To do this NIKS that expressed E6, E7 or E6/E7 from an integrated pLXSN retroviral plasmid were differentiated over 14 days to produce raft cultures. Western blot analysis of monolayer soluble extracts confirmed that each cell line expressed the transfected oncogenes (Figure 3.5a). After confirming this, an MCM-7 antibody was applied to each raft culture section. MCM-7 cells could be detected in every layer of E6/E7 and E7 raft cultures (Figure 3.5b). By comparison MCM-7 positive cells were only contained in the basal layer of E6 only raft cultures. This was identical to the MCM-7 pattern in HPV-negative NIKS raft cultures. This confirmed that the E7 oncogene alone is sufficient for the S-phase induction above the basal layer and we also demonstrated that MCM-7 could be used as an E7 surrogate marker in our NIKS raft system.

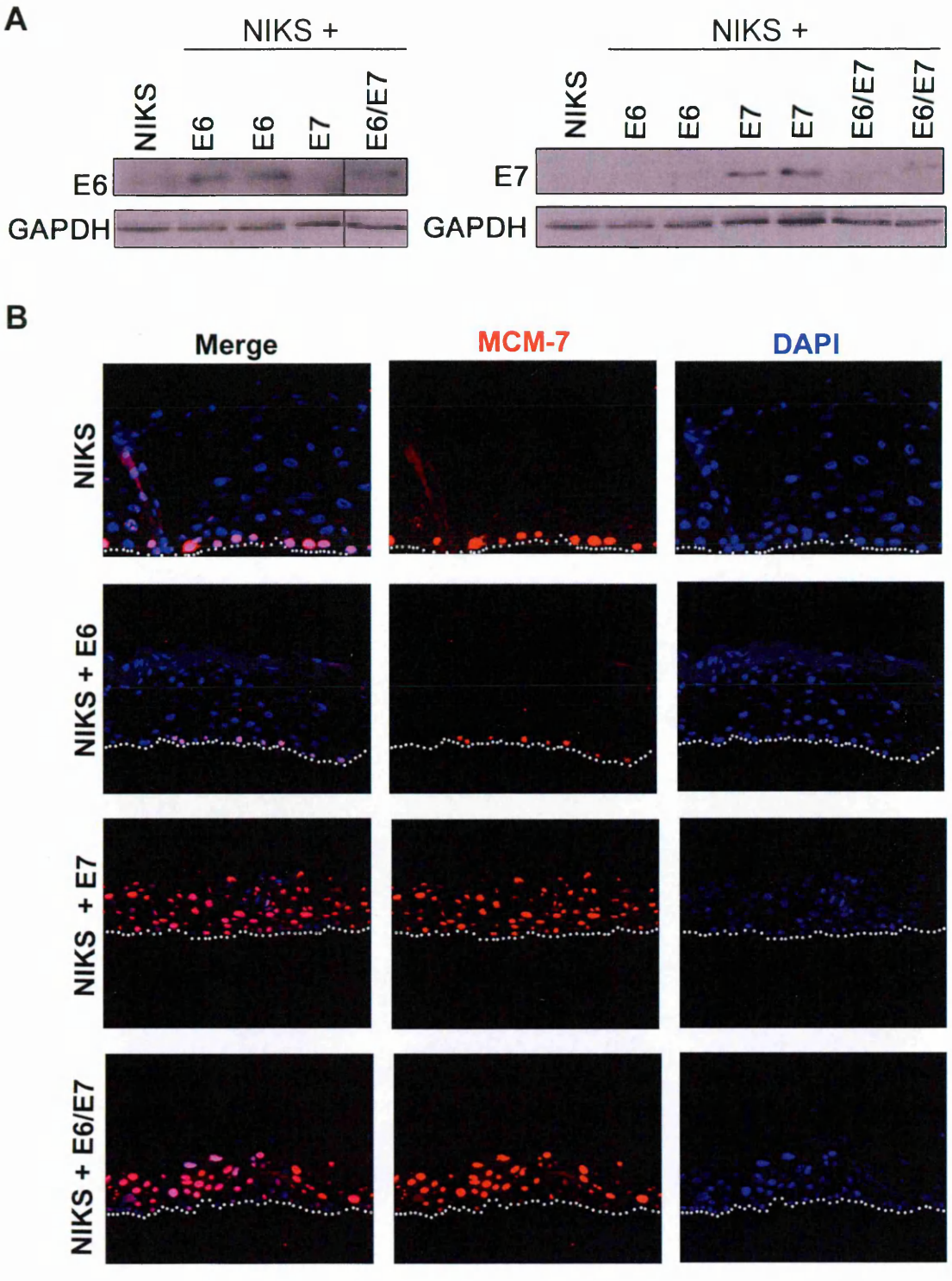

Figure 3.5 MCM-7 as surrogate marker for E7 expression in NIKS organotypic raft cultures
(A) Western blot analysis of soluble protein extracts from untreated NIKS monolayer cells or NIKS previously transduced with a retroviral plasmid expressing either E6, E7 or E6/E7. Antibodies specific for E6 or E7 show the expression of these oncogenes in the respective cells. (B) Untreated NIKS cells and NIKS cells expressing E6, E7 or E6/E7 were differentiated for 14 days to produce raft cultures. An antibody against MCM-7 was applied to formalin fixed raft sections to detect the layers of S-phase competent cells. All sections were counterstained with DAPI (blue) and were photographed at x20 magnification. The broken line on each raft culture indicates the basal layer.

3.2.6 S-phase is prolonged in wt-HPV-16 raft cultures

We next wanted to evaluate the extent of the S-phase compartment in raft culture sections of HPV-16 episomal cell lines. In these lines E7 should be expressed from the early p97 promoter of an intact 8 kb genome. To show that our HPV-16 episomal cell lines could express E7, we analyzed soluble lysates of sub-confluent monolayer cultures of each cell line, by Western blots. We detected E7 expression in all seven clones. The Western blot in Figure 3.6a shows E7 expression from three of these cell lines (2K, 4K and 9Q). Western blots that show E7 expression from additional cell lines will be presented in Chapter 5.

Endogenous E7 expression levels are typically hard to detect by Western blot therefore a high concentration of protein was loaded on each gel, as indicated by the high levels of the GAPDH loading control. Due to overloading, at this point, we were unable to make claims about differences in E7 protein levels between each cell line.

To evaluate E7 oncogene expression within our model system, we applied a MCM-7 antibody to adjacent sections of all seven HPV-16 raft cultures. We compared this staining pattern to several high-risk HPV induced cervical lesions that were previously stained with MCM-7. Figure 3.6b shows two of these HPV-16 raft culture sections alongside an HPV-16 induced cervical lesion. In both the HPV-16 raft epithelium and the high-risk HPV-16 induced cervical lesion we could detect MCM-7 expression in three to four layers of cells above the basal compartment. This MCM-7 pattern confirmed that E7 could prolong S-phase in our model system. It was also evident in both raft culture sections and the cervical

lesion that MCM-7 could not be detected within the last 3-4 layers of the epithelium. This was indicative of early promoter regulation in the raft epithelium. In productive infections it is thought that the early promoter is switched off in order to allow for late gene expression to occur (Middleton, Peh et al. 2003). Activation of the differentiation dependent late promoter is necessary to carry out the productive phase of the virus life cycle.

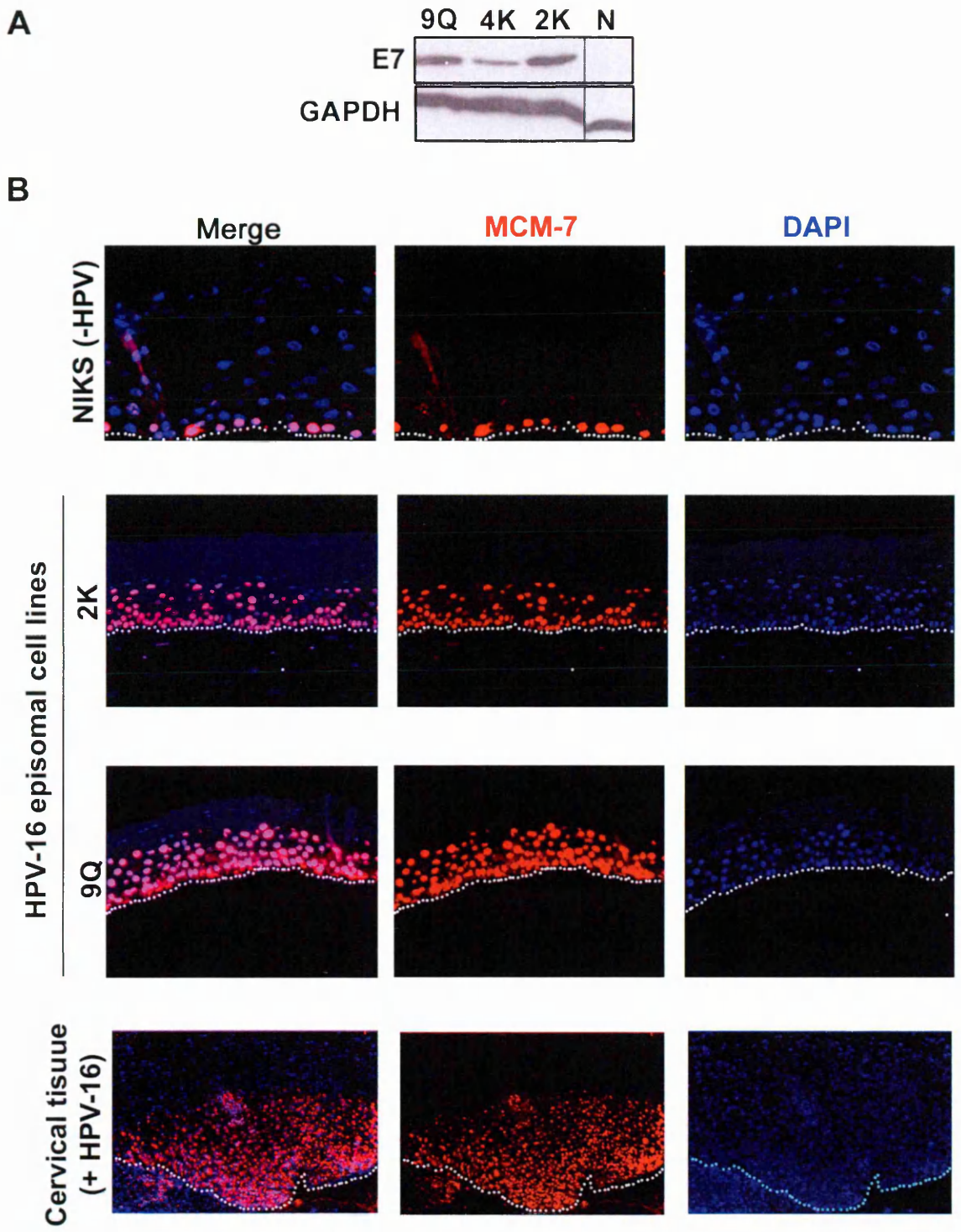

Figure 3.6 Expression of E7 and MCM-7 protein in HPV-16 raft cultures

(A) Western blot analysis of soluble protein extracts from three HPV-16 episomal cell lines and HPV-negative NIKS. Antibodies specific for the E7 protein show that E7 is expressed in all three HPV-16 cell lines. (B) HPV-negative NIKS and early passage (four to six) HPV-16 episomal cell lines were differentiated for 14 days to produce raft cultures. MCM-7 antibodies were applied to formalin fixed raft culture sections to assess the extent of S-phase competent cells. A section of HPV16-positive cervical tissue previously stained with MCM-7 was used for comparison (the cervical lesion was previously stained by Heather Griffin (NIMR, London, UK) and was used with permission). The broken line on each raft culture indicates the basal layer

3.2.7 A brief overlap of early and late viral gene expression occurs in wt-HPV-16 raft cultures

In this HPV-16 raft culture model we could only detect MCM-7 expression in three-four layers of cells above the basal compartment. The last layer of the S-phase compartment is thought to mark the end of early promoter expression. In a productive HPV-16 life cycle the last layer of the S-phase compartment also typically coincides with the first detectable levels of E4 (Peh, Middleton et al. 2002; Middleton, Peh et al. 2003). At this point in the virus life cycle it is thought that high levels of E4 expression are the result of the activation of the differentiation dependent late promoter. E4 has been previously identified as a major late transcript product (Milligan, Veerapraditsin et al. 2007). The first set of E4 positive cells are usually found in cells that still express MCM-7. It is thought that viral amplification begins in these specific cells where E4 is expressed and host replication machinery is still available.

To determine if a switch from early to late gene expression occurred in our system, we applied MCM-7 and E4 antibodies to all seven HPV-16 raft culture sections. Figure 3.7 contain three raft culture sections from our model and one typical high-risk HPV induced cervical lesion that had been previously stained with MCM-7 and E4. In both raft cultures and cervical epithelium we detected E4 protein in MCM-7 positive cells or just above an MCM-7 positive cell. MCM-7 was not detected in cells above the first E4 positive layer. The majority of the cells in this transient layer also contained both E4 and MCM-7, which likely marks the site of viral DNA amplification. We could therefore conclude that early and late promoter regulation was conserved in our HPV-16 raft culture model.

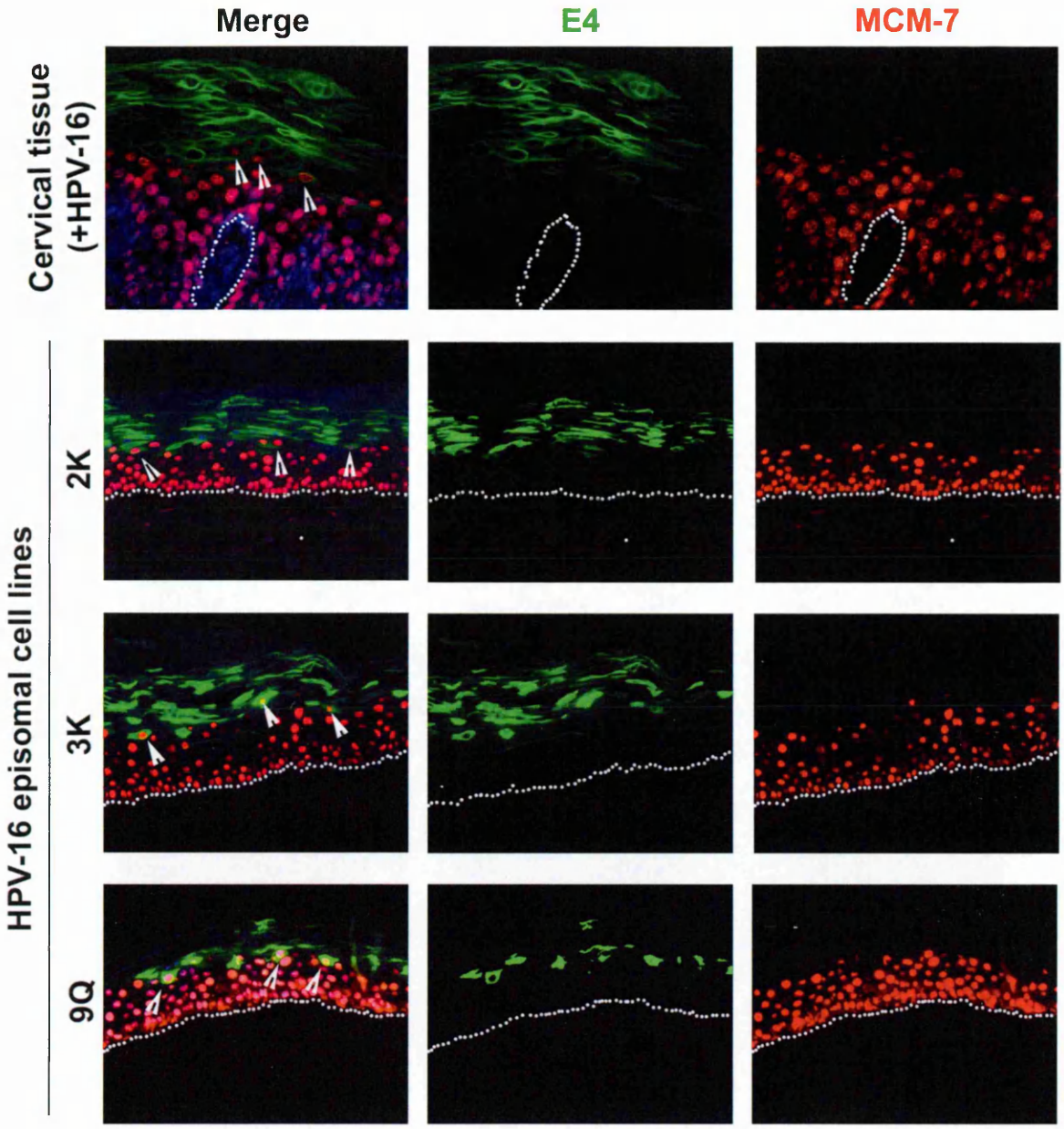

Figure 3.7 Expression of late gene E4 and MCM-7 protein in HPV-16 raft cultures

In order to assess where early and late gene expression overlap in the HPV-16 life cycle, raft culture sections of HPV-16-positive episomal cell lines were stained with antibodies specific for the E7 surrogate marker MCM-7 and E4 protein, respectively. A section of HPV-16 positive cervical tissue previously stained with MCM-7 and E4 was used for comparison (the cervical lesion was previously stained by Kate Middleton (NIMR, London, UK) and was used with her permission). White arrows indicate cells that are positive for both MCM-7 and E4 protein. All sections were counter-stained with DAPI (blue) and were photographed at x20 magnification. The broken line on each raft culture indicates the basal layer.

3.2.8 Viral DNA amplification and E4 expression commence in the same cells in HPV-16 raft cultures

The productive phase of the life cycle begins with amplification of the viral genome, which is thought to correlate with a thousand-fold increase in viral DNA (Bedell, Hudson et al. 1991). HPV amplified genomes first appear in the last layer of S-phase competent cells and also appear in the first cells that contain visible E4 expression. It is thought that both expression of E7 and E4 are necessary to begin the viral amplification process. E7 ensures that host replication machinery is still available for the virus to amplify its genome. E4 has a known ability to arrest cells in G2, which would prevent the cells from entering mitosis (Davy, Jackson et al. 2005). Preventing mitosis would give the virus a chance to replicate its own genome following cellular DNA replication.

To detect the amplified viral DNA in our system, HPV-16 raft culture sections were hybridized with a DIG labeled 8kb HPV-16 DNA probe. These sections were also stained with an E4 antibody. Amplified genomes were detected exclusively in E4 positive cells, and in cells where E4 first appeared in the epithelium (Figure 3.8). Amplified viral DNA could also be detected in E4 positive cells throughout the cornified layers where viral packaging is likely to occur. These are thought to be previously amplified genomes that are carried up to the surface. An HPV-16 cervical lesion also shows the typical staining pattern of E4 cells that contain amplified viral genomes. Here amplified genomes are also first detected in the first layer of E4 positive cells.

We were unable to show a triple stain of MCM-7, E4 and DNA due incompatible protocols. However, due to the location of the first amplified genomes it is likely that these cells also contain MCM-7. In conclusion we were able to show that viral amplification in the NIKS (cutaneus) HPV-16 raft system commences in the first layer of E4 positive cells, which is similar to the onset of viral amplification in real-life productive HPV-16 cervical lesions.

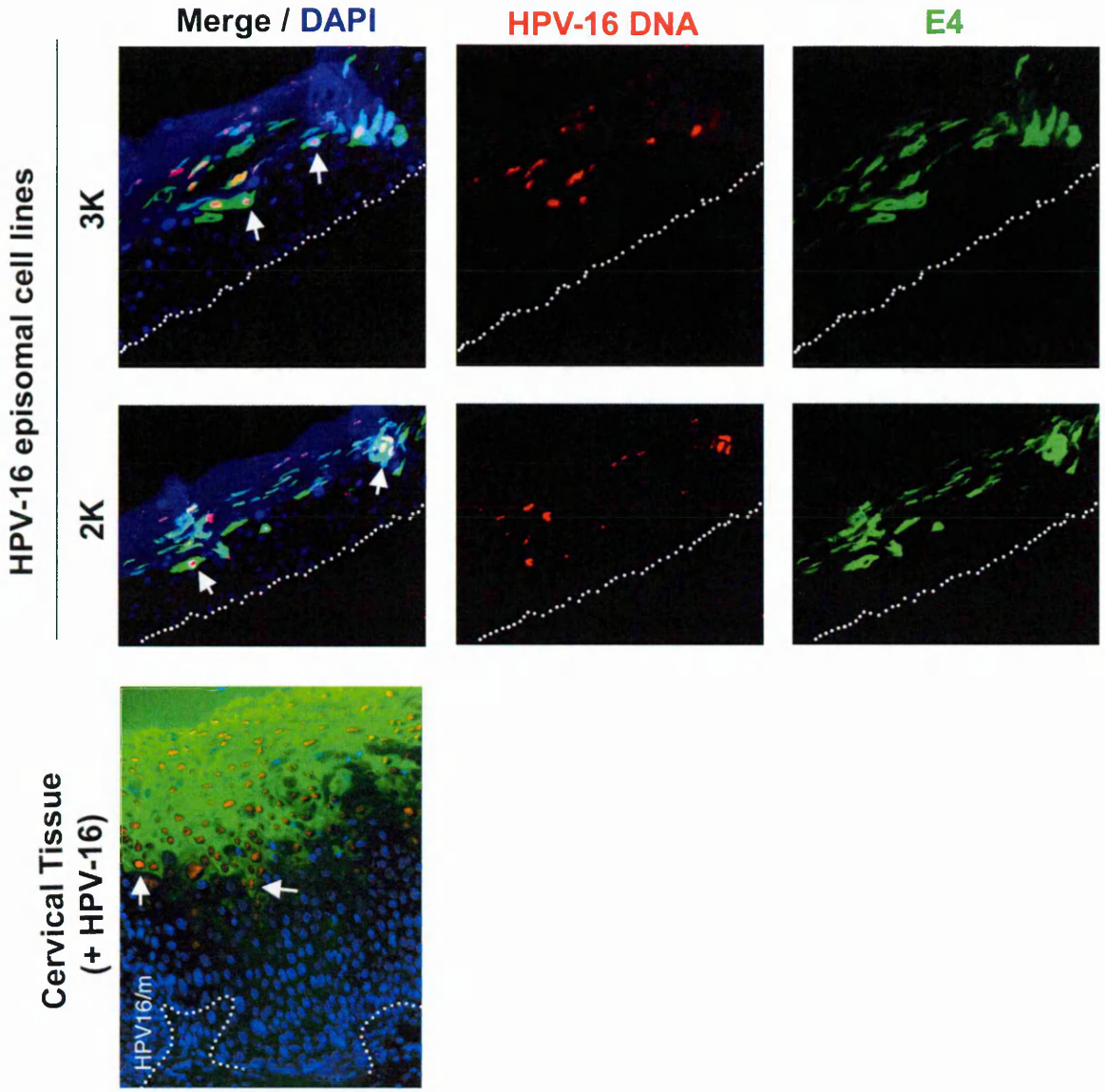

Figure 3.8 Detection of viral DNA amplification and E4 expression in HPV-16 raft cultures

To determine where viral DNA amplification starts relative to late life cycle events, raft cultures of HPV-16-positive episomal cell lines were hybridised with a DIG-labelled full length HPV-16 genome probe (HPV-16 DNA). Antibodies against HPV-16 protein E4 were applied to the same sections to detect late viral life cycle events. White arrows indicate cells that are positive for both HPV-16 DNA and E4 protein. A section of HPV-16-positive cervical tissue was stained the same way by Woei Peh (NIMR, London, UK) and used with permission for comparison. All sections were counter-stained with DAPI (blue) and were photographed at x20 magnification. The broken line on each raft culture indicates the basal layer.

3.2.9 The onset of early terminal differentiation commences normally in wt HPV-16 raft cultures and does not correlate with the appearance of late viral proteins.

The host cellular environment changes as the virus proceeds through the NIKS terminal differentiation program. It is widely established that the terminal differentiation program activates the late promoter, however the specific stage during terminal differentiation program has not been identified. We therefore wanted to establish whether late HPV gene expression in our system, correlated with any part of the NIKS terminal differentiation program. In addition we also wanted to evaluate if any alterations in the differentiation program occur as a result of the virus life cycle. Although this has not been extensively evaluated with HPV-16, previous work has shown that the expression of early keratins such as K10, are delayed in low–risk HPV-2 and HPV-63 induced cutaneous lesions. There was no such delay in low-risk HPV-11 induced cutaneous lesions. These studies also found no temporal relation between early terminal differentiation and late E4 expression. As this could be type-specific, we wanted to evaluate K10 expression alongside E4 in our HPV-16 raft system.

To evaluate regions of early terminal differentiation and late viral gene expression we applied a K10 and an E4 antibody to sections of the HPV-16 raft cultures. An HPV16 cervical lesion, was used for comparison. In our system, all seven HPV-16 raft culture sections showed little to no alterations in K10 expression compared to HPV negative NIKS rafts. In normal tissue K10 is expressed in the first layer above the basal compartment (Figure 3.9). By comparison K13 expression was slightly delayed above normal in the cervical/mucosal lesion. However, other HPV-

induced cervical lesions have shown that K13 is also expressed abnormally in the basal layer (data not shown (Kate Middleton NIMR, London, UK)). At this point we could only conclude that HPV-16 did not affect the start of early differentiation in the NIKS HPV-16 raft system.

E4 expression showed no clear correlation between the start of early terminal differentiation and late life cycle events. This was evident in our system and in the cervical lesion. This was also in line with the previous studies of low-risk viruses. Secondly no distinct alterations of K10 expression could be seen in the first one or two layers of E4-positive cells where active expression of K10 is still likely to occur.

In conclusion we can confirm that late HPV gene expression does not coincide with early terminal differentiation as determined by in our system or in HPV-induced cervical lesions. This suggests that late promoter activation is likely to occur in cells undergoing late terminal differentiation. In addition no distinct alterations in the start of early differentiation program or K10 expression could be detected in our system.

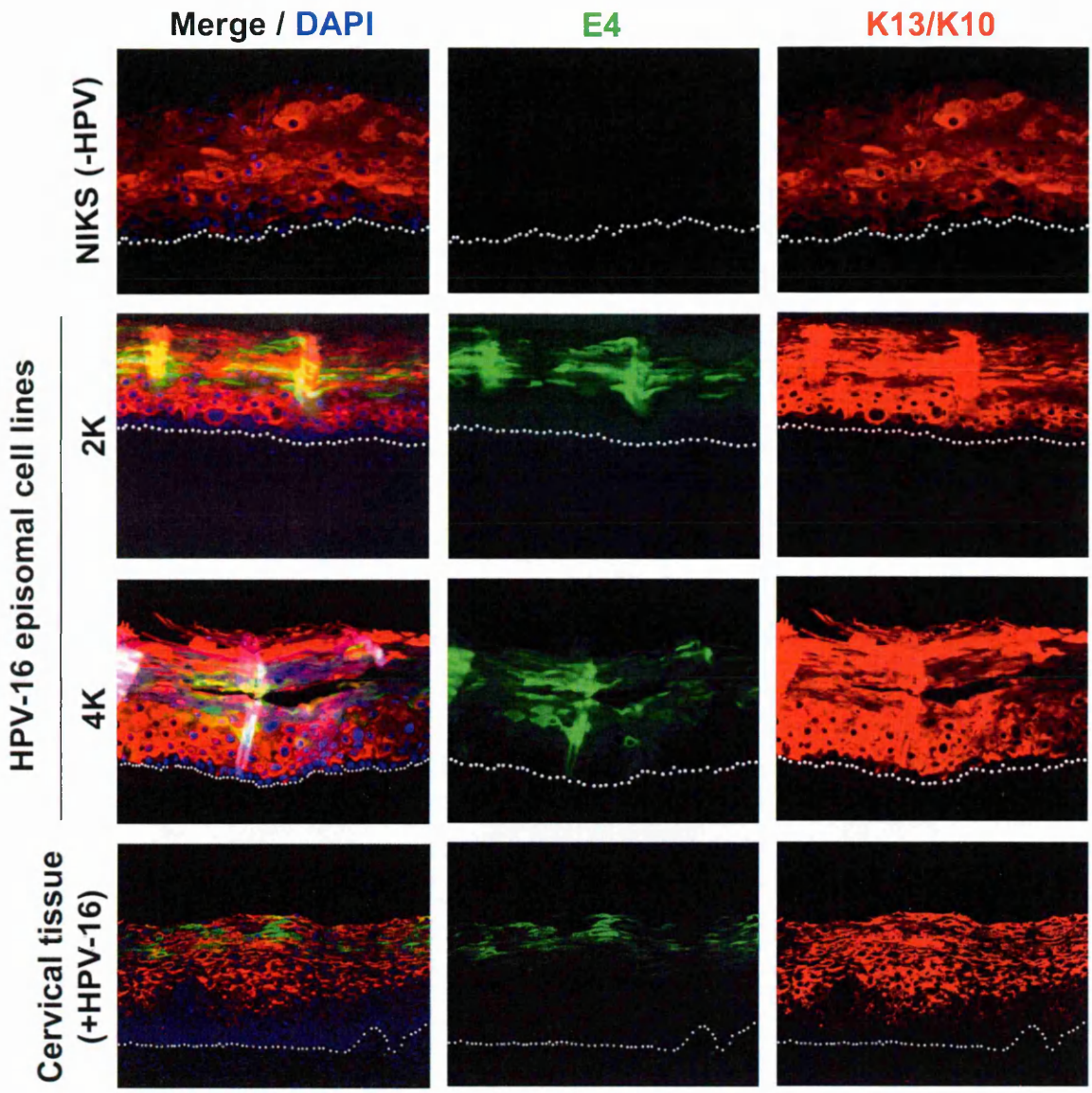

Figure 3.9 Expression of E4 protein and early terminal differentiation in HPV-16 raft cultures
To assess if E4 expression coincides with the onset of terminal differentiation, raft cultures sections of HPV-16-positive episomal cell lines were stained with the early differentiation marker K10 and an antibody against the HPV-16 protein E4. A section of HPV-16-positive cervical tissue previously stained with K13 and E4 antibody was used for comparison. All sections were counterstained with DAPI (blue) and were photographed at x20 magnification. The broken line on each raft culture indicates the basal layer. The Immunohistochemistry of the cervical tissue sections was previously carried out by Kate Middleton (NIMR, London, UK) and used with permission.

3.2.10 Late HPV-16 gene expression coincides with late terminal differentiation

As we had just shown that late viral gene expression did not coincide with the early part of the terminal differentiation program, we wanted to investigate whether the epithelial regions of late terminal differentiation coincide with late viral expression. To identify regions of late differentiation and late viral gene expression we applied antibodies, to pro-filaggrin/filaggrin and E4, to sections of all seven HPV-16 raft cultures. As mentioned earlier pro-filaggrin and filaggrin are highly abundant within the granular layer, which immediately precedes cornification.

When comparing the granular layer in HPV infected tissues to HPV negative NIKS raft cultures, the virus did not appear to compromise the formation of this layer. In the HPV-16 raft culture system we detected a granular layer consisting of two to three layers of pro-filaggrin granules and processed filaggrin (Figure 3.10).

Most interestingly, E4 is first detected at the start of granular layer or within the granular layer. E4 positive cells could not be detected below the filaggrin layer. The same staining patterns could also be demonstrated in an HPV-16 induced cervical mucosal lesion. This overlap is typically not easily identified in cervical lesions, as filaggrin is not as abundantly expressed in mucosal epithelium, when compared to cutaneous epithelium.

In our system, filaggrin was not highly abundant in every E4 positive cell so we could not conclude that filaggrin itself was necessary for E4 expression or vice

versa. It is however possible that the host cell environment during this stage of differentiation is necessary for late promoter activation and/or E4 accumulation.

These results highly suggest that E4 expression begins and/or E4 accumulates during late terminal differentiation, specifically in the granular layer. Secondly, it is possible that the formation of the granular layer is required for late viral events to occur.

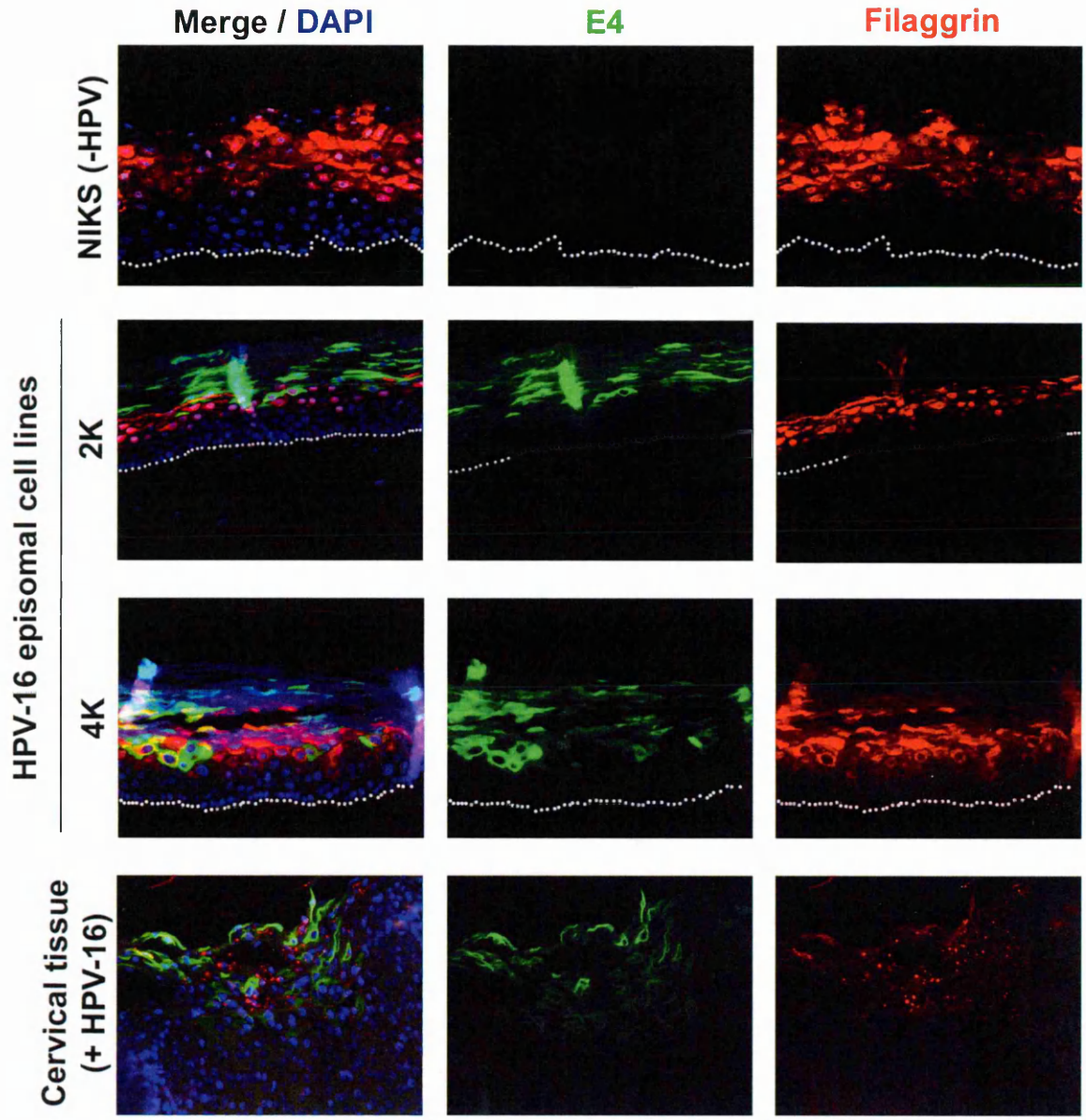

Figure 3.10 Expression of E4 protein and late terminal differentiation in HPV-16 raft cultures
To assess if late HPV-16 gene E4 expression correlates with late stages of cellular terminal differentiation, raft cultures sections of HPV-16-positive episomal cell lines were stained with antibodies against late terminal differentiation marker filaggrin and against E4 protein. A section of HPV-16-positive cervical tissue previously stained with filaggrin and E4 antibodies was used for comparison. All sections were counterstained with DAPI (blue) and were photographed at x20 magnification. The broken line on each raft culture indicates the basal layer. The Immunohistochemistry of the cervical tissue sections was previously carried out by Kate Middleton (NIMR, London, UK) and used with permission.

3.2.11 L1 capsid protein accumulates in the upper layers of E4 expressing cells

To complete a productive HPV life cycle L1 and L2 capsid proteins must be made and assembled into an intact capsid. Antibodies to L1 are primarily used to detect capsid protein in HPV induced lesions. L1 is a late transcript product, and is found in E4-positive cells of the cornified or superficial layers, of cutaneous or mucosal lesions respectively. L1 capsid protein has been also previously identified in first layer of E4 positive cells before the cornified layer. A temporal gap between the appearance of E4 and L1 is commonly detected in HPV lesions. It is possible that virus undergoes several rounds of genome amplification before L1 is expressed for virus packaging.

To assess where L1 capsid production occurred in our system, L1 and E4 antibodies were applied to adjacent sections of HPV-16 raft cultures. A typical L1/E4 staining pattern is also shown in a HPV induced cervical lesion (Figure 3.11). In our system L1 capsid was expressed in the upper layers of E4 cells (Figure 11). L1 was first detected in one or two E4 positive cells within the granular layer. However, most of the L1 capsid appeared to accumulate in E4 positive cells within the cornified or superficial layers.

There are still open questions regarding a possible role of E4 for L1 capsid assembly or infectivity. Current studies are evaluating if E4 enhances virions infectivity. (in personal communication with Pauline McIntosh, NIMR, London, UK). An alternative hypothesis is that E4 destabilizes cornified envelopes to allow for

virus release.regions that carry these mature capsids. As HPV is not a lytic virus this would allow for their release from the epithelium.

In conclusion we have demonstrated that early and late HPV-16 gene expression patterns in our cutaneous raft culture system are highly similar to high-risk HPV gene expression in the cervix. For future life cycle studies we have established a model that represents the HPV-16 life cycle in cervical (mucosal) tissue.

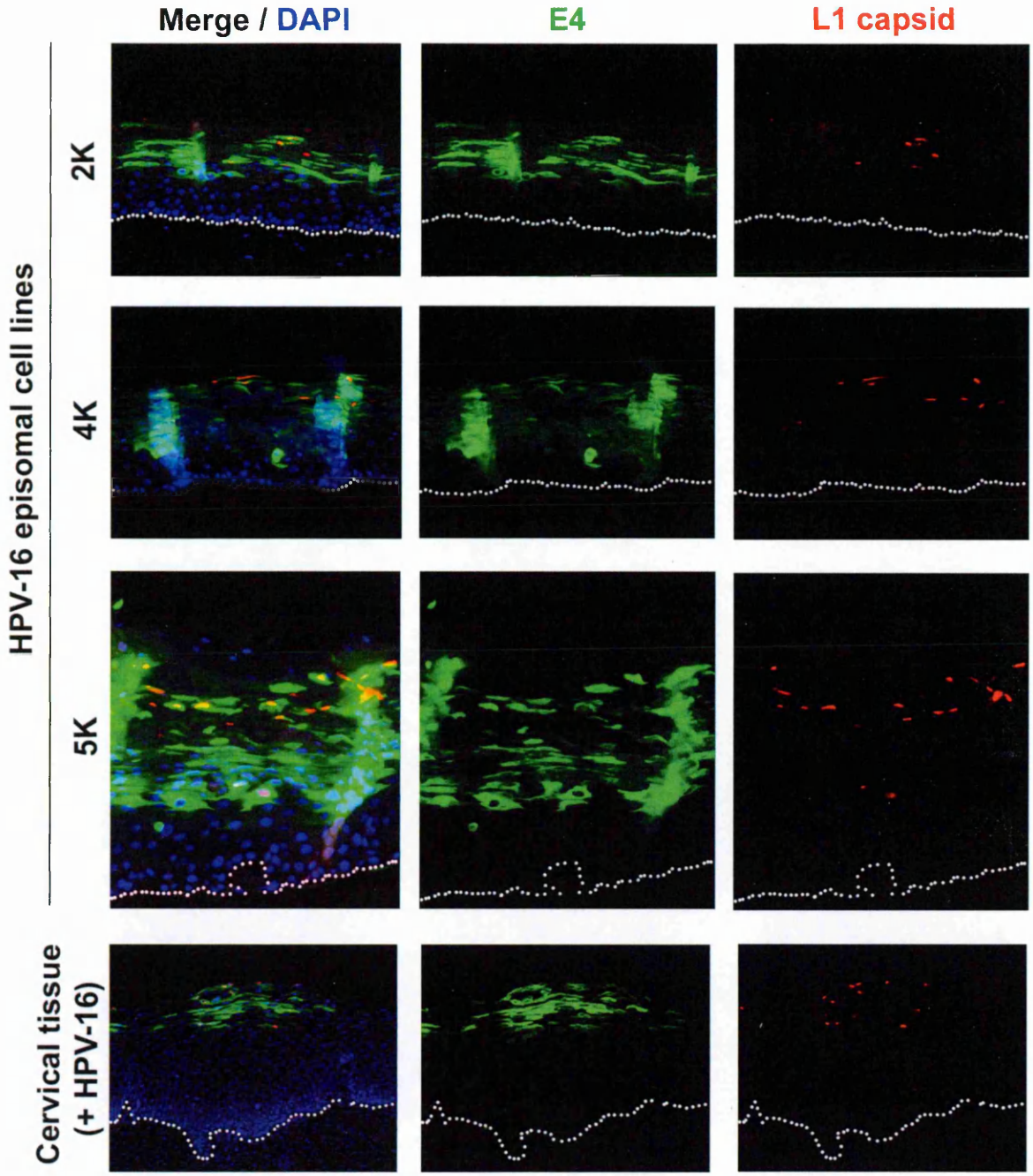

Figure 3.11 Expression of E4 protein and L1 capsid protein in HPV-16 raft cultures

To determine where L1 capsid protein accumulates within the virus life cycle, raft cultures sections of HPV-16-positive episomal cell lines were stained with antibodies against the L1 capsid protein and the E4 protein of HPV-16. A section of HPV-16 positive cervical tissue previously stained with antibodies against L1 capsid protein and E4 protein was used for comparison. All sections were counter-stained with DAPI (blue) and were photographed at x20 magnification. The broken line on each raft culture indicates the basal layer. The Immunohistochemistry of the cervical tissue section was previously carried out by Kate Middleton (NIMR, London, UK) and used with permission.

3.3 Discussion

The NIKS organotypic raft model has been widely used to investigate the functions of various HPV genes within the HPV-16 life cycle. However the HPV-16 life cycle in this NIKS (cutaneous) raft system has not been directly compared to the HPV-16 life cycle in cervical (mucosal) epithelium. Recent work, which has extensively analyzed HPV-16 gene expression patterns in cervical lesions, has given the opportunity to compare the NIKS raft system to real-life cervical biopsy material (Peh, Middleton et al. 2002; Middleton, Peh et al. 2003). We have shown that the early and late viral gene expression patterns in HPV-16 induced cervical (mucosal) lesions are conserved in the NIKS (cutaneous) raft system.

To evaluate viral gene expression patterns in the NIKS raft system, we conducted a side-by side comparison with low-grade HPV induced cervical lesions. Cervical lesions had been previously stained with antibodies specific for the E7 surrogate marker MCM-7 and the late viral genes, E4 and L1. Prior to this comparison we were able to confirm that MCM-7 was indeed a surrogate marker of E7 in the NIKS HPV-16 raft system. Only HPV-16 cell lines that expressed the E7 gene could produce MCM-7 positive cells above the basal layer, in raft culture. Although we were confident that the MCM-7 expression was a consequence of E7 expression only, for future studies, it will be important to find a good antibody that will specifically identify E7 proteins in these cells.

In direct comparison to cervical lesions, we were also able to confirm that the MCM-7 compartment was extended above the basal layer in raft cultures of HPV-16 episomal cell lines. In both the cervical and raft culture epithelium the extended

MCM-7 compartment was also maintained until a finite point in the epithelium, which likely identifies the end of early gene expression. It is currently not known as to where in the epithelium the early promoter is repressed, however one can speculate that the end of MCM-7 compartment marks the end of early gene expression in the epithelium. One possibility is that the early promoter is repressed by E2 in the upper layers. In addition to its role in viral DNA replication it has been shown that E2 also regulates transcription from the early p97 promoter (Tan, Leong et al. 1994). E2 is up-regulated by the differentiation dependent late promoter in the upper layers of the epithelium, in order to carry out viral amplification. It was also previously shown that high levels of E2 could specifically suppress E7 expression(Steger and Corbach 1997).

In both HPV induced cervical lesions and HPV-16 raft cultures we were able to show that the end of the MCM-7 compartment also coincided with the first identification of late E4 gene expression. In both cervical lesions and HPV-16 raft cultures the E4 protein was identified in the last layer of MCM-7/S-phase competent cells. As stated earlier It has been suggested that the overlap of S-phase competent cells and E4 is important for the start of viral amplification (Flores, Allen-Hoffmann et al. 2000; Peh, Middleton et al. 2002; Nakahara, Peh et al. 2005).

Similar to what was found in HPV-16 cervical lesions, amplified HPV-16 genomes were only detected in E4 positive cells and commenced in the first layer of E4 positive cells. Although we could not perform a double-stain of MCM-7 it was highly plausible that MCM-7 were also expressed in the first layer of cells that contained E4 and amplified genomes. In both HPV-16 raft cultures and HPV-16

cervical epithelium amplified genomes were also detected in E4 positive cells throughout the remainder of the upper layers.

Interestingly, late E4 expression also closely coincided with late terminal differentiation in the raft epithelium. The majority of E4 positive cells were localized in the granular layer in HPV-16 raft cultures. The granular layer was specifically marked by the presence of pro-filaggrin granules and cross-linked forms of filaggrin. One possibility is that the late promoter is upregualted specifically in this layer or cellular splice factors that generate late mRNAs (e.g. E4, L1) are more abundant in this layer.

Another possibility is that the granular layer is favorable for E4 accumulation. In the granular layer pro-filaggrin is processed into filaggrin by calpain cleavage (Presland, Kimball et al. 1997). E4 accumulates in cells following cleavage of its N-terminal domain. N-terminal cleavage of E4 is also carried out by calpain (in personal communication with Jameela Khan, NIMR, UK). It is possible that calpain is up-regulated in these cells during pro-filaggrin processing which is also favorable for the N-terminal cleavage of E4.

We were also able to identify several cervical lesions that expressed E4 only in filaggrin positive cells. Filaggrin is less abundant in cervical (mucosal) lesions, which has made this comparison more difficult. Additional analysis of cervical lesions will have to be completed before we can generally conclude that in both cervical (mucosal) and cutaneous lesions, E4 is expressed in cells that have entered late differentiation. It will perhaps be more beneficial to compare the NIKS

rafts to a more keratinizing epithelium (e.g. vulval epithelium), which contains higher levels of filaggrin.

Finally, we had identified that the productive phase of the life cycle was near completion in the HPV-16 raft culture. In both HPV-16 raft cultures and cervical lesion L1 proteins were expressed in upper layers of E4 positive cells. In addition to the identification of capsid proteins it has also been shown that virus capsids can be harvested from raft cultures of several of these HPV-16 cell lines. (in personal communication with Kenneth Raj, NIMR, London, UK).

Table 3.1 contains a summary of HPV-16 raft culture characteristics.

Table 3.1 HPV-16 raft culture characteristics

HPV-16 clone	2K	3K	4K	4Q	5K	9Q	13Q
Passage number	4-6	5	4-6	4-6	5	5	5
* MCM-7 above basal layer	Yes	Yes	Yes	Yes	Yes	Yes	Yes
* E4 protein	Yes	Yes	Yes	Yes	Yes	Yes	Yes
* MCM-7/E4 overlap	Yes	Yes	Yes	Yes	Yes	Yes	Yes
* Viral DNA amplification	Yes	Yes	NT	NT	NT	NT	NT
* L1 protein	Yes	Yes	Yes	Yes	Yes	Yes	Yes
* Timing of K10 expression	N	N	N	N	N	N	N
* Timing of filaggrin expression	N	N	N	N	N	N	N
Number of times rafted/observed	3	1	3	3	1	1	1

Key for Table 3.1

*= Viral or cellular protein expression/ viral DNA amplification in the HPV-16 NIKS raft epithelium is similar to HPV-16 positive cervical epithelium

NT=Not tested

N=Normal when compared to HPV negative NIKS raft culture

4.0 A raft based model of HPV-16 induced neoplasia

4.1 Introduction

In Chapter 3 we were able to show that the organization of early and late HPV gene expression in our cutaneous HPV-16 raft system is similar to a productive HPV-16 life cycle in HPV infected cervical (mucosal) tissue. Within the HPV disease spectrum these productive HPV-16 raft cultures also represent a pathologically low-grade HPV infection.

High-risk HPV types such as HPV-16 can cause a spectrum of precancerous dysplastic and neoplastic changes in the epithelium. Dysplasia refers to a decrease in cellular maturation like cytoplasmic maturation or cellular stratification and typically coincides with early stages of neoplasia. Neoplasia refers to the abnormal proliferation of cells, which can lead to tumor development and precedes cancer formation. Pathologists use a diagnostic grading scale to classify the extent of neoplastic changes in a lesion. Low-grade lesions that exhibit mild dysplasia in the bottom third of the epithelium are categorized as LSIL. High-grade lesions that exhibit moderate dysplasia to severe dysplasia throughout the middle third and upper third of the epithelium are categorized as HSIL (Diane Solomon 2004). Both LSIL and HSIL can be found in HPV-16-infected cutaneous and mucosal sites of the anogenital tract, which include the cervix, vulva, anus and penis. It is also not uncommon to find both LSIL and HSIL in the same lesion (in personal communication with Heather Griffin, NIMR, UK).

Beyond a pathological diagnosis, recent studies have correlated an alteration in early and late HPV gene expression with increasing neoplastic grades (Freeman, Morris et al. 1999; Middleton, Peh et al. 2003). Collectively these studies have identified that the number of layers that contain MCM-7 positive cells increases with advanced neoplastic changes in the epithelium. In addition, the increase of the S-phase compartment also coincided with a delay in E4 expression and L1 capsid within the upper layers (Middleton, Peh et al. 2003). Additionally, a high percentage of these high-grade lesions were associated with an incomplete HPV life cycle.

These studies led us to collectively evaluate the gene expression patterns and pathology of all ten of our NIKS HPV-16 raft cultures including the raft cultures that did not produce L1 capsid protein within the epithelium. This chapter will aim to show that the cutaneous NIKS HPV-16 episomal cell line model can represent a low-grade productive infection, but can also model the broader spectrum of HPV induced neoplasias. This is a presentation of the first known laboratory model of episomal HPV-16 induced neoplasia.

4.2 Results

4.2.3 Raft cultures of HPV-16 cell lines demonstrate three distinct patterns of MCM-7 expression

It was evident from our earlier life cycle validation panel that three out of ten differentiated HPV-16 episomal cell lines either produced only minimal amounts of L1 capsid protein or that L1 capsid protein was completely absent. The other seven of the raft cultures sections however produced abundant L1 capsid protein.

Middleton et al. (2003) had previously shown that the loss of L1 capsid in high-grade cervical lesions correlated with the persistence of the E7 surrogate marker, MCM-7, throughout the epithelial layers. We therefore proceeded to evaluate if any alterations in early and late viral gene expression in our system correlated with the loss of L1 capsids. To evaluate viral gene expression patterns we applied a panel of MCM-7, HPV-16 E4 and HPV-16 L1 capsid antibodies to raft culture sections of all ten HPV-16 episomal cell lines. We first applied an MCM-7 antibody to evaluate the early part of the viral life cycle (Figure 4.1). Interestingly, we could distinguish three distinct MCM-7 staining patterns in the ten HPV-16 raft culture sections. Each differentiated HPV-16 cell line showed reproducibly only one of these patterns throughout the majority of the raft culture sections. The observed MCM-7 expression patterns can be divided into three categories that we refer to as A, B and C.

Pattern A was found in raft culture 4K (Figure 4.1). In this pattern only a few positive MCM-7 cells could be detected in the basal layer. MCM-7-positive cells were only sporadic in the first several layers above the basal compartment and

clearly absent from the upper layers. Pattern B was detected in the majority of the raft cultures (2K, 3K, 4Q, 5K, 9Q and 13Q). In raft sections with this pattern, MCM-7 was detected in all cells within the basal compartment and in the majority of cells within the next two to three spinous layers. There was no sporadic distribution of MCM-7-positive cells as seen with pattern A, and the cells in the upper layers did not contain MCM-7. Interestingly, we recognized that the raft cultures with patterns A and B are the seven raft cultures from Chapter 3 that contained productive life cycles (Figure 3.4)

In raft cultures with pattern C, a greater number of layers contained MCM-7 positive cells. MCM-7-positive cells persisted throughout the entire epithelium and only a few sporadic MCM-7-negative cells were detected in the top layer. Interestingly raft cultures with pattern C represent the remaining three raft cultures from the original panel (1K, 6K and 6Q) that did not produce L1 capsid protein.

This led us to conclude that upon differentiation, individual early passage HPV-16 episomal cell lines could produce different phenotypes with respect to the degree of S-phase persistence in the epithelium. In addition, raft cultures with a less persistent S-phase compartment correlated with the presence of L1 capsid proteins whereas raft cultures with highly persistent S-phase compartments correlated with the loss of L1 capsid proteins.

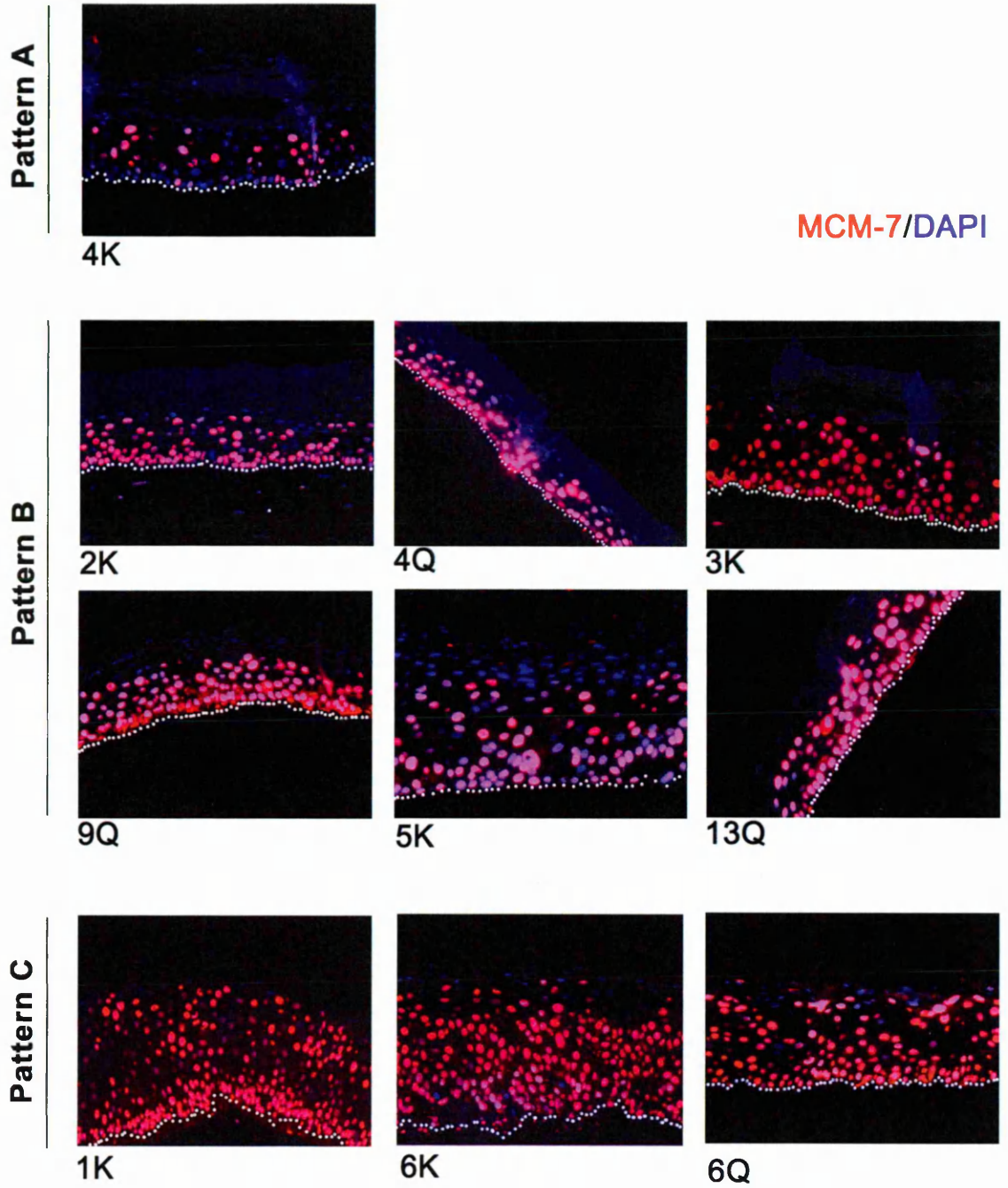

Figure 4.1 Three distinct patterns of MCM-7 expression in HPV-16 raft cultures

Sections of raft cultures from ten HPV-16 episomal cell lines were stained for MCM-7 protein (red) to identify the S-phase compartment and counterstained with DAPI (blue). The broken white line indicates the basal layer. Three distinct patterns of MCM-7 expression could be distinguished in these cell lines. Pattern A was identified in raft culture 4K and is characterized by the predominant absence of MCM-7 positive nuclei from the basal compartment and only sporadic presence in the second and third layers. Also, MCM-7 positive nuclei are absent from the upper layers. Pattern B was identified in raft cultures 2K, 3K, 4Q, 5K, 9Q and 13Q. In these raft cultures, MCM-7-positive cells are uniformly distributed but are only present in the first several layers of the epithelium and absent from the upper layers. Pattern C was found in raft cultures 1K, 6K and 6Q. In pattern C raft cultures, MCM-7-positive cells are contained in greater numbers and MCM-7 expression persists throughout the entire epithelium.

4.2.4 The persistence of MCM-7 in the upper layers of HPV-16 raft cultures correlates with a delay in late gene expression and an incomplete life cycle

After we found that expression of late gene E7 surrogate marker MCM-7 could persist in several of the raft cultures, we were curious to see if the onset of late E4 gene expression was also delayed. To evaluate this we applied an E4 antibody onto all ten raft culture sections that we had previously stained with MCM-7 (Figure 4.2). We observed that in fact E4 expression was dramatically delayed in the three raft culture epithelia with a persistent S-phase compartment (pattern C). In addition, E4 protein was only sporadically detected in the last layer of MCM-7 positive cells. In contrast, and as previously observed in Chapter 3, we detected an earlier onset of E4 expression in raft cultures with patterns A and B, which contained less persistent S-phase compartments. In these rafts E4 was also expressed at high levels throughout the remaining layers.

Next, we wanted to evaluate the timing of the expression of both late genes E4 and L1. To assess this we applied an E4 antibody to all ten raft culture sections previously stained with an L1 capsid antibody (Figure 4.3). In the HPV-16 raft culture epithelium with pattern A, E4 and L1 were both first detected in the lower third of the epithelium. L1 capsid protein could be mostly found in E4-positive cells within the last several layers of the epithelium. In all raft cultures with pattern B the first appearance of E4 and L1 expression was delayed when compared to pattern A. However we detected L1 capsid in E4-positive cells within the final few layers. Finally in the raft cultures with pattern C, we detected an extreme delay in E4 expression. L1 capsid was rarely detected or was completely absent.

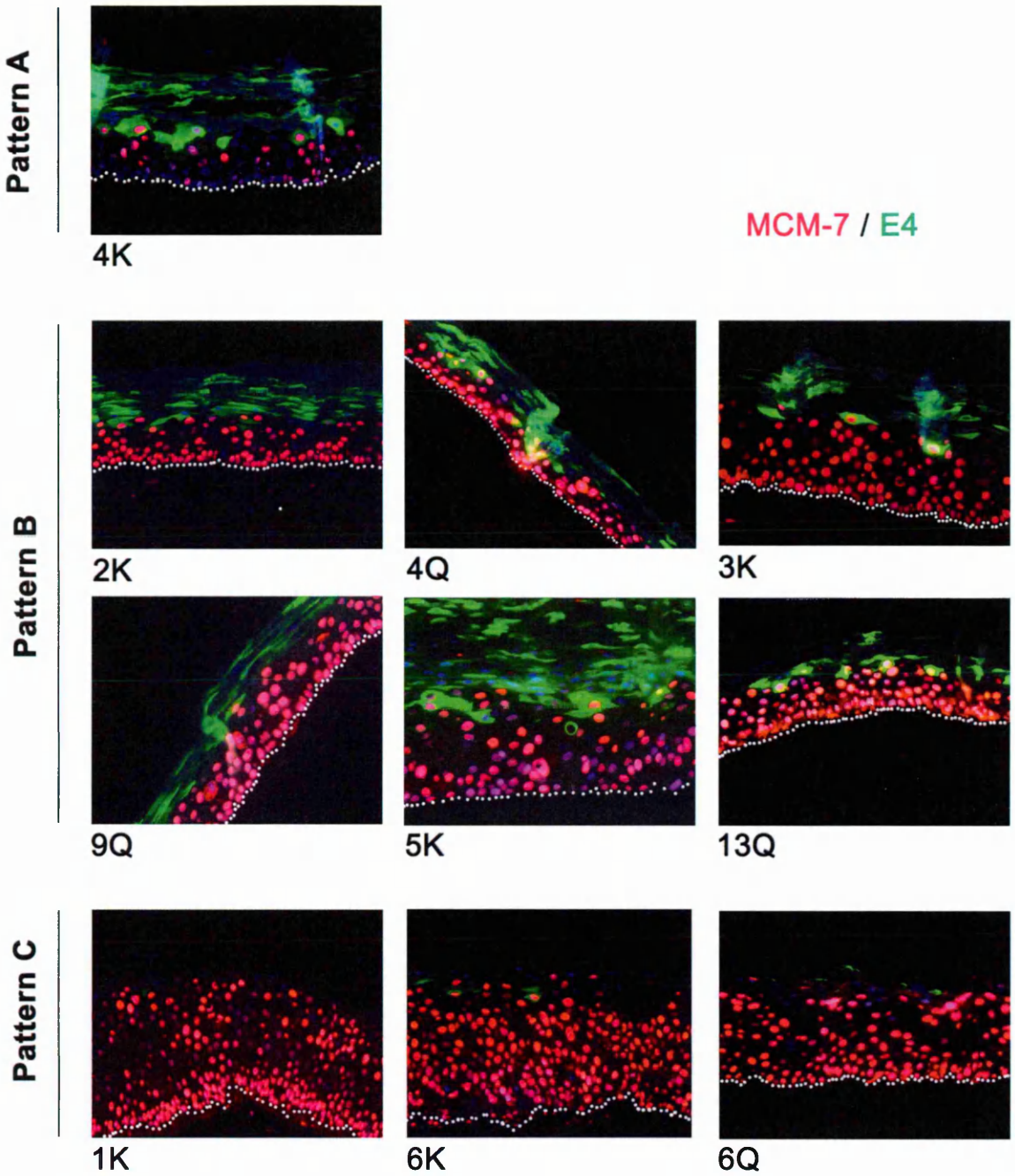

Figure 4.2 Onset of late E4 protein expression in HPV-16 raft cultures

Sections of raft cultures from ten HPV-16 episomal cell lines were stained for MCM-7 protein (red) and E4 (green, #248) to detect early and late HPV-16 gene expression in the epithelium. DAPI was applied as a nuclear counterstain (blue). The broken white line indicates the basal layer. An early onset of E4 expression is evident in raft culture 4K which contains a sporadic MCM-7 compartment (pattern A) and E4 remains highly abundant throughout the upper layers. In raft cultures with a uniform yet less persistent MCM-7 compartment (pattern B), E4 expression is in some cases slightly delayed compared to pattern A, but E4 is highly abundant throughout the upper layers. In raft cultures with a highly persistent MCM-7 compartment (pattern C) E4 expression is delayed until the last two cell layers and is only detected in sporadic MCM-7-positive cells.

As previously found in HPV-induced cervical lesions, the MCM-7, E4 and L1 gene expression patterns in the HPV16 raft cultures highly suggest that the level of S-phase persistence in the NIKS epithelium, has an impact on the timing of late gene expression in the upper layers. This also proposes that persistent early gene expression is less favorable for the virus to complete its life cycle and can consequently lead to high-grade neoplasia.

From these results we concluded that our HPV-16 raft culture model could possibly recapitulate the spectrum of viral gene expression patterns that are present in both low (LSIL) and high-grade (HSIL) HPV-induced neoplasia.

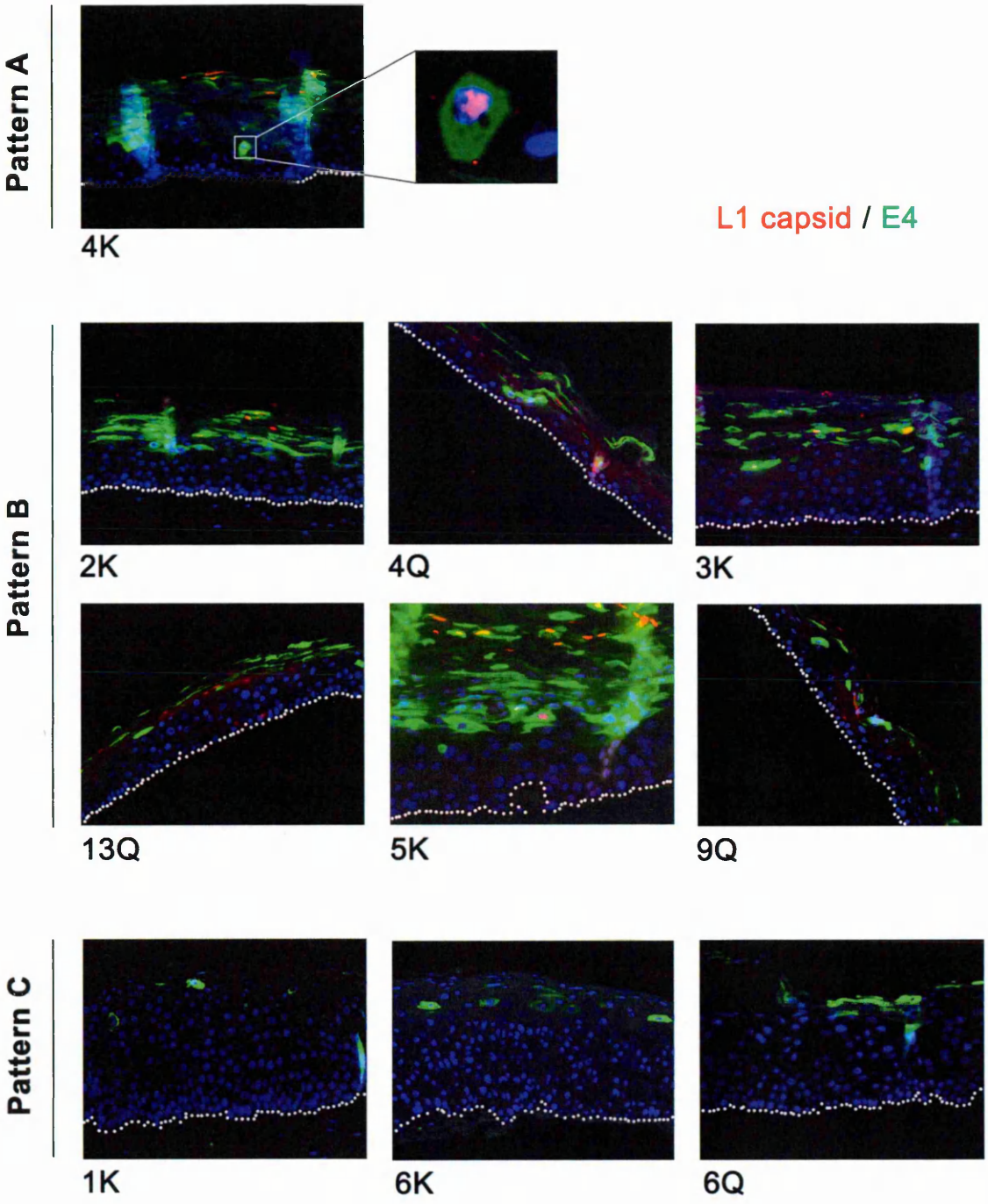

Figure 4.3 Onset of late L1 capsid protein expression in HPV-16 raft cultures

Sections of raft cultures from ten HPV-16 episomal cell lines were stained for L1 capsid protein (red) and E4 (green, #248) to detect late gene expression in the epithelium. DAPI was applied as a nuclear counterstain (blue). The broken white line indicates the basal layer. In raft culture 4K (pattern A) L1 capsid protein is detected early in the epithelium (magnified section from lower layer) in E4-positive cells and is detected throughout the cornified layers. In pattern B raft cultures (2K, 3K, 4Q, 5K, 9Q and 13Q), L1 capsid protein is also first detected in the first layer of E4 positive cells and remains highly abundant throughout the cornified layers. In pattern C raft cultures (1K, 6K and 6Q) E4 expression is delayed and L1 capsid protein can not be detected at all.

4.2.5 Raft cultures of early passage HPV-16 episomal cell lines mimic HPV induced LSIL and HSIL

So far we have established that MCM-7, E4 and L1 staining patterns in the NIKS HPV-16 raft system were reminiscent of HPV cutaneous and mucosal lesions with pathologically diagnosed LSIL and HSIL. Therefore, we attempted a side-by-side comparison between HPV-16 raft culture sections and sections of biopsied cutaneous and cervical (mucosal) lesions with MCM-7, E4 and L1 capsid as markers.

Pattern A can not be found in low-grade HPV-16 cervical lesions however it is commonly found in low-grade mucosal lesions infected with low-risk HPV types, such as HPV-11. Figure 4.4 shows the similarities in MCM-7 and E4 patterns between a low-grade HPV-11 mucosal lesion and raft culture 4K. These similarities include a sporadic S-phase compartment starting within the basal layer and a high abundance of E4 throughout the upper layers of the epithelium.

Pattern B raft cultures resemble the MCM-7 and E4 staining patterns of a typical HPV-16 cervical lesion with LSIL. In these HPV-16 low-grade lesions, MCM-7-positive cells are uniformly distributed in the first third of the epithelium. E4 expression is also highly abundant in the upper layers of the epithelium.

Pattern C raft cultures resemble the MCM-7/E4 staining pattern of a typical HPV-16 cervical lesion with HSIL. MCM-7-positive cells extend through the middle–third and final-third of the epithelium. Expression of E4 is delayed compared to the

other patterns and is only present in a subset of MCM-7 positive cells in the uppermost layers.

In Figure 4.5, the equivalent grades of cutaneous or cervical lesions are also comparable with the respective E4 and L1 staining patterns of the observed raft culture patterns. Low-grade (LSIL) HPV-1 cutaneous lesion and pattern A raft culture 4K both contain high levels of L1 capsid protein. In addition L1 capsid is detected early in the first several layers of the epithelium, which coincides, with the early onset of E4 expression. LSIL HPV-16 cervical lesions and raft cultures with pattern B also contain L1 capsid. However, late gene expression is slightly delayed compared to that of pattern A, and E4 and L1 capsid are starting to appear in the second-third of the epithelium. In HSIL HPV-16 cervical lesions and raft cultures with pattern C, late gene expression is delayed until the final third of the epithelium. Just like in Figure 4.4 this appears to confine E4 expression to the uppermost layers, while L1 capsid protein is reduced in the cervical lesion and seems to be completely absent from the raft cultures 1K and 6K.

We conclude that the spectrum of viral gene expression patterns observed in our HPV-16 raft culture system, is similar to those found in HPV-induced cervical lesions of LSIL and HSIL pathological grades. We have also found low-grade phenotypes that are commonly found in cutaneous lesions infected with low-risk HPV types. It is quite possible that these phenotypes exist in HPV-16- infected cervical lesions however due to their less neoplastic pathology, they are not frequently biopsied for analysis. This emphasizes that this system could potentially present intermediate phenotypes of the virus that we would not normally find in available biopsy material.

In order to continue with the evaluation of our model we have chosen three HPV-16 cell lines of both LSIL and HSIL phenotypes. In this thesis these cell lines are from now on grouped and named as LSIL phenotypes (cell lines 4K, 2K and 4Q) or HSIL phenotpyes (cell lines 1K, 6K, 6Q).

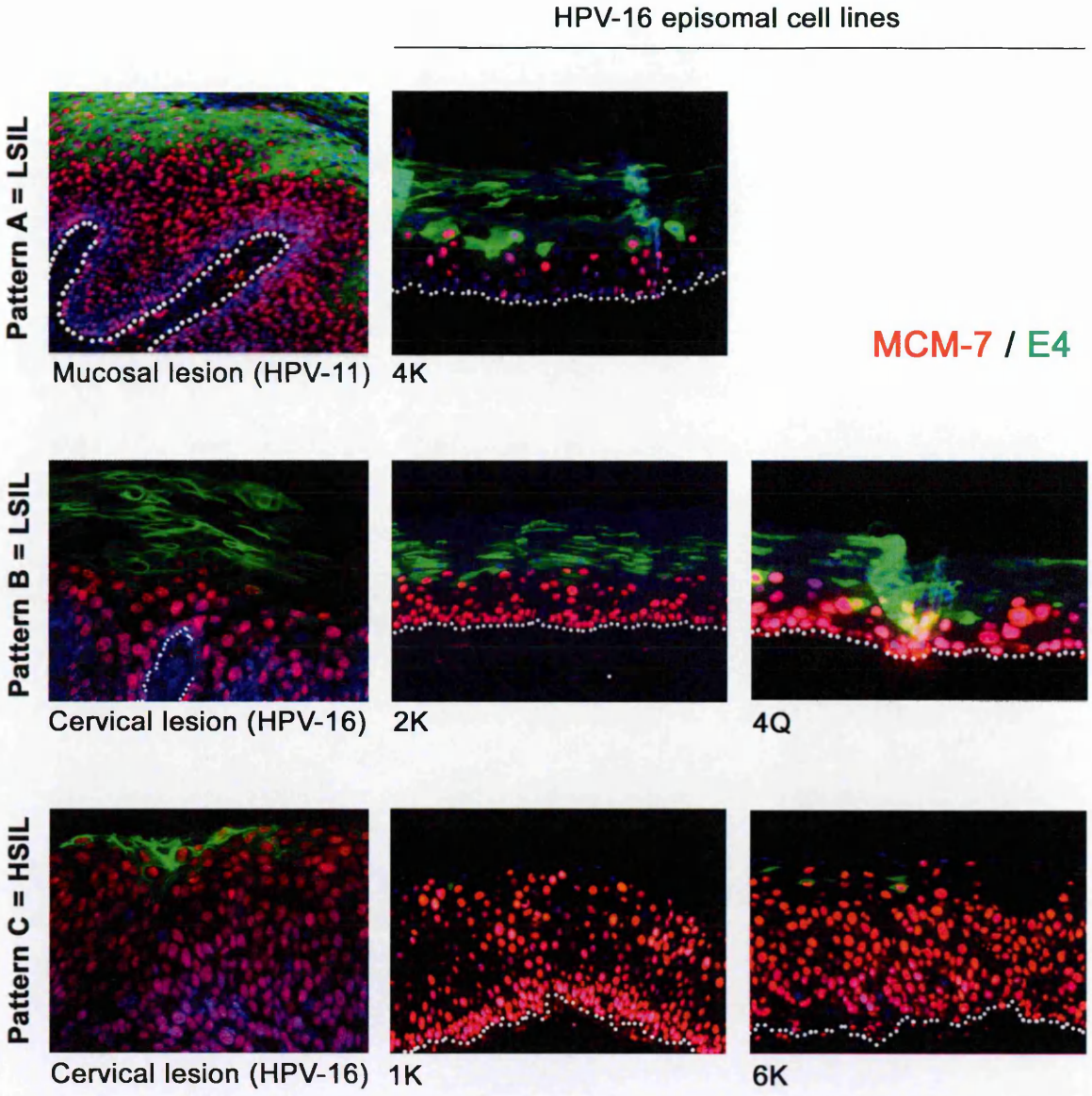

Figure 4.4 Comparison of MCM-7 and E4 expression between HPV-16 raft cultures and HPV-induced lesions with LSIL and HSIL.

Raft cultures sections of HPV-16-positive episomal cell lines and HPV induced lesions were stained against MCM-7 (red) and E4 (green, #248). DAPI was applied as a nuclear counterstain (blue). The broken white line indicates the basal layer. Pattern A raft culture resembles a pathologically diagnosed low-grade (LSIL) mucosal lesion infected with HPV-11. In both epithelia MCM-7 expression is less prominent in the basal layer, which correlates with high levels of E4 expression in the upper layers. Pattern B raft cultures resemble a pathologically diagnosed cervical lesion with LSIL. MCM-7 expression is more uniform and the S-phase compartment ends in the first to middle-third of the epithelium. This correlates with high levels of E4 expression in the upper layers. Pattern C raft cultures resemble high-grade cervical lesion (HSIL), where MCM-7 persists through the entire epithelium and E4 expression is delayed until the top layer.

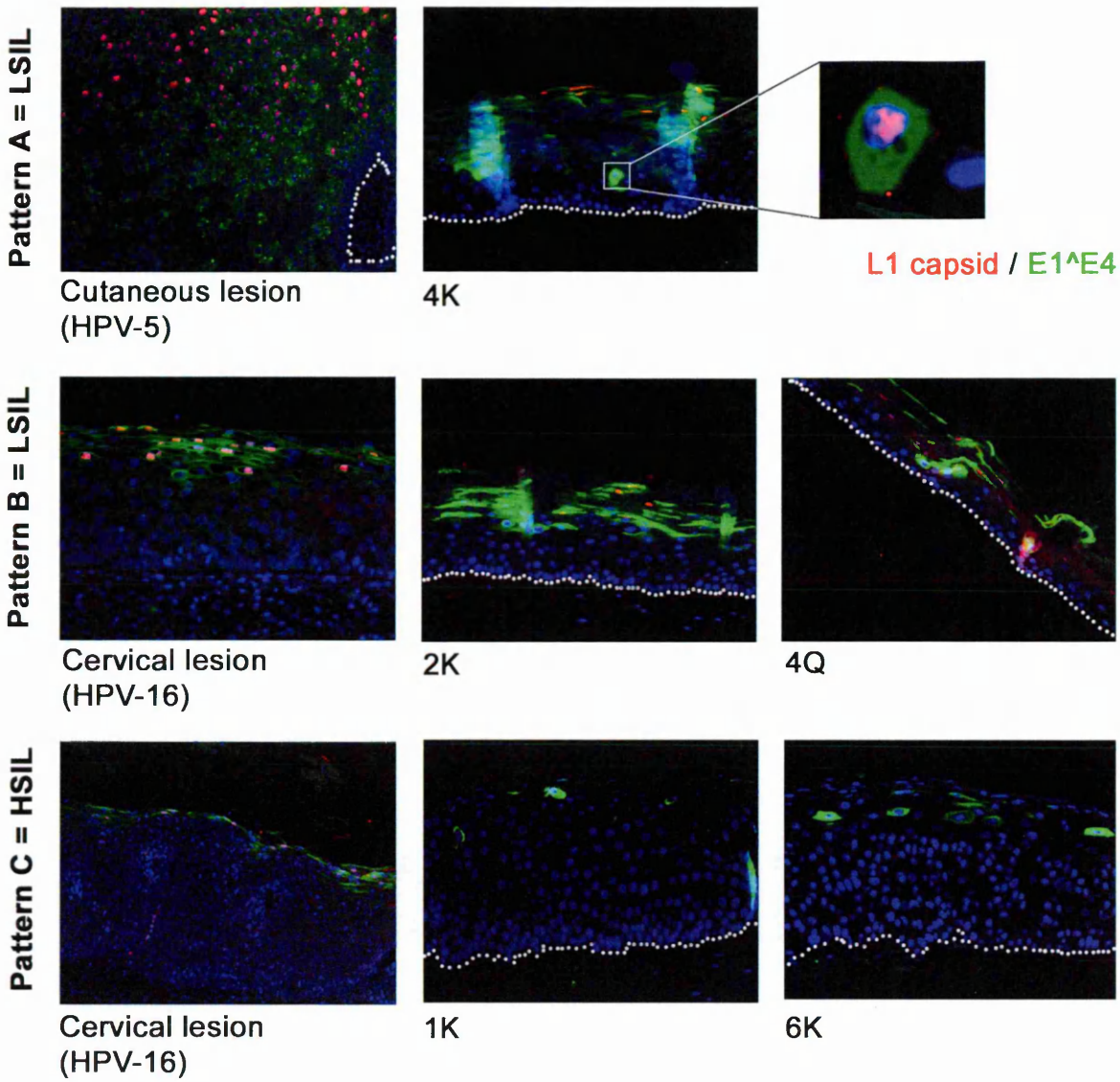

Figure 4.5 Comparison of L1 capsid protein and E4 expression between HPV-16 raft cultures and HPV-induced lesions with LSIL and HSIL.

Raft cultures sections of HPV-16-positive episomal cell lines and HPV-induced cervical lesions were stained against L1 capsid protein (red) and E4 (green, #248). DAPI was applied as a nuclear counterstain (blue). The broken white line indicates the basal layer. Pattern A resembles a low-grade (HSIL) cutaneous lesion infected with HPV-1. In this case L1 capsid protein is detected in E4- positive cells in the first third of the epithelium and in clusters throughout the upper layers. Pattern B raft cultures resemble a low-grade HPV-16 cervical lesion with LSIL. L1 capsid protein is detected in the middle to final third of the epithelium and is detected in clusters in the upper layers. In Pattern C raft cultures, E4 expression is delayed, which results in low levels of L1 capsid protein or it is completely absent from the epithelium

4.2.7 LSIL-like and HSIL-like phenotypes are reproducible in HPV-16 raft cultures with respect to MCM-7, E4 and L1 capsid expression.

We next wanted to show that the early and late HPV gene expression patterns were reproducible in independent raft culture experiments. To show their reproducibility, all six LSIL and HSIL cell lines were differentiated for 14 days to create two replicate raft cultures each (raft culture 1 and 2). Each HPV-16 cell line was differentiated at a similar early passage (passage four-six) as the first set of raft cultures. To quantify and compare replicate raft cultures of each cell line, the same combinations of either MCM-7 and E4 or E4 and L1 antibodies were applied as before (Figure 4.6). Three typical regions of equal measured size from each independent raft culture, were selected for counting. In order to quantify the S-phase compartment we counted the total number of MCM-7-positive cells from the basal layer to the top layer.

The mean of MCM-7 positive cells from three sections for each replicate raft culture was calculated, and the bar chart shows the mean of the means of both replicate rafts (Figure 4.6B). The error bars represent +/- the standard deviation between the two replicate raft cultures (Figure 4.6). Although we found that there was more variation in the number of cells that contained MCM-7 above the basal layer in the HSIL-like replicates, they consistently contain approximately twice as many MCM-7 cells above the basal compartment than the LSIL-like raft cultures. It was also apparent that the timing of E4 expression in the epithelium coincided with the end of the S-phase compartment in all six raft cultures. We noted that the two extreme phenotypes with respect to MCM-7 persistence expression were that of 4K (LSIL) with very low and 6K (HSIL) with very high persistence.

Figure 4.6 Reproducibility of early and late gene expression in HPV-16 raft cultures with LSIL and HSIL phenotype.

(A) Each three HPV-16-positive episomal cell lines with either the LSIL or HSIL phenotype were differentiated for 14 days to produce two replicate raft cultures (raft 1 and 2), respectively. Raft culture sections were stained against HPV-16 E7 surrogate marker MCM-7 (red) and HPV-16 E4 (green, #248) to observe early and late viral gene expression, respectively. DAPI was applied as a nuclear counterstain (blue). The broken white line indicates the basal layer. (B) In three separate sections from the raft cultures shown in (A) the number of MCM-7 positive cells above the basal layer was counted. The mean of MCM-7 positive cells for the three sections for each raft culture was calculated, and the bar chart shows the mean of the means of the replicate rafts. The error bars represent +/- the standard deviation between the two replicate raft cultures

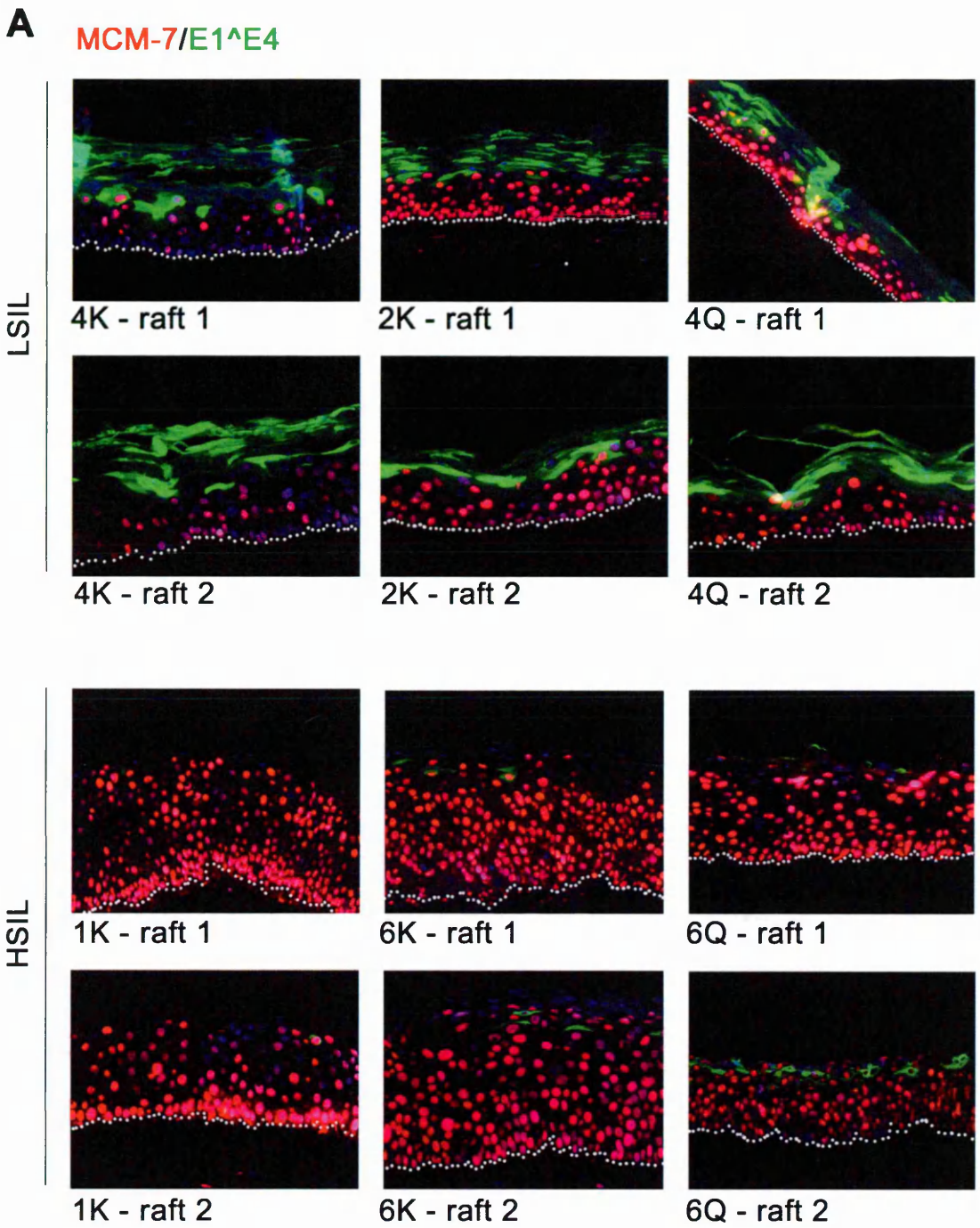
A
MCM-7/E1^E4
LSIL
4K - raft 1
2K - raft 1
4Q - raft 1
4K - raft 2
2K - raft 2
4Q - raft 2
HSIL
1K - raft 1
6K - raft 1
6Q - raft 1
1K - raft 2
6K - raft 2
6Q - raft 2

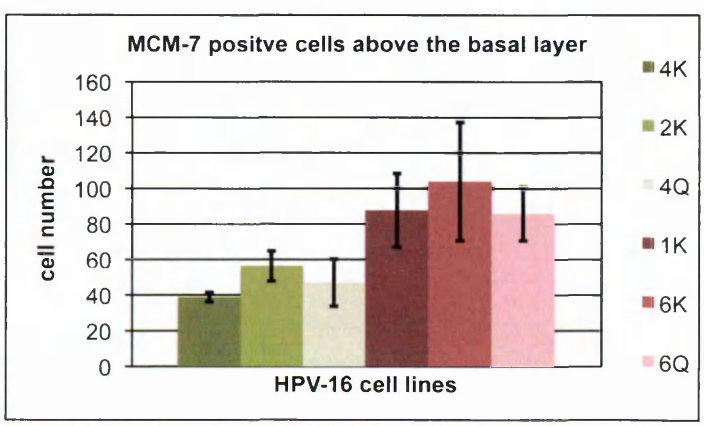
B
MCM-7 positve cells above the basal layer
cell number
160
140
120
100
80
60
40
20
0
HPV-16 cell lines
4K
2K
4Q
1K
6K
6Q

We also evaluated the reproducibility of L1 capsid protein abundance and virus productivity in replicate raft cultures (Figure 4.7). The mean of L1-positive cells of three sections for each raft culture was calculated, and the bar chart shows the mean of the means. The error bars represent +/- the standard deviation between the two replicate raft cultures (Figure 4.7B). The bar graph demonstrates that LSIL raft cultures on average contain much more L1-positive cells compared to HSIL-like raft cultures. We detected great variation in the number of L1-positive cells in raft culture 4Q. L1-positive cells are usually formed in the cornified layer and therefore we thought this inconsistency was potentially due to a variation in the degree of cornification at the top of the raft. We also detected L1-positive cells in HSIL raft culture 6Q but these were confined to sporadic pockets of E4-positive cells in the upper layers. It is worth mentioning that it is not untypical to find sporadic L1-positive cells in high-grade cervical lesions.

It was also interesting that we consistently identified raft cultures 4K (LSIL) and 6K (LSIL) as the two extremes with respect to both MCM-7 and L1 capsid abundance. This further suggests that the regulation of early oncogenes and/or the levels of early oncogenes in the epithelium can mark the region where late genes are expressed. From there we can conclude that the phenotypes presented in our HPV-16 episomal cell lines are reproducible with respect to their viral gene expression patterns. We are further able to consistently distinguish LSIL raft cultures from HSIL raft cultures based on observed differences in S-phase persistence and production of L1 capsid protein. This renders them valuable tools for future studies of HPV-induced neoplasia.

Figure 4.7 Reproducibility of L1 capsid expression in HPV-16 raft cultures with LSIL and HSIL phenotype.

(A) Each three HPV-16-positive episomal cell lines with either the LSIL or HSIL phenotype were differentiated for 14 days to produce two replicate raft cultures (raft 1 and 2), respectively. Raft culture sections were stained against HPV-16 L1 capsid protein (red) and HPV-16 E4 (green, #248). DAPI was applied as a nuclear counterstain (blue). The broken white line indicates the basal layer.

(B) In three separate sections from the raft cultures shown in (A) the number of MCM-7 positive cells above the basal layer was counted. The mean of MCM-7 positive cells for the three sections for each raft culture was calculated, and the bar chart shows the mean of the means of the replicate rafts. The error bars represent +/- the standard deviation between the two replicate raft cultures.

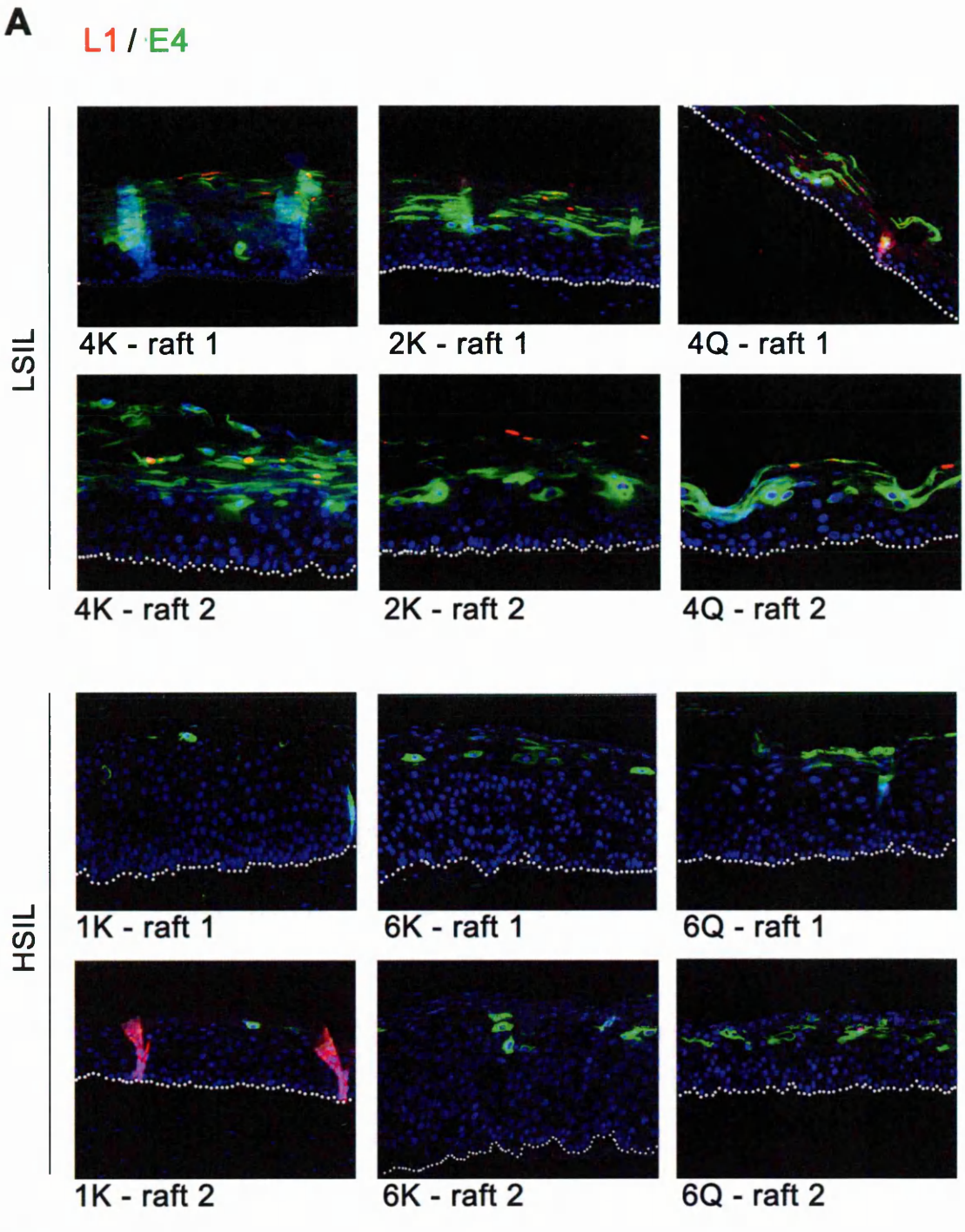
A
L1 / E4
LSIL
4K - raft 1
2K - raft 1
4Q - raft 1
4K - raft 2
2K - raft 2
4Q - raft 2
HSIL
1K - raft 1
6K - raft 1
6Q - raft 1
1K - raft 2
6K - raft 2
6Q - raft 2

B

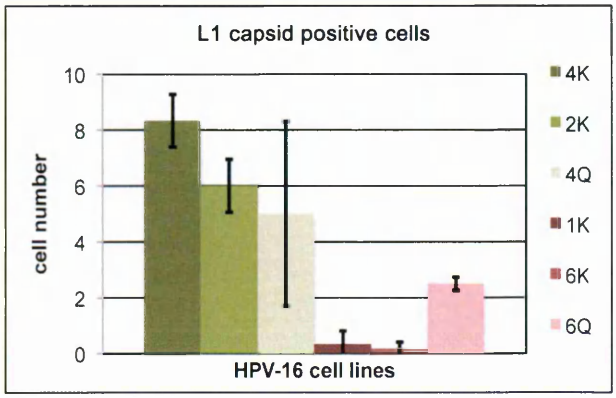
L1 capsid positive cells
cell number
10
8
6
4
2
0
HPV-16 cell lines
4K
2K
4Q
1K
6K
6Q

4.2.8 Early and late terminal differentiation is delayed in HSIL raft cultures

In HPV-16 raft cultures with detectable levels of L1 capsid protein expression (LSIL raft cultures) we have previously shown that early and late terminal differentiation followed a normal pattern of progression within the epithelium. We were also able to show that late E4 expression coincided with late terminal differentiation in the epithelium, specifically within the cells of the granular layer.

Previous studies have shown that the overexpression of the viral oncogenes E6 and E7 can affect the early and late stages of the cellular differentiation program. A delay or reduction in keratin expression and granular layer formation has also been correlated with high-grade HPV lesions, which do not support a complete HPV life cycle. We therefore wanted to evaluate if a delay in the terminal differentiation program occurred in the HSIL raft cultures. Secondly we wanted to evaluate if the delay in E4 and L1 expression was due to alterations in the terminal differentiation program.

To evaluate the early and late stages of the differentiation program in the HPV-16 raft cultures we applied keratin K10 and filaggrin antibodies to all six LSIL- or HSIL-raft cultures. In order to detect late viral gene expression. we stained for E4 protein expression. When we looked first at early stages of differentiation we found that HSIL-like raft cultures showed marked differences in the timing of K10 expression when compared to LSIL-like raft cultures. (Figure 4.8). In contrast to LSIL raft cultures where K10 expression commences just above the basal layer we detected a delayed K10 expression in HSIL raft cultures 1K and 6Q two to three cell layers above the basal compartment. In raft culture 6K we detected an even

more dramatic delay in early terminal differentiation, where K10 was first detected in the middle-third of the epithelium.

The onset of late terminal differentiation was also delayed in all HSIL raft cultures when compared to LSIL raft cultures (Figure 4.9). In HSIL raft cultures 6K and 6Q we detected a dramatic delay in filaggrin expression and a reduction of the overall size of the granular layer indicated by the amount of filaggrin positive cells. Although the granular layer in HSIL raft culture 1K was more extensive than in the other two HSIL raft cultures 6K and 6Q, similarly filaggrin was not detected until the final third of the epithelium.

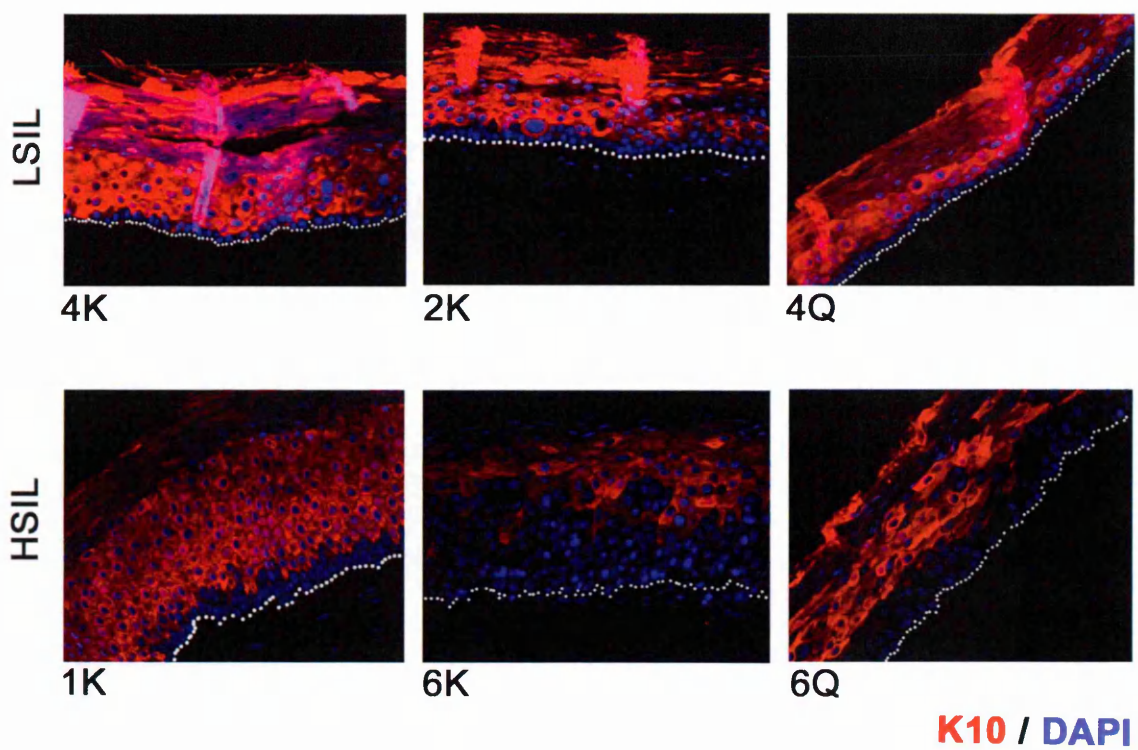

Figure 4.8. Early terminal differentiation in HPV-16 raft cultures with LSIL and HSIL phenotype.

To detect regions of early terminal differentiation in the epithelium sections of HPV-16 raft cultures with LSIL and HSIL phenotype, they were stained with an antibody against the early differentiation marker keratin K10. DAPI was applied as a nuclear counterstain (blue). The broken white line indicates the basal layer. K10 expression seemed to be overall delayed in raft cultures with HSIL phenotype compared to raft cultures with LSIL.

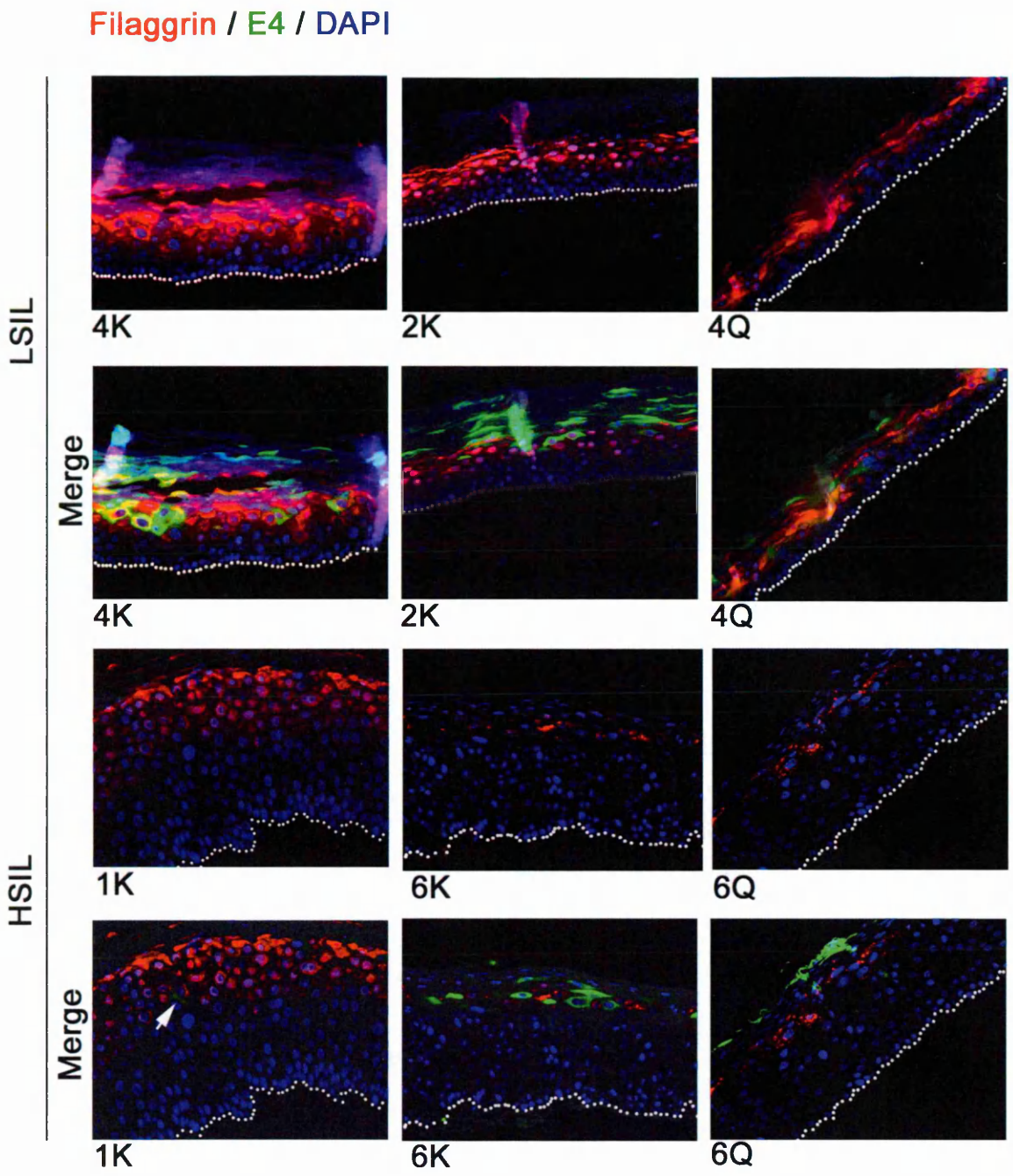

Figure 4.9. E4 expression and late terminal differentiation in HPV-16 raft cultures with LSIL and HSIL phenotypes

To detect regions of late differentiation in the epithelium, sections of HPV-16 raft cultures with LSIL and HSIL phenotypes were stained with antibodies against filaggrin (red) and late HPV-16 gene E4 (green, #248). DAPI was applied as a nuclear counterstain (blue). The broken white line indicates the basal layer. The white arrow in raft culture 1K identifies an E4 positive cell. The delay of late gene E4 expression in HSIL raft cultures seems to coincide with delayed filaggrin expression and late terminal differentiation

A delay in the formation of the granular layer also coincided with a delay in late E4 expression, as E4-positive cells were only first detected in this layer. We could however not correlate E4 abundance with the level of granular formation as HSIL raft culture 1K did not contain a higher level of E4-positive cells. This once again might suggest that the granular layer environment is favorable for E4 accumulation but it is unlikely that formation of the granular layer determines if the switch from the early to late gene expression will occur in this region.

We can conclude that in all HSIL raft cultures the terminal differentiation program is delayed compared to LSIL raft cultures that contain detectable numbers of L1-positive cells. We can also conclude that late viral gene expression is delayed and coincides with the onset of late cellular terminal differentiation in the epithelium. At this point however we cannot explain why the extent of the delay in terminal differentiation is different amongst the three HSIL like raft cultures. It is possible that alteration in the differentiation program are also linked to other viral induced pathological changes.

4.2.9 LSIL-like and HSIL-like HPV-16 raft cultures also contain pathological features of LSIL and HSIL

So far the identified phenotypic similarities between our system and low and high-grade cervical lesions are based on the viral gene expression patterns. However, the identification of LSIL and HSIL in medical screening programs is based primarily on a pathological diagnosis.

In lesions with LSIL, pathological changes are confined to the first third of the epithelium, whereas in lesions with HSIL, pathological changes are extended to the middle and final-third of the epithelium. The pathological changes of LSIL and HSIL include varying degrees of a) cellular hyperplasia (i.e. abnormal proliferation), b) cellular dysplasia (i.e. lack of squamous maturation), c) the lack of cellular polarity and d) pleomorphic nuclei which vary in size and shape.

We wanted to identify if pathological changes that occur in low and high-grade cervical lesions also occur in a similar fashion in the epithelium of our HPV-16 NIKS. To evaluate this, sections of HPV-16 raft cultures including the HPV-negative NIKS were stained with hematoxylin and eosin (H&E). This stain allowed us to visualize the described morphologies of the nucleus and cytoplasm within each epithelial layer.

It was first important to visualize the morphology of HPV-negative NIKS epithelium in order to show that pathological changes were not present in the absence of the virus. In raft cultures of HPV-negative NIKS, one or two layers of uniformly shaped nuclei could be seen in the basal compartment (Figure 4.10) and there was no

evidence of dysplasia. Similar to what is known about normal cervical and cutaneous tissues, nuclear abnormalities were not present above the basal compartment and normal squamous maturation and stratification also occurred above the basal compartment. Squamous maturation was also accompanied by a process of nuclear degeneration, which eventually presented as small uniform pycnotic[1] nuclei in the cornified layer. We therefore confirmed that no neoplastic changes were already evident in the HPV-negative NIKS epithelium.

In order to compare this to tissue with HPV-induced neoplasia, Figure 4.10 contains a cervical lesion with typical features of LSIL. In this lesion hyperplasia is evident in the first several layers, where cells fail to mature and seem to extend the basal layer. Their nuclei are pleomorphic and enlarged, which results in a high nuclear to cytoplasmic ratio. The cells in this region are also disordered and display a lack of polarity. In the middle of the epithelium, squamous maturation occurs and the cells become less dysplastic. This is accompanied by the presence of koilocytes, which are cells that represent a cytopathic effect of HPV viruses. Koilocytes typically contain darkened hyperchromatic nuclei, which is accompanied by a clearing of the cytoplasm. In the uppermost layer of this lesion then small pycnotic nuclei appear indicating the degeneration of nuclei.

We compared this lesion to the LSIL raft 4K and found that in addition to its LSIL-like viral gene expression patterns it also displays pathological features of LSIL. Similar to the cervical lesions with LSIL we found atypical nuclei in LSIL raft 4K to be confined to the first third of the epithelium. The first several layers include enlarged pleomorphic nuclei and a loss of cellular polarity is also evident in these

[1] The irreversible condensation of chromatin in the nucleus of a cell undergoing programmed cell death or necrosis

layers. The cells become less dysplastic above these layers, which is evident by squamous maturation presented as elongated cells in the middle-third of the epithelium. Koilocytes were however not as easily detectable in the raft culture sections. Nuclei were also less pronounced in the upper layers of raft 4K and which presents as pycnotic nuclei within the cornified layers. It should be noted that the cornified layers, which are only contained in cutaneous tissues, were extensive in this raft culture. This level of cornification suggested that the differentiation process began early on in the rafting process. In real life cutaneous tissue this layer would normally slough off when it is replaced by new cells, whereas in raft cultures this layer accumulates throughout the differentiation process.

We can now compare this to the pathology of cervical lesions and raft lesions with HSIL. In the cervical lesion with HSIL, increased hyperplasia is represented in more tightly packed layers of cells, which persists throughout the second to final third of the epithelium. The nuclei in all of these layers are pleomorphic and display a high nuclear to cytoplasmic ratio. The cells remain dysplastic until the final third of the epithelium where squamous maturation develops. Koilocytes are confined to the final third of the epithelium.

Similar to the HSIL cervical lesions with, HSIL raft culture 6K presented with an increase in tightly packed layers of pleomorphic nuclei, which extend throughout the first and second third of the epithelium. An extensive loss in cellular polarity is also evident starting from the basal compartment and persists throughout the epithelium. Squamous maturation did not occur until the last third of the epithelium. The cornified layer was less extensive which suggests that late

terminal differentiation was delayed and/or reduced in this epithelium relative to cell line 4K. We had previously identified that granular formation (late differentiation) in HSIL raft culture 6K is delayed and reduced in size when compared to LSIL raft culture 4K.

It is recognized that there are some variations between cutaneous and cervical/mucosal tissue and perhaps a more keratinizing tissue such as vaginal tissue could serve as a better comparison. However, we have shown that overall in this NIKS HPV-16 raft system we can correlate LSIL-like and HSIL-like viral gene expression patterns with their respective pathological grades.

Figure 4.10. Pathology of HPV-16 raft cultures with LSIL and HSIL phenotypes

Hematoxylin and eosin (H&E) were applied to raft culture sections of HPV-negative NIKS, HPV-16 raft culture 4K (LSIL) and HPV-16 raft culture 6K (HSIL)(For comparison H&E stained cervical sections of both LSIL and HSIL grades were taken from Branca, Ciotti et al. 2004.). HPV-negative NIKS display a normal pathology with small uniform sized nuclei in the basal compartment (MS). Normal stratification and cytoplasmic maturation occurs in the upper layers. This is accompanied by the degeneration of cellular nuclei, which are presented as small uniform pycnotic nuclei in the upper cornified layers (CL). Koilocytes are indicated by black arrows Both the LSIL cervical lesion and LSIL raft culture 4K displays a mild dysplasia (DC) in the first third of the epithelium. The nuclei are pleomorphic and a loss of cellular polarity is contained in this region. Normal stratification and cellular maturation occur in the middle and final-third of the epithelium. Small pycnotic nuclei are also present in the superficial and cornified layers (CL). The HSIL cervical lesion and HSIL raft culture 6K both display tightly packed basal-like cells, which extend through the final third of the epithelium. A loss in cellular polarity is evident throughout the first and middle-third of the epithelium. Cellular maturation is not evident until the upper two layers.

Cornified layer = CL

Mature squames = MS

Dysplastic cells = DC

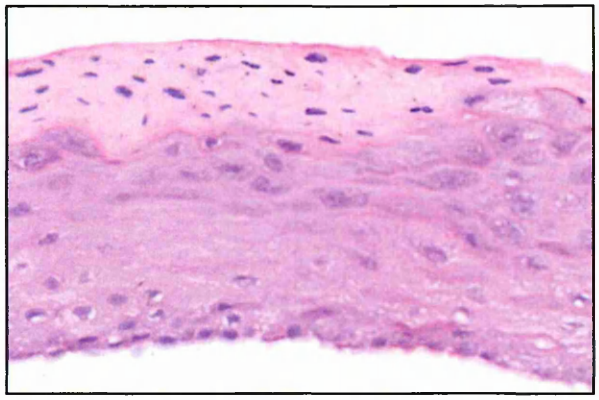

NIKS (- HPV)

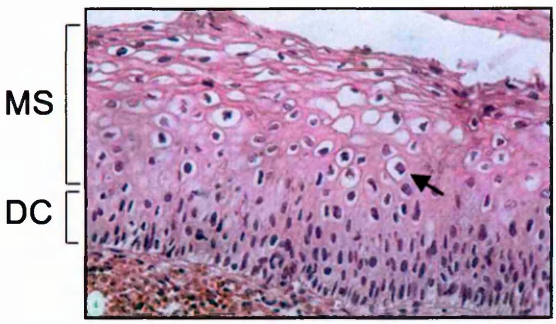

Cervical tissue (LSIL)
(+HPV-16)

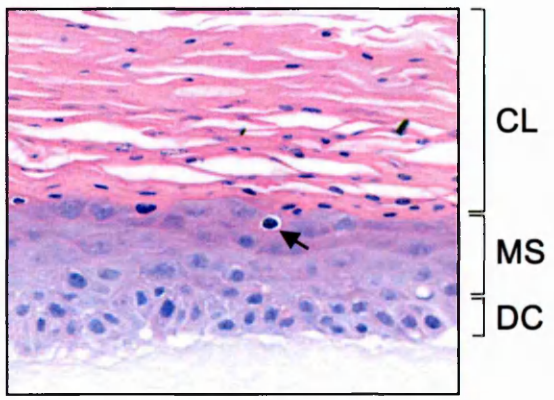

4K (LSIL)

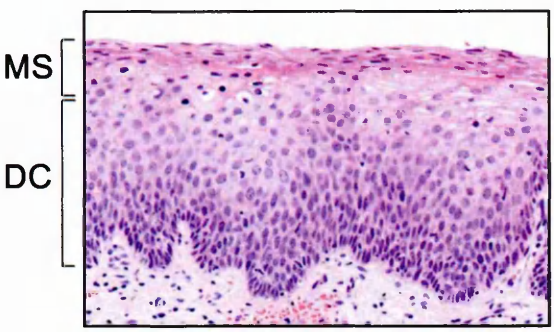

Cervical tissue (HSIL)
(+HPV-16)

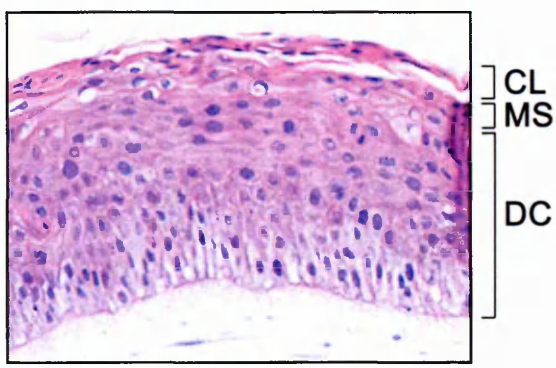

6K (HSIL)

4.2.10 p16 expression can be detected in cells in the upper layers of HSIL-like raft cultures but not in the upper layers of LSIL-like raft cultures

As mentioned before the identification of LSIL and HSIL phenotypes in cutaneous and cervical tissues relies heavily on a pathological diagnosis. However, the diagnoses are sometimes confounded by additional processes in the epithelium, such as inflammation. Due to these confounding factors many pathologists have adopted the use of a cellular marker in conjunction with the pathology, to diagnose the degree of neoplasia. The CDK4/CDK6 inhibitor, p16, has been shown to be a reliable diagnostic marker due to its accumulation in HPV-infected tissue (Klaes, Friedrich et al. 2001).

In normal tissue p16 prevents the phosphorylation of the Rb protein. The inhibition of Rb protein phosphorylation prevents entry in to the G1 phase of the cell cycle (Serrano, Hannon et al. 1993). A negative feedback loop through hypo-phosphorylated Rb then reduces p16 levels in order to allow for another around of proliferation to begin. During an HPV-16 infection the viral E7 oncogene degrades hypophosphorylated forms of the Rb protein and therefore p16 can accumulate in the cell (Li, Nichols et al. 1994). This suggests that p16 could be used as a marker of Rb protein degradation in the epithelium. It is important to mention that the reliability of p16 during diagnosis however has been entirely based on observational studies where the extent of p16 accumulation in the epithelial layers is shown to correlate with the grade of neoplastic severity. These studies have shown that in normal tissue, p16 is expressed at low levels and goes largely undetected. By comparison lesions with LSIL typically contain low levels of p16 in

the first third of the epithelium, whereas in lesions with HSIL, p16 is highly diffuse in the middle or final-third of the epithelium.

We therefore wanted to see if p16 could be detected in HPV-16 raft cultures according to our previous grading. To evaluate this, sections of all six raft cultures were stained with an antibody against p16 and additionally all sections were stained with hematoxylin to identify the cellular nuclei. In HPV-negative NIKS epithelium we detected p16 in sporadic basal cells but could not detect p16 above the basal compartment (Figure 4.11). In LSIL-like raft cultures we detected p16 in a sporadic number of basal cells and in sporadic cells within the second and third layers. Strikingly we detected p16 throughout the majority of the epithelium in HSIL raft cultures but with varying degrees of uniformity. For example, p16 was highly diffuse throughout HSIL raft culture 1K. In HSIL raft culture 6K we detected p16 in dense pockets of cells, which extended throughout the top layers of the epithelium however the staining was not as diffuse as in raft culture 1K. In raft culture 6Q we detected p16 in only sporadic cells however these cells were located throughout the upper layers of the epithelium. It was curious that p16 could also be detected in the cytoplasm of HSIL-raft cultures, and not in LSIL raft cultures. Because p16 can localize to both nucleus and cytoplasm this simply could be due to higher expression levels in these cells.

It was also surprising to see a sporadic distribution of p16 in the HSIL raft cultures as we expected its expression to mirror the diffuse staining of the E7 surrogate marker MCM-7. One explanation could be that Rb degradation does not always feature in the upper layers of the epithelium. The elevation of p16 however relies specifically on the degradation of Rb. Past studies have suggested that Rb degradation is mostly predominant in the basal layer where the degradation of

other Rb related pocket proteins lead to E2F activation and MCM expression in the suprabasal layers.

We conclude that all three of our LSIL raft cultures (4K, 2K, 4Q) and two of our HSIL raft cultures (6K and 1K) have typical p16 staining patterns that resemble those of cervical lesions with LSIL and HSIL, respectively. Although p16 staining patterns in 6Q are not as typical of high-grade cervical lesions, viral gene expression patterns together with pathological features place this raft culture in our high-grade category. This will lead us to further investigate if perhaps Rb protein degradation is not as prominent in this HPV-16 cell line, which would suggest MCM-7 to be a better marker of E7 detection in this system and possibly overall in HPV induced lesions.

Tables 4.1 and 4.2 summarise the raft characteristics for LSIL-like and HSIL-like raft cultures.

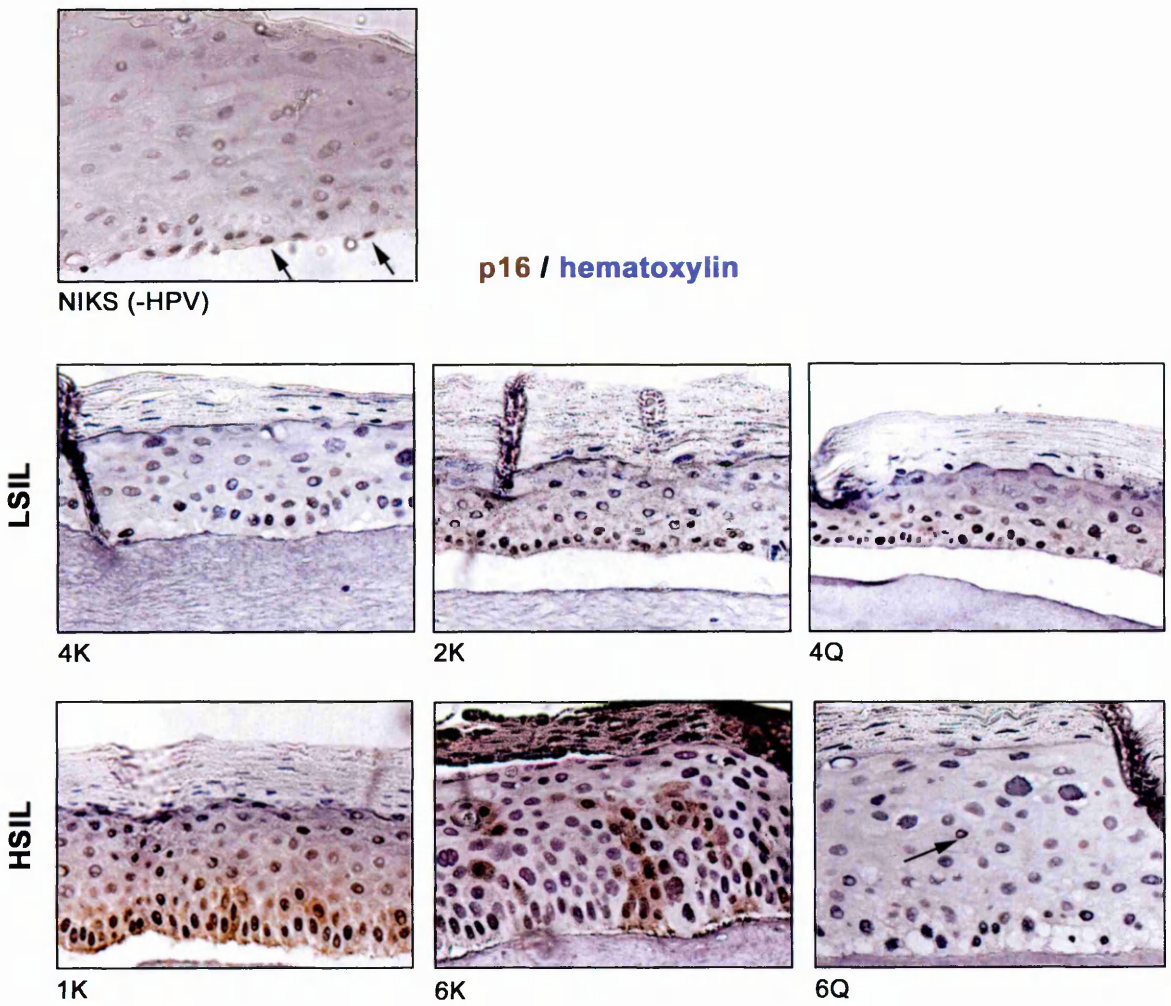

Figure 4.11 Detection of p16 in HPV-16 raft cultures with LSIL and HSIL phenotypes

HPV-negative NIKS raft cultures and HPV-16 raft cultures sections were stained with an antibody against p16 (brown). Hematoxylin was applied to identify cellular nuclei (blue). HPV-negative NIKS contain p16 in sporadic cells of the basal compartment (black arrows). In LSIL-like raft cultures p16-positive cells are sporadically located in the first and second layers. In HSIL-like raft cultures p16-positive cells are detected in most layers of the epithelium. Raft 1K contains highly diffuse p16 whereas raft 6K contains dense pockets of p16-positive cells. Raft 6Q contains highly sporadic p16-positive cells throughout the epithelium (black arrow).

Table 4.1 LSIL-like raft culture characteristics

HPV-16 Clone (passage number)	*2K (4-6)	3K (5)	*4K (4-6)	*4Q (4-6)	5K (5)	9Q (5)	13Q (5)
MCM-7	++	++	+	++	++	++	++
E4	++	++	+++	++	++	++	++
L1	++	++	+++	++	++	++	++
Timing of K10 expression	N	N	N	N	N	N	N
Timing of filaggrin expression	N	N	N	N	N	N	N
Number of times rafted/observed	3	1	3	3	1	1	1

(See key under table 4.2)

Table 4.2 HSIL-like raft culture characteristics

HPV-16 clone (passage number)	*1K (4-6)	*6K (8)	*6Q (4-6)
MCM-7	+++	+++	+++
E4	+	+	+
L1	-	-	+
Timing of K10 expression	D	D	D
Timing of filaggrin expression	D	D	D
Number of times rafted/observed	3	3	3

Key for Tables 4.1 and 4.2

* = HPV-16 cell lines chosen for more in depth analysis

MCM-7:
(+) = MCM-7 is expressed in a subset of cells within the first several layers
(++) = MCM-7 is expressed in the majority of cells within the first several layers
(+++) = MCM-7 is expressed in the majority of cells throughout the entire epithelium

E4:
(+) = E4 protein is expressed in a small number of cells in the uppermost layer
(++) = E4 protein is expressed in the majority of cells in the uppermost layers
(+++) = E4 protein is expressed in a small number of cells in the lower layers and in the majority of cell in the uppermost layers

L1: **(-)** = No L1 protein expression detected
(+) = L1 protein is rarely expressed in cells within the cornified layers
(++) = L1 protein is expressed in a small number of cells within the granular and cornified layers
(+++) = L1 protein is expressed in a greater number of cells within the granular and cornified layers

N = Normal when compared to HPV negative NIKS raft culture
D = Delay in raft epithelium when compared to HPV negative NIKS raft culture

4.3 Discussion

In Chapter 3 we had shown that the NIKS HPV-16 raft culture system models a productive HPV-16 infection of the cervix. We have now shown in Chapter 4 that the NIKS HPV-16 raft culture system also models the wide spectrum of HPV induced LSIL and HSIL. We have based these findings on the identification of viral gene expression patterns (i.e. MCM-7, E4 and L1) and pathological features that have been previously identified in cervical lesions of LSIL and HSIL grades. The respective HPV-16 cell lines have been phenotypically labelled as either LSIL-like or HSIL-like. Past studies in the field which have utilised this raft system, have not previously reported on this phenotypic variation. To our knowledge this phenotypic variation has not yet been identified in other HPV episomal systems.

We have also shown that HPV-16 episomal cell lines can reproduce their LSIL-like or HSIL-like gene expression pattern in repeated raft culture experiments. In addition LSIL and HSIL phenotypes are biologically reproducible within the NIKS cell line system as two different transfections yielded LSIL and HSIL-like cell lines (i.e. cell lines distinguished by Q and K). As these phenotypes are reproducible in independent transfections, it is possible that this system can be further developed as laboratory model of episomal HPV induced neoplasia.

As our HPV-16 cell lines are all at a low passage numbers we can conclude that the HSIL-like phenotype (i.e. high MCM-7 persistence) is not a consequence of long-term culturing. Past studies have suggested that E7 expression increases or becomes deregulated in cell lines that have reached high passage numbers. However, high passage numbers also led to viral integration, which likely explains the increase in E7 expression (Alazawi, Pett et al. 2002).

In our system, the phenotypic differences identified in early passage episomal cell lines, suggest that viral episomes potentially have different replication and/or transcription capacities following their early establishment in the host cell. This raises an important point more relevant to the time frame of neoplastic disease. Our results suggest that in real-life infection LSIL does not have to necessarily precede HSIL in the disease process. HSIL can therefore occur as an acute stage of infection. In personal communication with two pathologists (Rhona McVey, Manchester Royal Infirmary, Manchester, UK and Sue Ramachandra, Whittington Hospital; London, UK) it has been reported that many patients present with HSIL, at their first examination.

The phenotypic differences displayed in the NIKS HPV-16 raft culture system also show that E7 regulation can be highly diverse in the suprabasal compartment. Following immunohistochemical analysis, NIKS HPV-16 raft cultures presented with three patterns of MCM-7 expression that have been previously identified in mucosal lesions of LSIL or HSIL grades. Interestingly LSIL-like raft cultures presented with two distinct patterns of MCM-7 expression. One of these patterns being more typical of low-grade lesions associated with the low-risk type HPV-11 (Middleton, Peh et al. 2003). In raft culture 4K MCM-7 positive cells were mostly absent in the basal layer and were detected in small numbers in the suprabasal layers.

There are several possible explanations as to why some low-and high-risk viruses yield different levels of MCM-7 expression in the upper layers. In the case of both low and high-risk HPVs, It has been suggested that the E7 protein is continuously

driving S-phase re-entry in differentiating cells rather than preventing S-phase exit (Banerjee, Genovese et al. 2006) The ability of E7 to successfully drive cells into S-phase depends on several factors. S-phase entry is dependant on the ability of E7 to bind to and degrade hypophosphorylated Rb. In addition it has also been suggested that high levels of E7 are also needed to overcome the rise in the CDK2 and CDK4 inhibitors p21 and p27 (reviewed in (Doorbar 2006). p21 and p27 are likely elevated in the presence of E7, as a host defense mechanism, in order to prevent cellular replication in the differentiating layers.

It is established that E7 proteins of high-risk viruses have a higher affinity for Rb when compared to E7 proteins of low-risk risk viruses (Heck, Yee et al. 1992). This could explain why S-phase re-entry is less efficient in low-risk viruses. A second point is that low-risk viruses might have evolved to maintain steady levels of E7, which at times are not sufficient to overcome p21 and p27 levels induced by the cell. This has been suggested as a tactic of low-risk viruses, which is used to control proliferation (Banerjee, Genovese et al. 2006). This might further explain why low-risk viruses are less likely to cause high-grade disease and cancers.

Similar to what was described above for low-risk viruses it appears the virus in raft culture 4K is less efficient at inducing S-phase in differentiating cells. This raises the possibility that cell line 4K maintains a level of E7 expression that is not sufficient to consistently bypass p21 and p27 cell cycle inhibition or degrade Rb.

In contrast to this pattern, in LSIL raft cultures with pattern B, MCM-7 expression is more diffuse in the lower layers. This pattern is more typical of lesions induced by high-risk viruses such as HPV-16 (Middleton, Peh et al. 2003). This could indicate

that cell line 2K and 4Q contain sufficient levels of E7 to bypass CDK2 and CDK4 cell cycle checkpoints and therefore S-phase induction is more consistent in the upper layers.

Although there appears to be differences in E7 regulation in the lower layers of both LSIL-like raft cultures, early gene expression is tightly regulated in the upper layers in the case of both levels of S-phase induction. This appears to be a fundamental feature of all HPV viruses where early gene expression ends in order to carry out the productive phase of the life cycle. As we observed, both LSIL-like MCM-7 patterns correlated with L1 capsid protein expression.

In HSIL raft cultures MCM-7 expression persisted throughout the majority of the epithelium. This MCM-7 pattern is more typically detected in lesions caused by high-risk viruses. MCM-7 persistence is likely due to a deregulation of E7 expression from viral episomes, potentially leading to high levels of E7. These aspects will be discussed in more detail in Chapter 5.

LSIL and HSL gene expression patterns also show interesting features of early and late viral gene regulation. As shown earlier the end of MCM-7 compartment appears to identify when late gene expression beings. The order of gene expression is conserved however in both LSIL and HSIL lesions it appears that late gene expression is delayed relative to the levels of MCM-7 persistence. As observed with both cervical lesions and HSIL-like raft cultures, this delay in some cases leads to an incomplete life cycle. The switch between early to late gene expression is poorly understood. One possible explanation is that the delay in late gene expression could be due to splice factor regulation.

The cellular splice factor SRp20 is necessary for early gene expression, but at the same time represses late gene expression, including that of L1 capsid expression (Jia, Liu et al. 2009). In cervical lesions SRp20 is confined to the less differentiated layers where early genes would be expressed. SRp20 levels are subsequently reduced in the differentiated layers above, which coincides with late gene expression (Jia, Liu et al. 2009).

We have shown that the late differentiation program is delayed in HSIL-like raft cultures. This might indicate that splice factors like SRp20 are present at high levels throughout the epithelium and are not reduced until late differentiation occurs.

5.0 The analysis of monolayer LSIL-like and HSIL-like HPV-16 cell lines

5.1 Introduction

In Chapter 4 we have found that the viral gene expression patterns and pathological features of HSIL-like raft cultures were similar to that of high-grade cervical lesions. The fact that our HPV-16 raft model system can reflect these LSIL and HSIL phenotypes has given us the opportunity to ask new questions pertaining to the viral molecular basis of HPV-associated neoplasia.

The proposed viral mechanisms leading to HPV-induced neoplasia and HPV-related cancers have been heavily weighted on the E6 and E7 oncogenes as they have both been demonstrated to have transforming capabilities on the cell. Past studies have correlated the integration of E6 and E7 into a host chromosome with precancerous high-grade neoplasias and cancer (Klaes, Woerner et al. 1999) Separate studies have further shown that both E6 and E7 are more stably expressed following viral integration, presumably due the loss of viral regulatory elements during that process (Jeon and Lambert 1995). It has therefore been suggested that the deregulated and therefore persistent expression of E6 and E7 from viral integrants is necessary for cancer development.

More recently however it has been shown that 85% of precancerous high-grade lesions and 15% of HPV related cancers contain only viral episomes (Klaes, Woerner et al. 1999; Hafner, Driesch et al. 2008). It was further shown in these

high-grade lesions that E6 and E7 were only expressed from episomes. It is therefore possible that integration is likely to be more important for the final stages of cancer development and less important for the precancerous stages of neoplasia. This would therefore suggest that a deregulation of E6 and E7 expression could also occur from intact viral episomes.

Several studies using E6 and E7 transgenic mouse models have shown that persistent E6 and E7 expression is important for the development of neoplasia and cancer, however this has not been shown in systems that express endogenous levels of E6 and E7 from a full intact HPV-16 genome (Brake and Lambert 2005; Shai, Brake et al. 2007).

Other interesting questions are how cellular growth, viral copy number maintenance levels and E6 and E7 expression levels of the basal layer determine subsequent viral gene expression patterns, and if these lead to either LSIL- or HSIL-phenotypes. In this Chapter we have tried to address these questions using monolayer episomal LSIL- and HSIL- HPV-16 cell lines. Early passage monolayer cultures were used for these experiments as they represent the pre-differentiated basal layer of raft cultures, where early viral events (e.g. viral replication and viral oncogene expression) are likely to begin. Using monolayer LSIL-like and HSIL-like cultures we investigated in these cells if early E6 and E7 oncogene expression and/or cellular growth characteristics correlate with the levels of E7 surrogate marker MCM-7 persistence observed earlier in LSIL- and HSIL- raft cultures. In addition to investigating early viral oncogene levels we investigated in these early passage HPV-16 cell lines if early E7 oncogene expression was solely from episomal forms of the genome or if integrated forms of the genome also produced

a proportion of E7 transcripts. This would more fully address the hypothesis that early viral episomal establishment in the basal layer can lead to differences in viral oncogene expression levels thus potentially leading to more acute LSIL or HSIL phenotypes within the epithelium.

5.2 Results

5.2.1 HSIL-like monolayer episomal HPV-16 cell lines are not sensitive to contact inhibition

In Chapter 4 we showed that in raft culture, cell lines with HSIL phenotype maintained proliferating cells throughout the majority of the epithelium, which coincided with a delay in cellular differentiation and late viral gene expression. By comparison such cells were only detected in the first several layers of raft epithelium with LSIL phenotype, which coincided with a normal onset of cellular terminal differentiation and an earlier onset of late viral gene expression.

It is possible that the level of MCM-7 persistence in raft culture reflects a difference in the overall growth potential of LSIL- and HSIL-like cell lines. Therefore, we wanted to evaluate if HSIL-like cell lines have a higher growth potential than the LSIL-like cell lines. In order to compare the growth potentials of LSIL-like and HSIL-like cell lines, we seeded all six LSIL-like and HSIL-like cell lines at 1 x 10^5 cells per well in 6-well plates. Each cell line was harvested and counted in triplicates over a seven-day period (Figure 5.1). During sub-confluent growth densities (days one to four) all six HPV-16 cell lines maintained a growth advantage over the HPV-negative NIKS (Figure 5.1A), which was expected, as the viral oncogenes lead to higher levels of proliferation. At the end of the four-day period there were no differences between the total cell numbers between LSIL-like and HSIL-like cell lines (Figure 5.1B). This means that there is no significant difference in growth rate between the cell lines on the days one to four.

However, as the levels of cell to cell contact increased at days four to five we observed differences in the growth rates between LSIL-like and HSIL-like cell lines (Figure 5.1A).

The growth rate of all LSIL-like cell lines decreased following increased levels of cell to cell contact and reached growth saturation by day five. We also observed that the cells were completely confluent at day five. HPV-negative NIKS had a slower growth rate and reached growth saturation by day eight (data not shown). We also found that NIKS were also sensitive to contact inhibition at day eight and reached the same growth saturation cell number as LSIL-like cell lines.

In contrast to this a sharp increase in growth rate occurred for all HSIL-like cell lines as cell to cell contact increased (days four-five). All of the HSIL-like lines grew beyond the growth saturation point of HPV-negative NIKS and LSIL-like cell lines. When the HSIL cell lines reached growth saturation, their total cell numbers were approximately twice that of HPV negative NIKS and LSIL-like cell lines (Figure 5.1c). Two of the HSIL-like cell lines (1K and 6Q) reached saturation by day seven. However, we were unable to determine a saturation point for HSIL clone 6K at day seven, as its initial growth rate was slightly lower compared to the other HSIL clones 1K and 6Q. Additional experiments have shown that 6K and 6Q have similar growth saturation densities.

This data suggests that similar to HPV-negative NIKS, the LSIL-like cell lines can become contact inhibited when they reach 100% confluency. Normally, when keratinocytes reach maximum cell-to-cell contact cell proliferation is inhibited. and they default into their differentiation program. This is consistent with our LSIL-like

raft cultures, where we found that these cell lines can default normally into their differentiation program as the cells move above the basal layer (Figure 4.8). In contrast to this, HSIL-like cell lines were not initially sensitive to contact inhibition. Their ability to grow beyond complete confluency could potentially explain the observed delays in the terminal differentiation program in HSIL-like raft cultures as well as their ability to maintain MCM-7 expression throughout the raft culture epithelium.

A

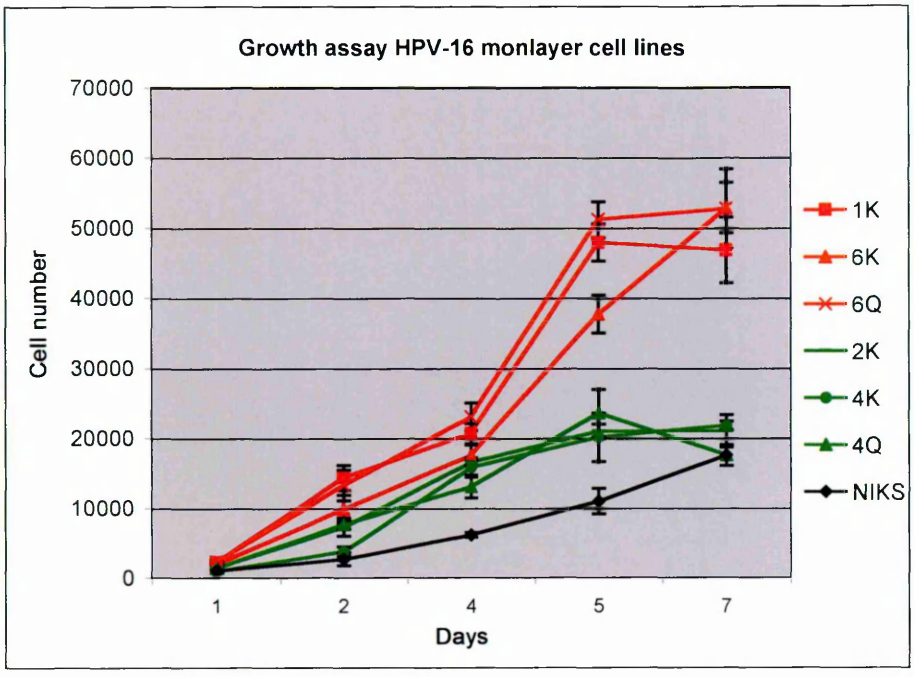

B

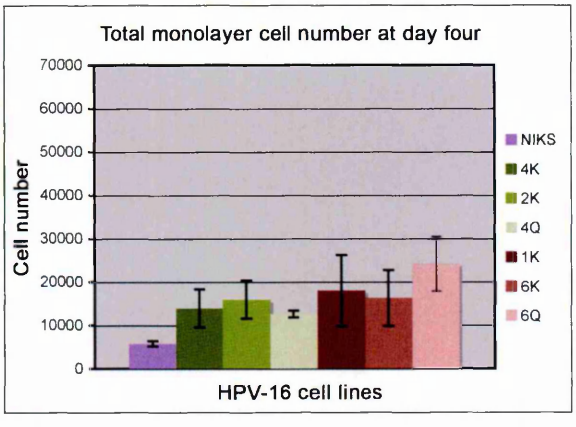

C

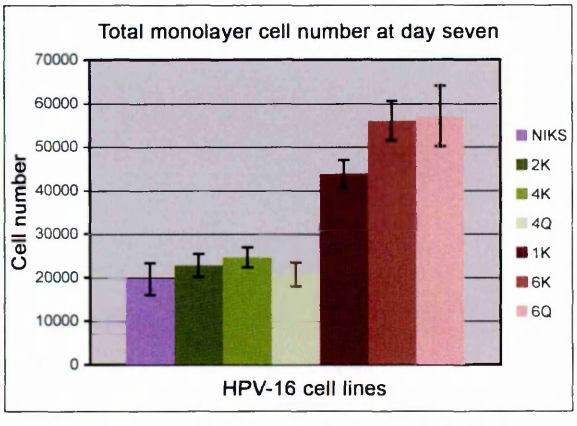

Figure 5.1.Growth characteristics of LSIL and HSIL HPV -16 cell lines

(A) Monolayer cultures of LSIL and HSIL cell lines were counted in triplicate over seven days until reaching post-confluent cell densities (day seven). The mean total cell numbers from triplicate counts for each cell line were plotted against days of growth. The error bars represent the standard deviation of the triplicate counts. LSIL cell lines approach confluent densities (day four-five) and further growth beyond confluence is inhibited (day five). An increase in growth rate is observed in HSIL cell lines as the cells approach confluence (days four-five) where growth is maintained after reaching the growth saturation points of LSIL-like cell lines. (B-C) The bar graphs show the mean cell numbers for LSIL and HSIL HPV-16 cell lines at day four (sub-confluence) and day seven (post-confluence). The error bars represent the standard deviation of the triplicate counts.

5.2.2 HPV-16 cell lines have similar morphologies prior to cell-cell contact but have different morphologies following cell-cell contact

After our observation that HSIL-like clones could proliferate beyond the cell saturation numbers of LSIL-like clones, we wanted to exclude the possibility that this was due to inherent differences in the size and morphology of the HSIL-like cell lines. We therefore visualized the morphologies of LSIL-and HSIL-like cell lines at sub-confluent (day three) and post-confluent levels (day seven) by phase contrast microscopy. Figure 5.2 includes a typical representation of the LSIL and HSIL-like cell lines at sub-confluent and confluent levels of growth.

In sub-confluent cultures HPV negative NIKS, LSIL cell line 4Q, and HSIL cell line, 6K, grew at similar densities and there were no remarkable differences in their sizes and morphologies. At post confluent levels, HSIL cell line 6K had a different morphology compared to NIKS and LSIL cell line 4K. This was evident by a more basal-like appearance and a high nuclear to cytoplasmic ratio in HSIL cell line 6K, which both indicated ongoing proliferation. In contrast, clusters of differentiating cells were apparent in LSIL cell line 4Q, where the nuclei looked degraded and less pronounced. These morphologies are typical of keratinocytes that have stopped proliferating.

We have therefore confirmed that HSIL-like cell lines did not grow to higher numbers at post confluent levels as a result of their inherent cell morphology. We further observed the onset of morphological differences between the LSIL and HSIL cell lines when they reach complete confluency.

Lastly, we made a very important realization, which lends to the relationship between monolayer growth characteristics at complete confluency and raft culture phenotypes. We observed that the cell density at confluence rather than at sub-confluence would likely be more similar to the cell density of the basal layer in raft cultures. This led us to consider that confluent monolayer cultures rather than sub-confluent monolayer cultures more closely mimic the cell environment of tightly packed basal layer of raft culture epithelium. It is therefore possible that the growth characteristics at complete confluency more closely reflect the growth potential of cell lines in raft culture.

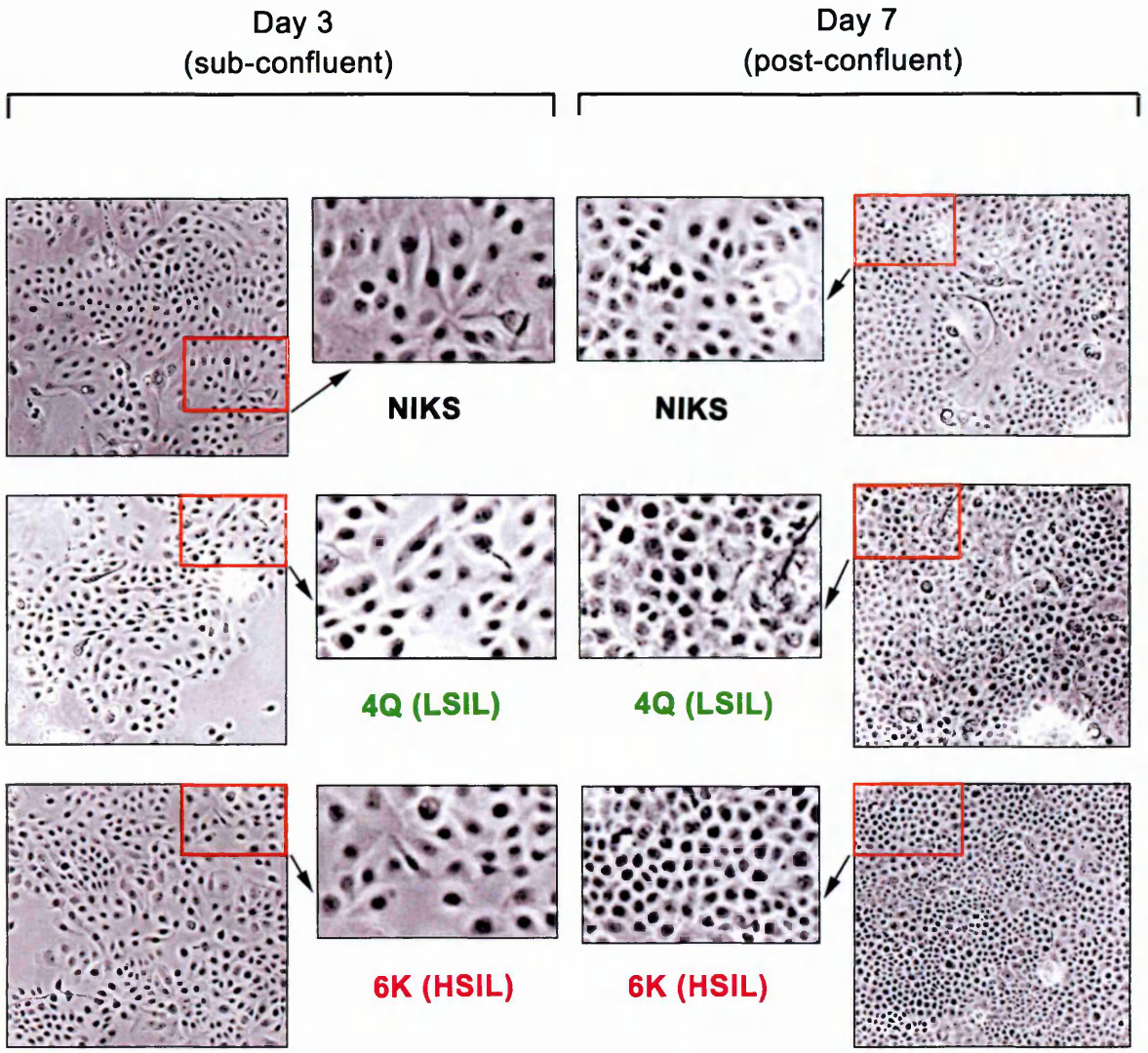

Figure 5.2 Cell morphology of LSIL-like and HSIL-like cell lines at pre and post confluent densities

The HPV-16 monolayer cell lines were analyzed at 20x magnification by phase contrast at day three (sub-confluence) and day seven (post-confluence). The smaller boxes contain an expanded view of the uniformly sized, marked bordered areas. The cell size and morphology of HSIL, LSIL cell lines and NIKS are similar at sub-confluent cell densities. At post-confluent cell densities NIKS and LSIL cell lines display the typical morphology of keratinocytes that have undergone growth inhibition. Their cytoplasms are enlarged relative to the size of the nuclei. At day seven LSIL cell line 4Q also shows evidence of differentiation where the nuclei appear dissolved. At post-confluent densities the HSIL-like cell lines remain basal-like with high nuclear to cytoplasmic ratios. This morphology is typical of cells that are still proliferating

5.2.2.1 HSIL-like cell lines display mitotic activity at post-confluent growth densities

In order to further assess the mitotic activity of our HPV-16 episomal cell lines we stained confluent monolayer HPV-16 cell lines with H&E. The use of H&E allows for the visualization of nuclear and cytoplasmic morphologies and mitotic figures.

Mitotic figures are a snapshot of the chromosomal aggregations that occur during the different stages of mitosis. Mitotic figures of cells that are in metaphase display chromosomes that are aligned at the metaphase plate (Figure 5.3A). Mitotic figures of cells in anaphase show previously paired chromosomes, which have separated to opposite poles of the cell. Atypical mitotic figures can form during abnormal mitotic spindle formation. Atypical mitotic figures include tripolar mitoses, which are commonly found in malignant cells and are associated with HPV-induced neoplasias (Figure 5.3A),

In H&E stained, confluent monolayer cultures, mitotic figures were rarely detected in any LSIL- cell lines and HPV-negative NIKS (Figure 5.3b). We detected active mitosis in approximately 0.2% (1 out of 400) of the LSIL-like cells and HPV-negative NIKS. LSIL-like cell lines and HPV-negative NIKS also contained low nuclear to cytoplasm ratios, which as explained earlier are typical for keratinocytes that have stopped proliferating. In contrast, all HSIL-cell lines were morphologically basal-like, with high nuclear to cytoplasmic ratios. We detected the highest number of mitotic figures in confluent cultures of HSIL-cell line 6K, where approximately 7.5% (30 out of 400) of cells were in active mitosis. The other two HSIL cell lines, 1K and 6Q, were less mitotically active, with approximately 4% (16 out of 400) and 3% (12 out of 400) mitotically active cells, respectively.

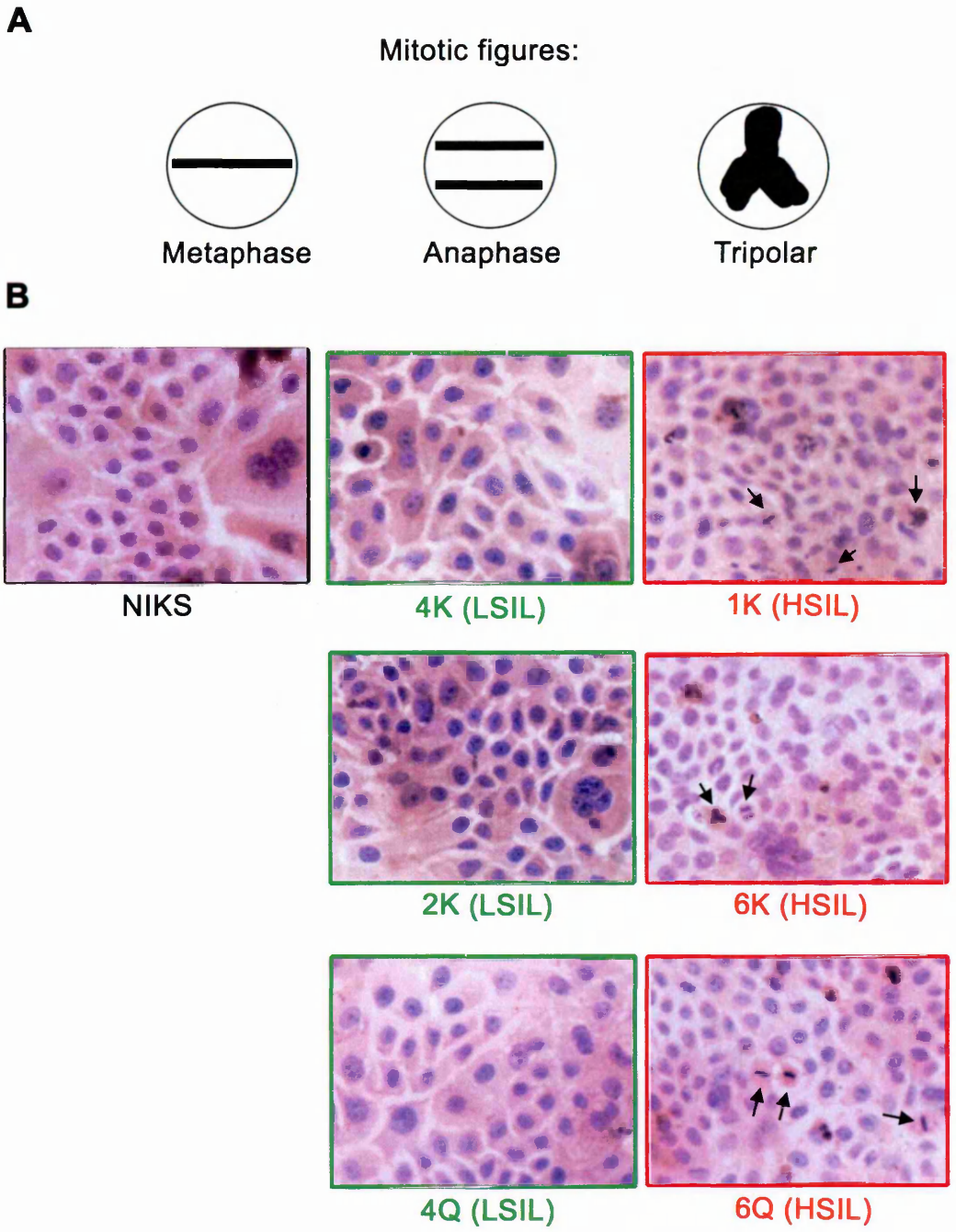

Figure 5.3 Mitotic activity of LSIL-like and HSIL-like cell lines at post-confluent growth densities

(A) This cartoon shows two types of mitotic figures, which can be detected when cells are in metaphase and anaphase. Tripolar mitoses are an example of an atypical mitotic figure, which is commonly found in HPV-induced neoplasias. (B) Cells at post-confluent densities were stained with H&E to observe nuclear and cytoplasmic morphologies and mitotic figures. NIKS and LSIL cell lines contain low nuclear to cytoplasmic ratios, reflecting a typical morphology of keratinocytes that have stopped proliferating. Mitotic figures are also extremely rare in these cell lines. HSIL cell lines display typical morphologies of cells that are proliferating. This is evident by their basal-like appearance and their high nuclear to cytoplasmic ratios. Mitotic figures are present in all HSIL cell lines, indicated by the arrows, and include atypical mitoses (e.g. tri-polar mitoses).

These numbers include also atypical mitotic figures, such a tripolar mitoses that we found in all three HSIL-like cell lines but not at all in LSIL-like cell lines or HPV-negative NIKS.

These results confirm our previous conclusion that HSIL cell lines remain mitotically active at fully confluent densities, whereas LSIL cell lines, just like HPV-negative NIKS, display the normal growth inhibitory characteristics of confluent keratinocytes.

5.2.3 HPV-16 E7 oncogene expression levels increase in HSIL cell lines at confluence

We had previously established using two methods that HSIL-like cell lines continue to proliferate at fully confluent densities, whereas LSIL-like cell lines stop proliferating at this point. Since the E6 and E7 oncogenes have been shown to drive proliferation in HPV-infected cells we wanted to test if the were in part responsible for the observed growth characteristics.

The E6 and E7 oncogenes have established consequences on the host cell, which allow the cell to maintain a proliferative state and also bypass apoptotic pathways. The E6 and E7 oncogenes are also associated with the reduction in levels of several cellular proteins that regulate proliferation with respect to cell-cell contact. For example it has been shown that the adherin junction (AJ) protein, E-cadherin, is delocalized from cell membranes and reduced in the presence of the viral oncogene E7(Wilding, Vousden et al. 1996; Yuan, Ito et al. 2009). In HPV-negative cells E-cadherin binds to cellular membranes during cell-cell contact, where it helps to maintain cellular adhesion (reviewed in (Balda and Matter 2003). It has also been shown that E-cadherin can bind to other cellular proteins at the cell membranes, which are important for cell cycle regulation. For example it can bind to Beta-catenin and retain it outside of the nucleus. Because nuclear Beta-catenin can transactivate pro-proliferative genes such as Cyclin D, this function of E-cadherin is considered to be anti-proliferative. Accordingly, the loss of E-cadherin has been associated with HPV-related neoplasias and various cancers and is therefore regarded as a tumour suppressor gene (Vessey, Wilding et al. 1995).

To evaluate E7 expression levels in the monolayer NIKS HPV-16 system, we first wanted to see if the levels of E7 expression in monolayer remained constant at sub-confluent (day three), confluent (day five) and post-confluent (day seven) culture conditions. To evaluate E7 expression we harvested each clone during the monolayer growth assay at days three, five and seven and evaluated E7 expression levels by western blot (Figure 5.4A). The bar graph reflects the relative change in band intensity compared to day three (Figure 5.4B). To compensate for unequal loading the E7 band intensities were also normalised against GAPDH band intensities.

We found that relative to day three, E7 band intensities increased between days three, five and seven in all HSIL-like cell lines. By comparison the E7 band intensities of LSIL-like cell lines either decreased or increased moderately between days three, five and seven. We therefore concluded that E7 gene expression increased more dramatically in confluent and post-confluent cultures of HSIL cell lines when compared to LSIL-like cell lines.

For each level of confluency we also wanted to compare the E7 expression levels between all HPV-16 cell lines. To do so we analysed the identical lysates of each cell line, side by side by western blot against E7 (Figure 5.4C). At sub-confluent levels of growth (day three) there was no correlation with E7 expression levels and the respective phenotypes. At confluent (day five) and post-confluent (day seven) levels of growth, all of the HSIL-like cell lines expressed higher levels of E7 when compared to LSIL-like cell lines.

We concluded that E7 expression increased and persisted at higher levels in confluent HSIL-like cell lines compared to LSIL-like cell lines. The increased E7 expression levels in confluent HSIL-like cultures correlated with their ability to proliferate beyond confluent cell densities. This might also be indicative of the level of E7 expression in the basal cells of HSIL-like HPV-16 raft cultures, which could explain their ability to remain in a proliferative state longer.

At this point we cannot explain why only HSIL-like cell lines have dramatically increased levels of E7 expression at complete confluency. It could be due to subtle differences in promoter activity or regulation acted upon by the host cell or differences in viral protein stability.

Interestingly, we also made the observation that E7 expression levels were considerably lower in LSIL cell line 4K when compared to the remaining five HPV-16 cell lines. Raft cultures of LSIL cell line 4K presented with a sporadic MCM-7 compartment (Pattern A), which closely resembles the MCM-7 patterns found in LSIL lesions cause by low-risk viruses such as HPV-11. Apart from confirming that initial E7 expression is a good indicator of the later proliferative potential in raft culture this suggests that in the case of HPV-16, E7 oncogene regulation is extremely variable. This then can potentially lead to a wide range of possible LSIL-like and HSIL-like viral gene expression patterns.

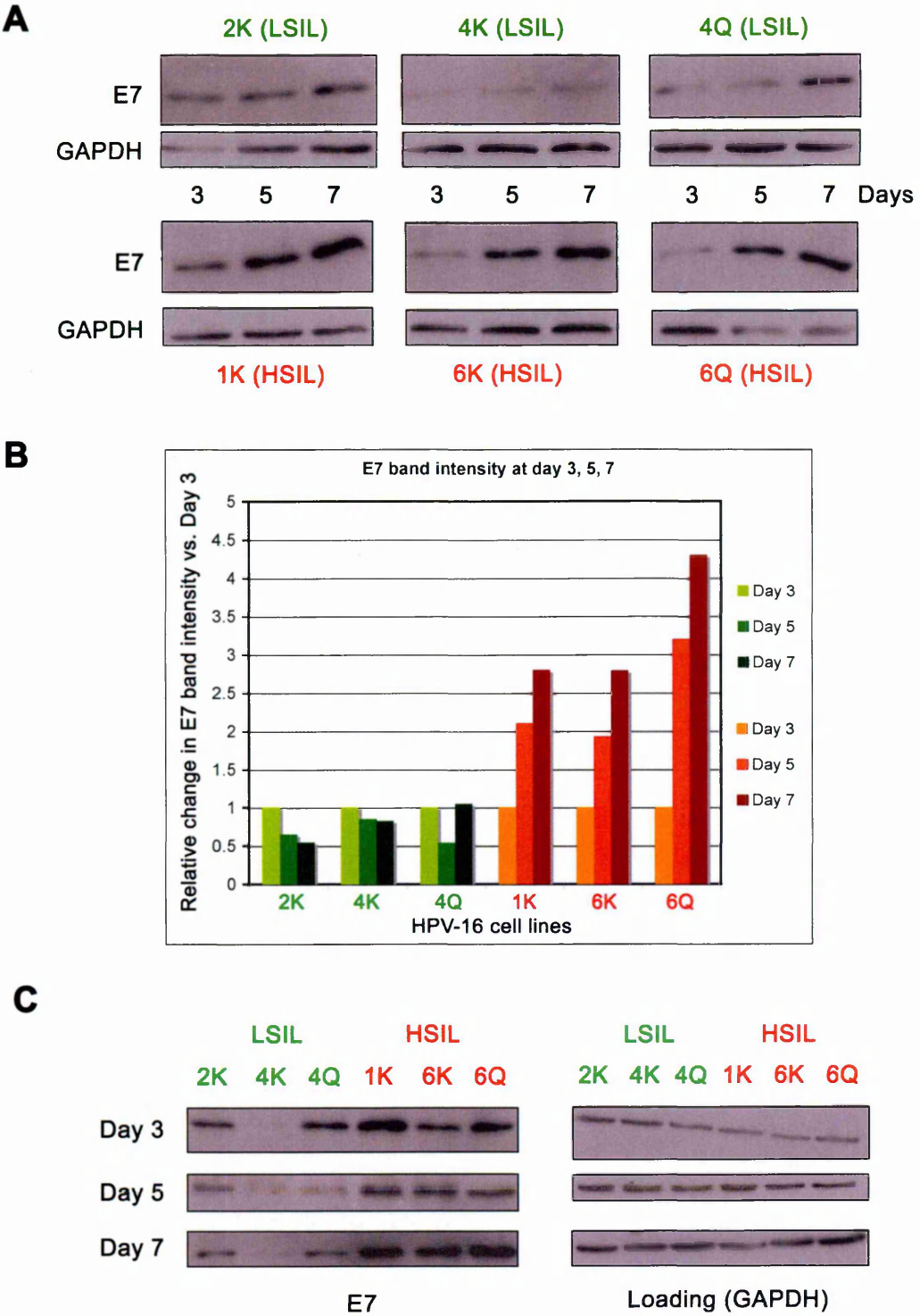

Figure 5.4. Relative changes in E7 expression levels over days three, five and seven in LSIL-like and HSIL-like cell lines.

(A) Each cell line was harvested at days three, five and seven to assess E7 expression levels by western blot. (B) The bar graph represents the changes in E7 band intensities within each individual cell line over days five and seven relative to day three. All E7 band intensities were normalised against the GAPDH band intensity for each individual cell line. (C) Western blots show side-by-side comparisons of E7 expression levels in LSIL and HSIL cell lines for days three, five and seven. Equal loading is shown by western blot against GAPDH.

5.2.4 HPV-16 E6 oncogene expression levels increase in HSIL cell lines at confluence

We had previously shown that at confluent and post-confluent growth densities viral oncogene E7 expression levels were higher in HSIL cell lines compared to LSIL cell lines. Next we wanted to evaluate if E6 oncogene levels increase in a similar fashion when HSIL-like cell lines reach complete confluency.

The HPV oncogene E6 interacts with and degrades several AJ proteins, which include the PDZ domain proteins, hDlg, Scribble and Z0-1 (reviewed in (Thomas, Narayan et al. 2008). PDZ proteins also bind to cell membranes during cell-cell contact and modulate cell growth and cell polarity. It has been shown that the degradation of PDZ proteins is likely to be important for episomal maintenance during the viral life cycle (Lee and Laimins 2004). Further reduced levels of PDZ proteins have been associated with a loss in cell polarity and abnormal proliferation when cell-cell contact is achieved. PDZ proteins are commonly reduced in HPV-related neoplasias and various cancers (Nakagawa, Yano et al. 2004).

To evaluate E6 expression in our HPV16 episomal cell lines we measured the E6 expression levels from the identical lysates taken at days three, five and seven by western blot (Figure 5.5A). The bar graph contains the relative changes in band intensity that occurred in each HPV-16 cell line, from day three to days five and seven (Figure 5.5B).

At confluent and post-confluent levels of growth, E6 band intensity decreased or remained similar to the band intensity at sub-confluency (day three). By comparison we detected a modest but marked increase in E6 band intensity in all HSIL-like cell lines at full confluency (day five) and post-confluency (day seven). When we directly compared E6 expression levels between each cell line at day three we found that there was no obvious correlation between E6 expression levels and the growth phenotype (Figure 5.5C). In contrast at complete confluency (day five) and post confluency (day seven), E6 expression levels were slightly higher in all HSIL cell lines compared to the LSIL cell lines.

From these observations we conclude that both E6 and E7 levels increased and persisted at higher levels in fully confluent cultures of HSIL cell lines when compared to LSIL cell lines.

However, overall we found that E6 levels did not rise proportionally to E7 levels and we did not detect the same relative differences in HSIL cell lines to LSIL cell lines. We expected to see proportional rises of the two oncogenes as they are transcribed from a single bicistronic message. Although this could be attributed partly to technical difficulties, this may also hint at differences in E6 and E7 regulation. This could either happen at the RNA level by transcript processing and/or splicing. Alternatively this could point to differences in protein stability of E6 and E7, which occur at complete confluency.

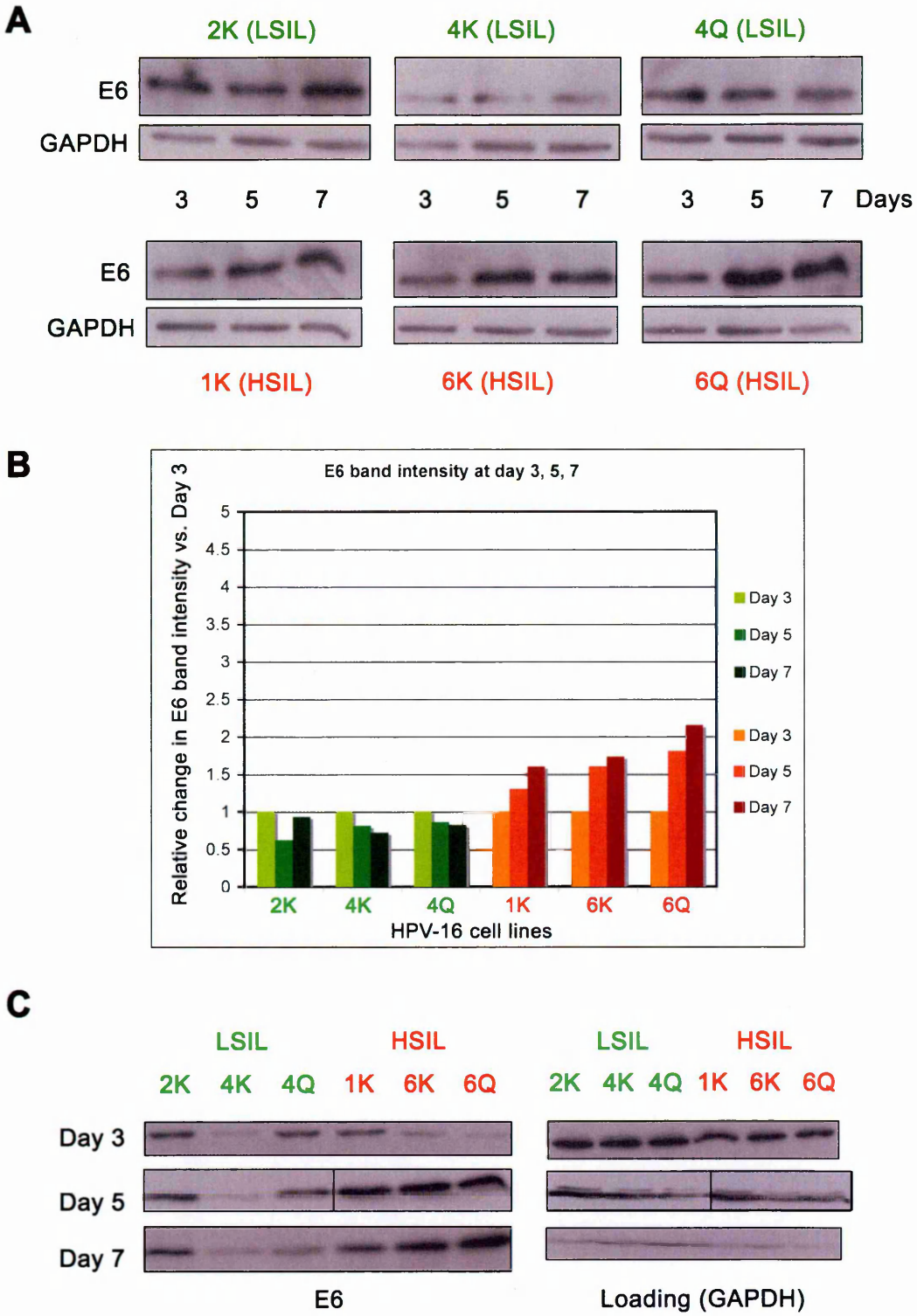

Figure 5.5 Relative changes in E6 expression levels over days three, five and seven in LSIL-like and HSIL-like cell lines.

(A) Each cell line was harvested at days three, five and seven to assess E6 expression levels by western blot. (B) The bar graph represents the changes in E6 band intensities within each individual cell line over days five and seven relative to day three. All E6 band intensities were normalised against the GAPDH band intensity for each individual cell line. (C) Western blots show side-by-side comparisons of E6 expression levels in LSIL and HSIL cell lines for days three, five and seven. Equal loading is shown by western blot against GAPDH.

5.2.5 The E7 oncogene is expressed from an episomal form of the HPV-16 genome in LSIL-like and HSIL-like HPV-16 cell lines.

In previous studies E6 and E7 viral integrants versus intact 8kb episome have been detected in the majority of HPV-related cancers and also in a percentage of pre-cancerous HPV-induced high-grade lesions. It further has been shown that the stable expression of E6 and E7 following integration can lead to chromosomal abnormalities, which pushes the cells further through the transformation process.

More recently alternative molecular assays, such as Amplification of Papillomavirus Oncogene Transcript (APOT), have been used to distinguish if E7 transcripts are produced from episomal versus integrated forms of the viral genome. Several studies using the APOT method have surprisingly found that the majority HPV-induced high-grade lesions contain E7 transcripts that are produced from only the episomal form of the virus. In one study the APOT method identified that in 85% of the lesions with HSIL, E7 transcripts were produced from only episomal forms of the virus (Klaes, Woerner et al. 1999). In contrast, in the majority of carcinomas in-*situ* they have found that E7 transcripts were produced predominantly from integrated viral genomes. Therefore it has recently become more accepted that the integration of E6 and E7 is likely to be a later event in the pathological process and more important for the final stages of cancer development.

We had previously shown by Southern blot that all of the HPV-16 cell lines contained predominantly episomal forms of the HPV-16 virus. We decided to use the APOT assay as a way to ask more specifically if oncogene E7 expression

came from episomal or integrated forms of the virus. The APOT method specifically involves RT-PCR analysis of two primer sets, which are specific for the E7 ORF and the early viral poly (A) region, which lies downstream of E7. In this method, if E7 transcripts are created from a non-disrupted episomal form of the HPV-16 genome these primers will amplify a single 1.1 kb cDNA fragment. However, if E7 transcripts are created from multiple E7 integration sites within the cellular genome, a series of different size fragments is generated.

To conduct our APOT experiment we used RNA extracts from sub-confluent cultures of each HPV-16 cell line. The APOT procedure resulted in the generation of a single 1.1 kb band for all three LSIL and HSIL clones (Figure 5.6). By comparison multiple bands were generated from our positive integration control sample.

These results confirm that E7 transcripts are produced from episomal forms of the HPV-16 genome in both LSIL-like and HSIL-like cell lines. This further suggests that differences in E7 viral gene expression in high-grade lesions could arise from differences in episomal copy number availability or differences in early promoter regulation, rather than E6 and E7 integration. Future work will also address if E6 and E7 transcript levels also correlate with E6 and E7 protein levels.

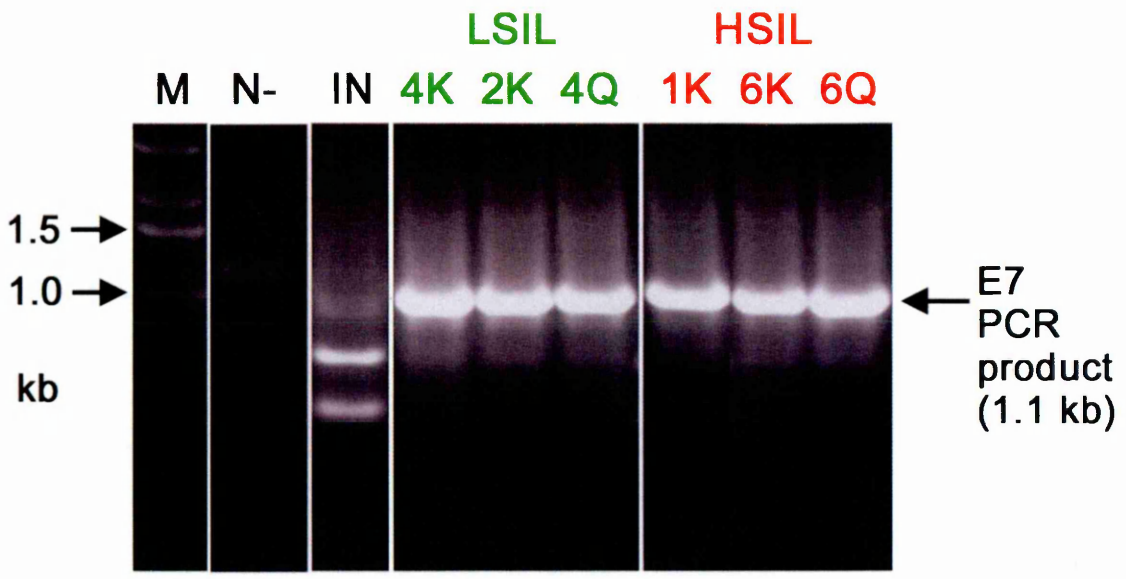

Figure 5.6. APOT analysis of E7 transcripts from HPV-16 monolayer cell lines (in collaboration with Emilio Pagliarulo, NIMR, London, UK)

The agarose gel shows a single amplified 1.1 kb E7 PCR product in all LSIL and HSIL cell lines, which indicates that E7 transcripts have come from an intact episome. For the DNA marker (M) the size of two bands is shown. The integrated control (IN) contains several amplified bands, which represent E7 transcripts, which are produced from several E7 integration sites in the host genome. HPV-negative NIKS (N-) were used as a negative control. All tested HPV-16 cell lines show only the 1.1kb amplification product indicative of episomal forms of the viral genome.

5.2.6 LSIL-like cell lines are more likely to contain higher viral copy numbers per cell than HSIL-like cell lines

We had previously shown that E7 transcripts were produced from only episomal forms of the virus in both LSIL and HSIL-like HPV-16 cell lines. This led us to investigate if episomal copy numbers in LSIL-like and HSIL-like lines account for the differences in E6 and E7 protein expression at complete confluency. Past studies have correlated the development of HSIL with a high viral load. However the majority of these studies were assessing the viral DNA levels of cells taken from cytological smears. These cells were taken from the top of the lesion and therefore their copy numbers did not necessarily reflect the viral DNA replication levels from the basal layer. However, using our monolayer HPV-16 cell lines we were able to assess the viral DNA replication levels, which would more closely resemble those found in the basal layer, where E7 expression is initiated.

To evaluate the viral copy number per cell in monolayer HPV-16 cell lines we used Q-PCR methods on total genomic DNA. In order to detect HPV-16 DNA we used primers specific for the HPV-16 E4 ORF. In order to quantify the total number of cells in each reaction we used primers specific for cellular GAPDH. We isolated the total genomic DNA from each cell line on day four of the growth assay, because this time-point was likely to reflect downstream expression levels of E7 protein one day later at complete confluency (day five). In order to be statistically accurate we harvested each cell line in triplicates and also each cell line was grown separately in two more independent cell cultures to test for biological reproducibility. The mean from these nine independent samples was calculated for each cell line.

Due to the fact that we could not run all nine samples from every cell line on the same plate, we carried through one identical sample in each run. All of our copy number values were then normalised to this sample. The bar graph in Figure 5.7 shows the means of all nine samples for each cell line. The error bar represents the standard deviation of the mean.

Surprisingly, the LSIL cell lines on average had higher HPV copy numbers per cell, when compared to HSIL-like cell lines. We did however find that HPV-16 copy numbers varied more in the LSIL-like cell lines. We therefore conducted an unpaired t-test on all LSIL-like and HSIL-like cell lines. When we conducted statistical test between individual cell lines we found that in most comparisons LSIL and HSIL cell lines had significantly different copy numbers. We also found that overall LSIL-like cell lines as a phenotypic group have significantly higher copy numbers when compared to the copy numbers of HSIL-cell lines. This suggests that cells that maintain high copy numbers are more likely to correlate with LSIL phenotypes.

One possible explanation for this is that high copy numbers might lead to more controlled and therefore lower levels of E7 expression, due to higher levels of the HPV-16 E2 protein. It is widely established that the E2 replication protein can bind to several sites within the HPV-16 LCR, which then can lead to the repression of the early promoter and early oncogene transcription. However it has also been shown that high E2 levels are needed to repress transcription (Steger and Corbach 1997). A lower copy number could therefore cause low E2 protein levels, which would possibly not be sufficient to repress E7 transcription.

To test this hypothesis we attempted to evaluate E2 protein levels in all six monolayer HPV-16 cell lines. We were however unable to detect endogenous levels of E2 with the current available E2 antibodies.

A

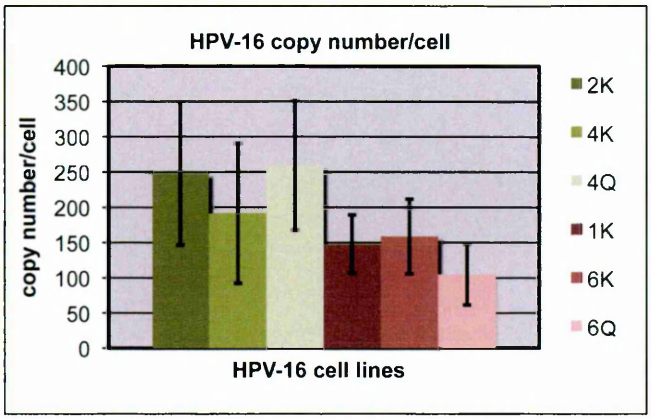

B

Data	P value	Significance = p < 0.05
2K vs 4K	0.151	Not significant
2K vs 6K	0.003	Significant
2K vs 6Q	0.0002	Significant
2K vs 1K	0.0002	Significant
2K vs 4Q	0.151	Not significant
4K vs 6K	0.154	Not significant
4K vs 6Q	0.0144	Significant
4K vs 1K	0.0127	Significant
4K vs 4Q	0.0088	Significant
6K vs 6Q	0.03	Significant
6K vs 1K	0.0192	Significant
6K vs 4Q	0.0001	Significant
6Q vs 1K	0.986	Not significant
6Q vs 4Q	0.0001	Significant
1K vs 4Q	0.0001	Significant

Data	P value	Significance = p < 0.05
All values of LSIL vs. all values of HSIL	0.0001	Significant

Data	P value	Significance = p < 0.05
Means of LSIL vs. means of HSIL	0.025	Significant

Figure 5.7 HPV-16 viral copy numbers

(A) Quantitative-PCR was used to detect the HPV-16 DNA copy numbers per cell in LSIL and HSIL cell lines. The bar graph shows the mean copy numbers/cell values for each cell line, from nine individual samples. The error bar represents (+/-) standard deviation of copy numbers values from the nine samples. (B) An unpaired T-test was conducted to show the significance of the measured differences of HPV-16 copy numbers between LSIL and HSIL cell lines. The table below contains the respective P-values. All values with $p<0.05$ were considered significant.

5.2.7. Cellular p53 expression levels are more reduced in HSIL-like cell lines compared to LSIL-like cell lines when at post-confluent monolayer growth densities

So far we have shown that the levels of the E6 and E7 oncogenes correlate with the level of MCM-7 persistence in raft culture, validating the use of MCM-7 as E7 surrogate marker. One possibility is that the level of MCM-7 persistence could be directly due to the reduced levels of the main E6 and E7 cellular binding partners Rb protein and p53. E7 can bind to Rb protein and induce its degradation. This is critical, because Rb protein allows the transcription factor E2F to remain in an active state, which then leads to the expression of MCM-7 and G1 to S-phase entry. Therefore it is conceivable, that E7 expression can lead to Rb protein degradation, activate E2F, which increases MCM-7 expression and cell proliferation. The activation of E2F however also causes increased expression of p16, which normally then antagonizes Rb protein function in cell cycle regulation. Rb however then degrades p16 in order to ensure the cell cycle can proceed again. In the case of Rb degradation p16 is not reduced and therefore accumulates in the cell. Accordingly, it has been shown in the case of HPV infection that Rb degradation is inversely related to p16 levels in the cell.

Another cellular protein marker that is changed after HPV infection is the tumour suppressor gene p53. As a result of continuous Rb protein degradation and MCM-7 induction by viral E7 it has been shown that cells will express high levels of p53. During cellular stress p53 can act as a G1 to S-phase checkpoint protein, which prevents the cell from proceeding through S-phase. In a separate pathway p53 can also induce cellular apoptosis. To counteract these effector functions of p53 during an infection, the virus has developed a way to degrade p53 by the action of

the E6 oncogene. This happens through ubiquitination and proteasomal degradation of p53.

Because of the described biological relationships and due to the lack of good E6 and E7 antibodies, Rb protein and p53 degradation have been used as markers for E7 and E6, respectively. However, it has never been shown before whether the levels of Rb protein and p53 degradation exactly correlate with E7 and E6 protein levels. To test this for the time in the context of the NIKS HPV-16 system we evaluated if the level of Rb protein and p53 degradation in each cell line correlates with their respective E6 and E7 levels. Also, we looked if this correlated with the level of MCM-7 persistence observed in their raft cultures.

In order to evaluate this, we used the identical lysates from cells harvested at day three, five and seven from our previous growth assays for Western blot against Rb protein, p16 and p53. At day three and five, Rb protein degradation did not correlate with E7 levels or the level of S-phase persistence in raft culture (Figure 5.7). We did however find that as expected p16 was inversely related to Rb protein levels. At day seven Rb protein levels were decreased in all cell lines whereas there were no dramatic changes in p16 levels compared to day five. We further concluded that the level of Rb protein degradation did not correlate with the level of MCM-7 persistence.

When we evaluated p53 levels at day three and five, we found that they were were consistently lower in all HPV-16 cell lines compared to HPV-negative NIKS. However, there did not seem to be a correlation with their respective E6 levels.

Interestingly, at day seven, p53 was reduced more in the HSIL- cell lines compared to the LSIL cell lines. Furthermore, this correlated nicely with elevated E7 and E6 levels at this time point.

In summary the data suggests that the increased levels of E6 and E7 by day seven allowed for the further reduction of both Rb protein and p53 in HSIL-like cell lines. As stated earlier it is unlikely that reduced Rb levels directly lead to higher levels of S-phase persistence or growth inhibition as we found it to be was degraded in both LSIL and HSIL cell lines. It is more remarkable that p53 levels are lower in post-confluent HSIL cell lines compared to LSIL cell lines.

It is unlikely that MCM-7 persistence in HSIL raft cultures is due to the loss of p53-related G1 phase CDK4 checkpoint pathways. As Rb levels are already degraded in all of the HPV-16 cell lines, the G1-S-phase transition would likely proceed, even in the presence of high p53 levels. However, it is possible that we have identified a new cellular marker that can be used to distinguish between LSIL and HSIL lesion.

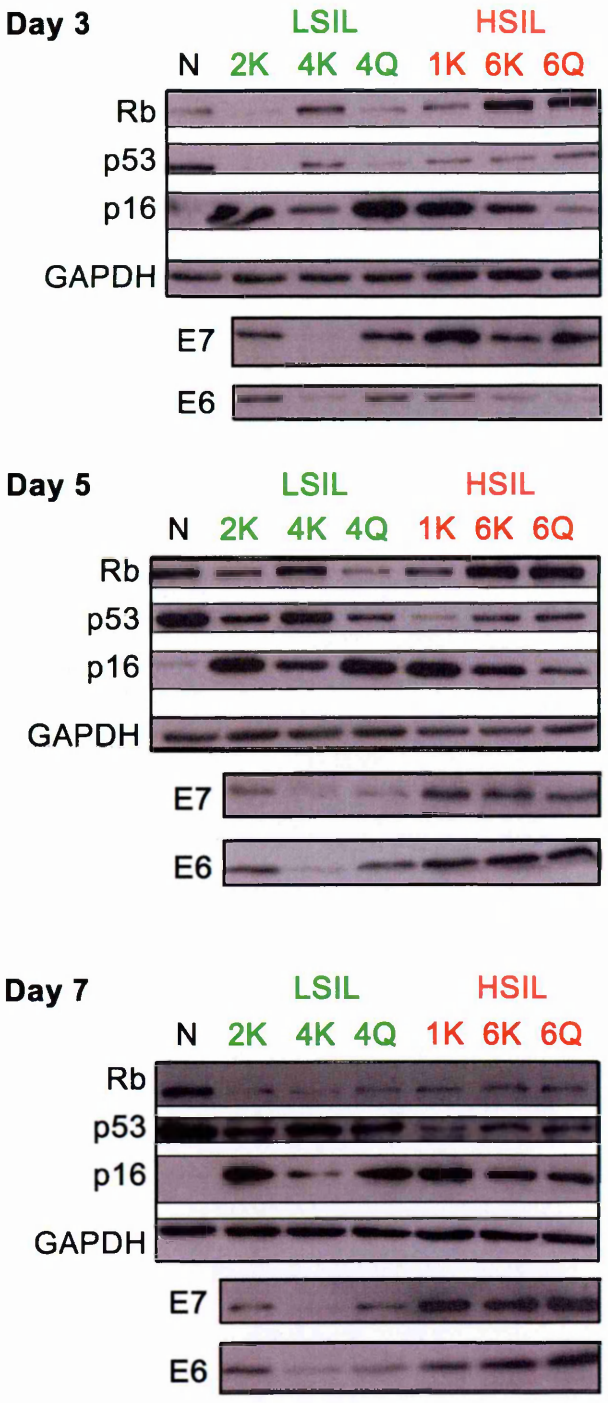

Figure 5.8. Expression of E6 and E7 binding partners in LSIL and HSIL cell lines

Rb, p53 and p16 protein expression levels in HPV-16 cell lines were assessed by western blot. Expression levels for each protein were assessed on days three (sub-confluence), five (confluence) and seven (post-confluence) of the previous growth assay. The respective E6 and E7 protein expression levels at the same time points are shown below (identical with the data from figures 5.3 and 5.4).

5.2.9 Beta-catenin activity is higher in HSIL-like cell lines

We had previously shown that HSIL-like cell lines continued to proliferate when cell-cell contact was established, whereas LSIL-like cell lines were sensitive to contact inhibition. The E6 and E7 oncogene levels also increased and persisted at higher levels in confluent HSIL-like cell lines compared to LSIL-like cell lines.

One explanation for this is that an increase in E6 and E7 levels at cell contact allowed HSIL-like cell lines to bypass contact inhibition pathways. As mentioned earlier, E7 and E6 oncogenes can reduce the levels of adherin junction proteins such as E-cadherin and Scribble, respectively. The reductions in these proteins lead to a loss in G1 to S-phase inhibition. One way that adherin junction proteins regulate S-phase at cell-cell contact is through their ability to sequester Beta-catenin from the nucleus (reviewed in Balda and Matter 2003). Additionally, Beta-catenin is also tightly regulated by the canonical Wnt pathway and by adherin junction proteins as a measure to control cell proliferation. When Beta-catenin is active, it binds to the T-cell factor/lymphoid enhancer (TCF/LEF) transcription factors in the nucleus, by use of a specific binding site on TCF/LEF complex (reviewed in (Huelsken and Behrens 2002). The newly formed Beta-catenin/TCF complex then transactivates the expression of several genes such as Cyclin D and c-Myc, which lead to proliferation. When cell-cell contact is established Beta-catenin is degraded or is sequestered to adherin junctions to prevent further proliferation.

Recent work has shown that Beta-catenin activity is higher in NIKS that overexpress the E6 and E7 oncogenes, when compared to HPV-negative NIKS (personal communication with Kenneth Raj, NIMR, London, UK). We therefore

wanted to evaluate if perhaps Beta-catenin activity was elevated more in HSIL-like cell lines which might lead to their ability to maintain proliferative capabilities at increasing cell densities.

To test this we transfected sub-confluent LSIL-like cell lines, HSIL-like cell lines and HPV-negative NIKS with the Topflash *Photinus* luciferase reporter plasmid. The Topflash plasmid contains the specific TCF/LEF binding site for Beta-catenin. The *Renilla* luciferase reporter plasmid (pRL) was co-transfected with the Topflash plasmid, as a transfection control. All transfections were carried out in duplicate. The cells were subsequently harvested at 72 hours post-transfection after reaching complete confluency. To assess the Beta-catenin activity we quantified the *Photinus* luminescent signal from the Topflash vector. The *Photinus* luciferase levels were then normalised to the luminescent signals from the *Renilla* plasmid alone. The bar graph in Figure 5.9 shows the standard deviation from duplicate transfections, for each cell line. All of the HPV-16 cell lines contain higher levels of beta-catenin activity compared to HPV-negative NIKS. In addition HSIL-like cell lines contain higher levels of Beta-catenin activity compared to LSIL-like cell lines.

As Beta-catenin activity is higher in all HPV-16 cell lines compared to HPV negative NIKS, we can first suggest that the virus might increase or sustain Beta-catenin activity as another means of maintaining cells in S-phase. It is possible that the increased levels of E6 and E7 oncogene in confluent HSIL-like cell lines leads to a further increase in the Beta catenin activity, thus allowing the cells to maintain proliferative capabilities. Furthermore it is possible that the level of Beta-catenin activity in HSIL-like cell lines leads to S-phase persistence in raft culture epithelium. Further work will be needed to determine if the increase in Beta-

catenin activity is due to a reduction in specific adherin junction proteins. Furthermore we will have to establish if the increase in Beta-catenin activity is due to an increase in one or both of the HPV oncogenes in HSIL-like cell lines.

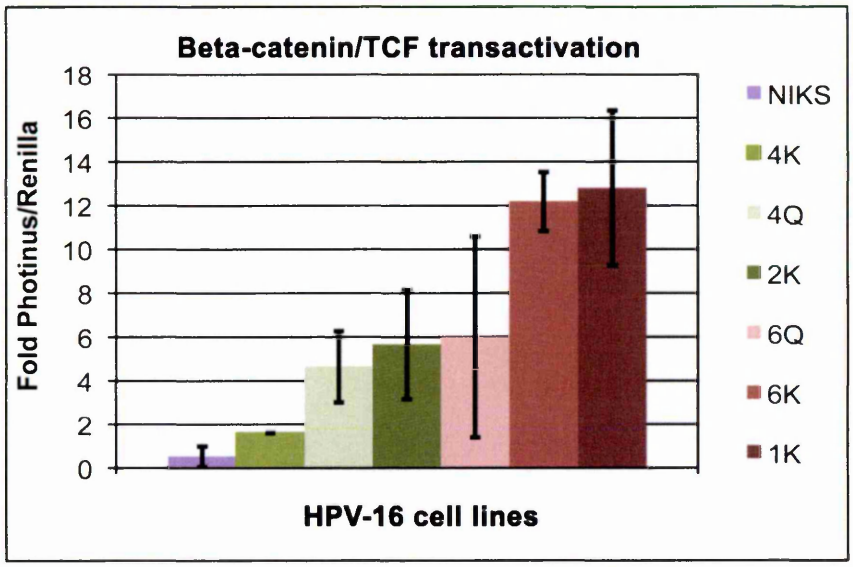

Figure 5.9 Beta catenin-TCF transactivation in LSIL and HSIL cell lines

LSIL and HSIL cell lines and HPV negative NIKS were transfected in duplicate with the Topflash *Photinus* luciferase reporter vector, which contains the TCF transcription factor Beta-catenin binding site. All cell lines were co-transfected with a *Renilla* luciferase reporter plasmid (pRL), which was used as a transfection control. The level of Beta-catenin activity for each cell line was assessed by quantification of the luminescent signal from the Topflash *Photinus* reporter vector. The bar graph shows the fold increase of *Photinus* above the *Renilla* transfection control. The error bars represent the standard deviation of the duplicate transfections.

5.3 Discussion

In Chapter 5 we have shown that LSIL-like cell lines differ from HSIL-like cell lines with respect to their growth characteristics and E6 and E7 oncogene levels. More specifically growth assay experiments have shown that HSIL-like cell lines have the ability to proliferate in confluent cultures whereas LSIL-like cell lines appear to be sensitive to contact inhibition. We have also observed that the E6 and E7 protein levels of HSIL-like cell lines are elevated in confluent cultures compared to sub-confluent cultures. By comparison the E6 and E7 protein levels in LSIL-like cell lines decrease or moderately increase in confluent cultures. Overall, the E6 and E7 protein levels are higher in confluent cultures of HSIL-like cell lines compared to LSIL-like cell lines.

Although we can not at present explain why E6 and E7 levels rise in confluent HSIL-like cell lines, we have made the observation that confluent cultures likely mimic the cell density of the basal layer in raft cultures, more so than sub-confluent cultures. We can speculate that the growth potential and viral oncogene levels in confluent monolayer cultures are likely to be similar to that of the basal layer cells in raft culture epithelium. We can therefore raise the possibility that the high levels of E6 and E7 observed in "basal-like" confluent cultures are responsible for the level of MCM-7 persistence in HSIL-like raft cultures. Recent studies have shown that persistent E7 expression in mice is necessary for the development of HSIL, however there was no indication if the level of E7 protein contributed to this disease grade (Jabbar, Abrams et al. 2009).

The coincidental rise in oncogene levels during confluency has been only a recent find with this system. Prior to culturing HPV-16 cell lines in six-well plates we were unable to consistently detect endogenous E6 and E7 levels. HPV-16 cell lines were originally grown in six-well plates to carry out growth assays. The detection of viral oncogenes by Western blot has been historically difficult within the HPV field, as it has been mostly claimed that endogenous levels of E6 and E7 are difficult to detect by these methods. In our case growing the cell lines in a tight confined space increased our chances of detecting E6 and E7 expression compared to growing the same cell lines in larger flasks. Using this method of growth has subsequently allowed us to make these correlations between growth density and oncogene levels.

We have also made an interesting correlation between E6 and E7 protein levels and the different LSIL-like MCM-7 patterns in raft culture. Raft culture 4K, which like low-risk HPV-11 lesions, contains a sporadic S-phase compartment. We also observed that E6 and E7 protein levels are dramatically lower in cell line 4K compared to the remaining LSIL-like cell lines. Raft culture 4Q and 2K by comparison contained moderate levels of E7, which correlated with a more diffuse MCM-7 compartment. We have now shown that low and moderate levels of E6 and E7 expression from are more favorable for productive infection whereas high levels of E6 and E7 correlate with a highly persistent MCM-7 compartment and an incomplete life cycle. A next step forward will therefore be to knockdown the E6 and E7 protein levels in HSIL-like cell lines. Ideally we would recover a more LSIL-like phenotype following the reduction of E6 and E7 in HSIL-like cell lines.

Results in this chapter also suggest the possibility that the virus interferes with contact inhibition pathways such as those involving active beta-catenin. Preliminary data suggests that the virus allows beta-catenin to remain active at times of cell-cell contact. When in the nucleus beta-catenin forms a complex with the TCF/LEF transcription factors leading to the transactivation of cellular genes that are necessary for cells to proceed through S-phase (Huelsken and Behrens 2002). Beta-catenin is degraded or is sequestered to the cell membranes at times of cell-cell contact. We have found that confluent LSIL-like and HSIL-like HPV-16 cell lines have increased beta-catenin activity compared to HPV negative NIKS. It is possible that the virus keeps beta-catenin active in cell-cell contacted areas such as the basal layer, as another means to ensure that cell replication machinery is available in the suprabasal layers. As this would be a normal mechanism of the virus, high levels of E6 and E7 would possibly sustain this activity in the upper layers of the epithelium. Coincidently HSIL like cell lines all display higher levels of beta-catenin activity when compared to LSIL-like cell lines.

It is also possible that the increased beta-catenin activity is due to a reduction of PDZ proteins, such as hScrib and hDlg. In the absence of E6 these PDZ proteins normally control Beta-catenin activity via their interactions with the tumor suppressor gene APC.(Matsumine, Ogai et al. 1996; Takizawa, Nagasaka et al. 2006) In cases of high E6 expression, high reductions of PDZ proteins could lead to an increase in active beta-catenin. In collaboration with Lawrence Banks and colleagues we have preliminary data that shows both hScrib and hDlg proteins are more reduced in HSIL-like raft cultures when compared to LSIL-like raft cultures. Future work will be aimed at investigating the role of these pathways in HPV inducedneoplasia.

6.0 Final Discussion

In this thesis we have shown that the NIKS HPV-16 raft culture system can model a wider spectrum of HPV disease than we had previously envisioned. Surprisingly we have found that early passage HPV-16 episomal cell lines were heterogeneous in their ability to complete a HPV life cycle. After propagating these lines in organotypic raft cell culture we identified that a subset of raft cultures contained viral gene expression patterns that were reminiscent of low-grade HPV-16 induced cervical lesions (i.e.LSIL-like), where another subset contained viral gene expression patterns that were reminiscent of high-grade cervical lesions (i.e. HSIL-like) (Middleton, Peh et al. 2003). We have specifically based these findings through the identification of MCM-7 (E7 surrogate marker) and, HPV-16-E4 and HPV-16- L1 gene expression patterns. In addition, we have identified that LSIL-like raft cultures and HSIL-like raft cultures display pathological features that are similar to those found in cervical lesions of a similar pathological grade. This is the first report of LSIL-like and HSIL-like phenotypic variation in episomal HPV raft culture systems. We have therefore presented a novel laboratory model of HPV induced neoplasia. This has allowed us to ask new questions pertaining to the molecular basis of HPV induced neoplasia

The focuses of these questions were mainly towards the understanding of early events in the virus life cycle including viral copy number and E6 and E7 oncogene levels. Through this analysis we have found that viral copy number and E6 and E7 protein levels vary between early passage monolayer episomal cell lines, which point to possible differences in early episomal establishment in the host cell. In addition we have found that the major difference in E6 and E7 protein level

variation occur at high cell densities, a time when keratinocytes would normally stop proliferating, in order to default into the terminal differentiation program. We have found that E6 and E7 protein levels rise in confluent HSIL-like cell lines where E6 and E7 protein levels decrease or increase moderately in confluent cultures.

Interestingly the rise in E6 and E7 protein levels in HSIL-like cell lines at high cell density, also correlate with their ability to bypass density-dependent growth arrest. In contrast to this, as with HPV- negative NIKS, LSIL-like cells lines stop proliferating when cell-cell contact is achieved. We have further hypothesized that a lack of cell-cell sensing in the case of HSIL-like cell lines possibly allows these cells to persist in cycle in the raft epithelium, above the threshold of LSIL-like cell lines. Past work has not identified changes in oncogene levels at confluency or if lack of cell-cell sensing is important for increased cell-cycle persistence in the suprabasal layers

We have also made the observation that confluent cultures likely mimic the tightly packed basal layer environment more so than sub-confluent cultures. We therefore hypothesize that the basal oncogene level likely determines the level of cell cycle persistence in the suprabasal layers. Recent studies have suggested that persistent E6 and E7 expression is indeed important for the development of neoplasia however their studies did not evaluate if basal E6 and E7 levels lead to different LSIL or HSIL phenotypes (Brake and Lambert 2005; Jabbar, Abrams et al. 2009).

More immediate future work will be to directly assess if the E6 and E7 oncogene levels are responsible for these phenotypes. This question can be directly addressed by using the shRNA knockdown technique. The successful knock down of E6 and E7 using shRNA has been previously achieved in cervical cancers lines (Gu, Putral et al. 2008). We can therefore select for HSIL-like clonal cell lines that display different levels of E6 and E7 knockdown efficiencies. HSIL-like cell lines with reduced levels of E6 and E7 will be propagated in organtotypic raft culture. Ideally we would want to show that a reduction of the E7 oncogenes leads to a reduction of the MCM-7 compartment and a regression to LSIL-like phenotype

The diversity of E7 regulation in HPV-16 raft cultures

Interestingly LSIL-like raft cultures contained two distinct MCM-7 expression patterns previously detected in mucosal HPV induced LSIL lesions, one being more typically associated with low-risk viruses such as HPV-11 (Middleton, Peh et al. 2003). Raft 4K, which displayed similar early gene expression patterns to that of HPV-11 lesions contained a sporadic MCM-7 compartment where MCM-7 was predominantly absent from the basal layer. We have found that this pattern correlates with the dramatically low E6 and E7 protein level that is produced by this particular HPV-16 cell line.

It has been previously suggested E7-mediated S-phase induction can be inhibited by anti-proliferative signals imposed by the cell. More specifically the (Cyclin E) cdk2/ (Cycllin D) cdk4 inhibitor p21 has been shown to rise in the presence of E7 (Noya, Chien et al. 2001). In cases of low E7 it has been suggested that E7 forms a complex with p21 and Cyclin E, which leads to G1 arrest. However when E7 levels are high it is has been suggested that E7 can inactivate p21 and which

allows S-phase progression to proceed (reviewed in (Doorbar 2006). The low level of E7 expression in cell line 4K might therefore be less optimal for p21 inactivation leading to less efficient S-phase induction.

In the remaining two LSIL raft cultures 2K and 4Q, MCM-7 expression was more diffuse and was first identified in the basal layer. We have correlated this with higher E6 and E7 levels when compared to that of cell line 4K. We can speculate that the level of E7 is sufficient for inactivating p21 more consistently in the lower basal layers. In contrast to LSIL raft cultures MCM-7 positive cells were detected throughout majority of the epithelium in HSIL-like raft cultures. As stated earlier MCM-7 persistence is likely related to the dramatically higher levels of E7, which likely saturate any host cell defenses.

A further step in this evaluation could first entail identifying the p21 levels in LSIL-like and HSIL-like raft culture epithelium. In the case of raft culture 4K it is possible that we might identify that MCM-7 negative cells are positive for p21. This would indicate alternate regions in the epithelium where S-phase induction did not occur as a consequence to cell cycle inhibition. This mode of E7 cell cycle regulation appears to be favorable for the virus and might well serve to control host cell proliferation in order carry out a complete life cycle.

Through identifying these different MCM-7 patterns we can further suggest that the virus does not always adhere to a strict method of E7 gene regulation and S-phase induction. At present this model could be useful for identifying HPV-16 intermediate LSIL-like phenotypes that will potentially not be identified in biopsy material due to the fact that low-grade lesions are biopsied less frequently. This

could undoubtedly lead to further studies of early HPV-16 gene regulation. In addition to evaluating MCM-7 expression patterns, identifying a good E7 antibody for raft culture experiments would greatly strengthen these studies.

Beta-catenin and cell-cell sensing

Preliminary results also suggest that the virus sustains active beta-catenin, which likely also interferes with cell cycle inhibition. Active beta-catenin forms a complex with TCF/LEF transcription factors in the nucleus, which leads to the transactivation of cell cycle proteins such as Cyclin D (Huelsken and Behrens 2002). At times of cell-cell contact Beta-catenin is degraded or is sequestered to the cell membranes in order to control proliferation. As we have found elevated levels of active beta-catenin in all LSIL and HSIL-like cell lines above that of HPV negative NIKS, we can hypothesize that in normal circumstances the virus interferes with Beta-catenin pathways as another means to persist in the cell cycle above the tightly packed basal layer. HSIL cell lines appear to activate Beta-catenin at higher levels, which might consequently lead to increased cell cycle persistence in the epithelium.

Recent work has shown that Beta-catenin activity is increased in E6 only NIKS cell lines when compared to E7 only NIKS cell lines and HPV negative NIKS. (In personal communication with Kenneth Raj, NIMR, London, UK). This might suggest then that both E6 and E7 are needed to extend the S-phase compartment above the basal layer however by different mechanisms.

Although we are not certain of a direct interaction with E6 and beta-catenin there are several possible scenarios that might explain a role of E6 in sustaining active

beta-catenin. One scenario is related to a reduction of p53, which is directly mediated by E6. Past studies have shown that beta-catenin interacts with p53 via a negative feedback loop (Oren, Damalas et al. 2002). Mutations in p53 have been shown to result in abnormal beta-catenin accumulation (Cagatay and Ozturk 2002). In the case of highly reduced levels of p53 as observed in HSIL-like cell lines, this might lead to abnormal levels of active beta-catenin.

We have also preliminary data also suggests that PDZ domain cellular proteins such as hDlg and hScrib are more reduced in HSIL-like raft cultures compared to LSIL-like raft cultures (data not shown). It is widely established that E6 degrades PDZ domain proteins, which is thought to be important for neoplastic development and carcinogenesis (Thomas, Narayan et al. 2008). The reduction of hScrib and hDlg could also potentially interfere with their binding of the tumor suppressor APC (Matsumine, Ogai et al. 1996; Takizawa, Nagasaka et al. 2006). APC functions to regulate beta-catenin activity in the cytoplasm in order to control proliferation. The high reduction of hScrib and hDlg proteins might therefore contribute to high Beta-catenin activity.

The further evalauation of the NIKS raft culture system as laboratory model of HPV-induced neoplasia

Through these studies we have also found that LSIL-like and HSIL-like phenotypes are biologically reproducible in the NIKS system. We have concluded this based on the fact that two different transfections yielded LSIL-like and HSIL-like phenotypes. This is in support of this system as a potential laboratory model of episomal HPV induced neoplasia. At present LSIL-like and HSIL-like phenotypes

have not been identified in any other system that maintains viral episomes. However, this does not discount that these phenotypes do not exist in other keratinocyte cell line systems that maintain viral episomes.

At present the data in this thesis suggests that the oncogene levels are regulated differently from viral episomes and are responsible for the LSIL-like and HSIL-like phenotypes. This however does not rule out that a level of heterogeneity in the host cell line could also be contributing to these phenotypes in individual clonal cell lines. As mentioned earlier NIKS arose as a spontaneously immortalized cell line with a near diploid genome, and was also shown to be maintained as an isogenic cell line (Allen-Hoffmann, Schlosser et al. 2000). It will be necessary to verify that the parental NIKS are still homogeneous cell line and the cells did not acquire further genomic instability over time that might contribute to these phenotypes. We are currently karyotyping the NIKS and HPV-16 each cell lines to look for additional chromosomal rearrangement and base ploidy levels. Secondly it is possible that chromosomal rearrangement can lead to elevations or decreases in gene dosage. To evaluate this Array comparative genomic hybridization (aCGH) can be carried out on genomic DNA (gDNA). aCGH is a highly sensitive assay that identifies gene copy number changes within a specific chromosomal region (Strefford and Parker 2009).

Future work will be aimed at evaluating if this phenotypic variation also exists in primary cell lines. Past studies have shown that both cervical and foreskin keratinocytes can been successfully transfected with high-risk HPV genomes (Lace, Anson et al. 2009). Primary HPV-16 cell lines can be subsequently maintained for up to 30 passages. We have also recently harvested primary

cervical cell lines from cervical biopsies, which could be used to establish a model of HPV-16 cervical disease.

References

Alazawi, W.,Pett, M.,Arch, B.,Scott, L.,Freeman, T.,Stanley, M. A. and Coleman, N. (2002). "Changes in cervical keratinocyte gene expression associated with integration of human papillomavirus 16". Cancer Res **62**(23): 6959-65.

Allen-Hoffmann, B. L.,Schlosser, S. J.,Ivarie, C. A.,Sattler, C. A.,Meisner, L. F. and O'connor, S. L. (2000). "Normal growth and differentiation in a spontaneously immortalized near-diploid human keratinocyte cell line, NIKS". J Invest Dermatol **114**(3): 444-55.

Androphy, E. J.,Lowy, D. R. and Schiller, J. T. (1987). "Bovine papillomavirus E2 trans-activating gene product binds to specific sites in papillomavirus DNA". Nature **325**(6099): 70-3.

Baker, C. C.,Phelps, W. C.,Lindgren, V.,Braun, M. J.,Gonda, M. A . and Howley, P. M. (1987). "Structural and transcriptional analysis of human papillomavirus type 16 sequences in cervical carcinoma cell lines". J Virol **61**(4): 962-71.

Balda, M. S. and Matter, K. (2003). "Epithelial cell adhesion and the regulation of gene expression". Trends Cell Biol **13**(6): 310-8.

Balsitis, S.,Dick, F.,Dyson, N. and Lambert, P. F. (2006). "Critical roles for non-pRb targets of human papillomavirus type 16 E7 in cervical carcinogenesis". Cancer Res **66**(19): 9393-400.

Balsitis, S. J.,Sage, J.,Duensing, S.,Munger, K.,Jacks, T. and Lambert, P. F. (2003). "Recapitulation of the effects of the human papillomavirus type 16 E7 oncogene on mouse epithelium by somatic Rb deletion and detection of pRb-independent effects of E7 in vivo". Mol Cell Biol **23**(24): 9094-103.

Banerjee, N. S.,Genovese, N. J.,Noya, F.,Chien, W. M.,Broker, T. R.andChow, L. T. (2006). "Conditionally activated E7 proteins of high-risk and low-risk human papillomaviruses induce S phase in postmitotic, differentiated human keratinocytes". J Virol **80**(13): 6517-24.

Bedell, M. A.,Hudson, J. B.,Golub, T. R.,Turyk, M. E.,Hosken, M.,Wilbanks, G. D. and Laimins, L. A. (1991). "Amplification of human papillomavirus genomes in vitro is dependent on epithelial differentiation". J Virol **65**(5): 2254-60.

Berg, M. and Stenlund, A. (1997). "Functional interactions between papillomavirus E1 and E2 proteins". J Virol **71**(5): 3853-63.

Bernard, H. U.,Chan, S. Y. and Delius, H. (1994). "Evolution of papillomaviruses". Curr Top Microbiol Immunol **186**: 33-54.

Bernard, H. U.,Chan, S. Y.,Manos, M. M.,Ong, C. K.,Villa, L. L.,Delius, H.,Peyton, C. L.,Bauer, H. M. and Wheeler, C. M. (1994). "Identification and assessment of known and novel human papillomaviruses by polymerase chain reaction amplification, restriction fragment length polymorphisms, nucleotide sequence, and phylogenetic algorithms". J Infect Dis **170**(5): 1077-85.

Bernard, H. U. (2005). "The clinical importance of the nomenclature, evolution and taxonomy of human papillomaviruses". J Clin Virol **32 Suppl 1**: S1-6.

Black, A. R. and Azizkhan-Clifford, J. (1999). "Regulation of E2F: a family of transcription factors involved in proliferation control". Gene **237**(2): 281-302.

Bosch, F. X. and De Sanjose, S. (2003). "Chapter 1: Human papillomavirus and cervical cancer--burden and assessment of causality". J Natl Cancer Inst Monogr(31): 3-13.

Boyer, S. N.,Wazer, D. E. and Band, V. (1996). "E7 protein of human papilloma virus-16 induces degradation of retinoblastoma protein through the ubiquitin-proteasome pathway". Cancer Res **56**(20): 4620-4.

Brake, T. and Lambert, P. F. (2005). "Estrogen contributes to the onset, persistence, and malignant progression of cervical cancer in a human papillomavirus-transgenic mouse model". Proc Natl Acad Sci U S A **102**(7): 2490-5.

Branca, M.,Ciotti, M.,Santini, D.,Bonito, L. D.,Benedetto, A.,Giorgi, C.,Paba, P.,Favalli, C.,Costa, S.,Agarossi, A.,Alderisio, M. and Syrjanen, K. (2004). "Activation of the ERK/MAP kinase pathway in cervical intraepithelial neoplasia is related to grade of the lesion but not to high-risk human papillomavirus, virus clearance, or prognosis in cervical cancer". Am J Clin Pathol **122**(6): 902-11.

Brehm, A.,Nielsen, S. J.,Miska, E. A.,Mccance, D. J.,Reid, J. L.,Bannister, A. J. and Kouzarides, T. (1999). "The E7 oncoprotein associates with Mi2 and histone deacetylase activity to promote cell growth". EMBO J **18**(9): 2449-58.

Bryan, J. T. and Brown, D. R. (2000). "Association of the human papillomavirus type 11 E1()E4 protein with cornified cell envelopes derived from infected genital epithelium". Virology **277**(2): 262-9.

Buchkovich, K.,Duffy, L. A. and Harlow, E. (1989). "The retinoblastoma protein is phosphorylated during specific phases of the cell cycle". Cell **58**(6): 1097-105.

Cagatay, T. and Ozturk, M. (2002). "P53 mutation as a source of aberrant beta-catenin accumulation in cancer cells". Oncogene **21**(52): 7971-80.

Candi, E.,Schmidt, R. and Melino, G. (2005). "The cornified envelope: a model of cell death in the skin". Nat Rev Mol Cell Biol **6**(4): 328-40.

Chan, S. Y.,Bernard, H. U.,Ratterree, M.,Birkebak, T. A.,Faras, A. J. and Ostrow, R. S. (1997). "Genomic diversity and evolution of papillomaviruses in rhesus monkeys". J Virol **71**(7): 4938-43.

Chen, X. S.,Garcea, R. L.,Goldberg, I.,Casini, G. and Harrison, S. C. (2000). "Structure of small virus-like particles assembled from the L1 protein of human papillomavirus 16". Mol Cell **5**(3): 557-67.

Cheng, S.,Schmidt-Grimminger, D. C.,Murant, T.,Broker, T. R. and Chow, L. T. (1995). "Differentiation-dependent up-regulation of the human papillomavirus E7 gene reactivates cellular DNA replication in suprabasal differentiated keratinocytes". Genes Dev **9**(19): 2335-49.

Chow, L. T.,Duffy, A. A.,Wang, H. K. and Broker, T. R. (2009). "A highly efficient system to produce infectious human papillomavirus: Elucidation of natural virus-host interactions". Cell Cycle **8**(9): 1319-23.

Cohen, J. (2005). "Public health. High hopes and dilemmas for a cervical cancer vaccine". Science **308**(5722): 618-21.

Collins, A. S.,Nakahara, T.,Do, A. and Lambert, P. F. (2005). "Interactions with pocket proteins contribute to the role of human papillomavirus type 16 E7 in the papillomavirus life cycle". J Virol **79**(23): 14769-80.

Cornelissen, M. T.,Smits, H. L.,Briet, M. A.,Van Den Tweel, J. G.,Struyk, A. P.,Van Der Noordaa, J. and Ter Schegget, J. (1990). "Uniformity of the splicing pattern of the E6/E7 transcripts in human papillomavirus type 16-transformed human fibroblasts, human cervical premalignant lesions and carcinomas". J Gen Virol **71 (Pt 5)**: 1243-6.

Dale, B. A.,Salonen, J. and Jones, A. H. (1990). "New approaches and concepts in the study of differentiation of oral epithelia". Crit Rev Oral Biol Med **1**(3): 167-90.

Davy, C. E.,Jackson, D. J.,Wang, Q.,Raj, K.,Masterson, P. J.,Fenner, N. F.,Southern, S.,Cuthill, S.,Millar, J. B. and Doorbar, J. (2002). "Identification of a G(2) arrest domain in the E1 wedge E4 protein of human papillomavirus type 16". J Virol **76**(19): 9806-18.

Davy, C. E.,Jackson, D. J.,Raj, K.,Peh, W. L.,Southern, S. A.,Das, P.,Sorathia, R.,Laskey, P.,Middleton, K.,Nakahara, T.,Wang, Q.,Masterson, P. J.,Lambert, P. F.,Cuthill, S.,Millar, J. B. and Doorbar, J. (2005). "Human papillomavirus type 16 E1 E4-induced G2 arrest is associated with cytoplasmic retention of active Cdk1/cyclin B1 complexes". J Virol **79**(7): 3998-4011.

Day, P. M.,Baker, C. C.,Lowy, D. R. and Schiller, J. T. (2004). "Establishment of papillomavirus infection is enhanced by promyelocytic leukemia protein (PML) expression". Proc Natl Acad Sci U S A **101**(39): 14252-7.

De Geest, K.,Turyk, M. E.,Hosken, M. I.,Hudson, J. B.,Laimins, L. A. and Wilbanks, G. D. (1993). "Growth and differentiation of human papillomavirus type 31b positive human cervical cell lines". Gynecol Oncol **49**(3): 303-10.

De Villiers, E. M.,Fauquet, C.,Broker, T. R.,Bernard, H. U. and Zur Hausen, H. (2004). "Classification of papillomaviruses". Virology **324**(1): 17-27.

Delvenne, P.,Hubert, P.,Jacobs, N.,Giannini, S. L.,Havard, L.,Renard, I.,Saboulard, D. and Boniver, J. (2001). "The organotypic culture of HPV-transformed keratinocytes: an effective in vitro model for the development of new immunotherapeutic approaches for mucosal (pre)neoplastic lesions". Vaccine **19**(17-19): 2557-64.

Demers, G. W.,Halbert, C. L. and Galloway, D. A. (1994). "Elevated wild-type p53 protein levels in human epithelial cell lines immortalized by the human papillomavirus type 16 E7 gene". Virology **198**(1): 169-74.

Demeter, L. M.,Stoler, M. H.,Bonnez, W.,Corey, L.,Pappas, P.,Strussenberg, J. and Reichman, R. C. (1993). "Penile intraepithelial neoplasia: clinical presentation and an analysis of the physical state of human papillomavirus DNA". J Infect Dis **168**(1): 38-46.

Desaintes, C. and Demeret, C. (1996). "Control of papillomavirus DNA replication and transcription". Semin Cancer Biol **7**(6): 339-47.

Doorbar, J.,Parton, A.,Hartley, K.,Banks, L.,Crook, T.,Stanley, M. and Crawford, L. (1990). "Detection of novel splicing patterns in a HPV16-containing keratinocyte cell line". Virology **178**(1): 254-62.

Doorbar, J.,Foo, C.,Coleman, N.,Medcalf, L.,Hartley, O.,Prospero, T.,Napthine, S.,Sterling, J.,Winter, G. and Griffin, H. (1997). "Characterization of events during the late stages of HPV16 infection in vivo using high-affinity synthetic Fabs to E4". Virology **238**(1): 40-52.

Doorbar, J. (2006). "Molecular biology of human papillomavirus infection and cervical cancer". Clin Sci (Lond) **110**(5): 525-41.

Duensing, S.,Duensing, A.,Flores, E. R.,Do, A.,Lambert, P. F. and Munger, K. (2001). "Centrosome abnormalities and genomic instability by episomal expression of human papillomavirus type 16 in raft cultures of human keratinocytes". J Virol **75**(16): 7712-6.

Duensing, S. and Munger, K. (2003). "Human papillomavirus type 16 E7 oncoprotein can induce abnormal centrosome duplication through a mechanism independent of inactivation of retinoblastoma protein family members". J Virol **77**(22): 12331-5.

Dyson, N.,Howley, P. M.,Munger, K. and Harlow, E. (1989). "The human papilloma virus-16 E7 oncoprotein is able to bind to the retinoblastoma gene product". Science **243**(4893): 934-7.

Eckert, R. L.,Crish, J. F. and Robinson, N. A. (1997). "The epidermal keratinocyte as a model for the study of gene regulation and cell differentiation". Physiol Rev **77**(2): 397-424.

Eichner, R.,Sun, T. T. and Aebi, U. (1986). "The role of keratin subfamilies and keratin pairs in the formation of human epidermal intermediate filaments". J Cell Biol **102**(5): 1767-77.

Eichten, A.,Rud, D. S.,Grace, M.,Piboonniyom, S. O.,Zacny, V. and Munger, K. (2004). "Molecular pathways executing the "trophic sentinel" response in HPV-16 E7-expressing normal human diploid fibroblasts upon growth factor deprivation". Virology **319**(1): 81-93.

Flores, E. R. and Lambert, P. F. (1997). "Evidence for a switch in the mode of human papillomavirus type 16 DNA replication during the viral life cycle". J Virol **71**(10): 7167-79.

Flores, E. R.,Allen-Hoffmann, B. L.,Lee, D. and Lambert, P. F. (2000). "The human papillomavirus type 16 E7 oncogene is required for the productive stage of the viral life cycle". J Virol **74**(14): 6622-31.

Freeman, A.,Morris, L. S.,Mills, A. D.,Stoeber, K.,Laskey, R. A.,Williams, G. H. and Coleman, N. (1999). "Minichromosome maintenance proteins as biological markers of dysplasia and malignancy". Clin Cancer Res **5**(8): 2121-32.

Fuchs, E. (1990). "Epidermal differentiation: the bare essentials". J Cell Biol **111**(6 Pt 2): 2807-14.

Fujii, T.,Masumoto, N.,Saito, M.,Hirao, N.,Niimi, S.,Mukai, M.,Ono, A.,Hayashi, S.,Kubushiro, K.,Sakai, E.,Tsukazaki, K. and Nozawa, S. (2005). "Comparison between in situ hybridization and real-time PCR technique as a means of detecting the integrated form of human papillomavirus 16 in cervical neoplasia". Diagn Mol Pathol **14**(2): 103-8.

Funk, J. O.,Waga, S.,Harry, J. B.,Espling, E.,Stillman, B. and Galloway, D. A. (1997). "Inhibition of CDK activity and PCNA-dependent DNA replication by p21 is blocked by interaction with the HPV-16 E7 oncoprotein". Genes Dev **11**(16): 2090-100.

Gallie, B. L. (1994). "Retinoblastoma gene mutations in human cancer". N Engl J Med **330**(11): 786-7.

Gammoh, N.,Grm, H. S.,Massimi, P. and Banks, L. (2006). "Regulation of human papillomavirus type 16 E7 activity through direct protein interaction with the E2 transcriptional activator". J Virol **80**(4): 1787-97.

Gammoh, N.,Isaacson, E.,Tomaic, V.,Jackson, D. J.,Doorbar, J. and Banks, L. (2009). "Inhibition of HPV-16 E7 oncogenic activity by HPV-16 E2". Oncogene **28**(23): 2299-304.

Gissmann, L.,Pfister, H. and Zur Hausen, H. (1977). "Human papilloma viruses (HPV): characterization of four different isolates". Virology **76**(2): 569-80.

Gissmann, L.,Wolnik, L.,Ikenberg, H.,Koldovsky, U.,Schnurch, H. G. and Zur Hausen, H. (1983). "Human papillomavirus types 6 and 11 DNA sequences in genital and laryngeal papillomas and in some cervical cancers". Proc Natl Acad Sci U S A **80**(2): 560-3.

Grassmann, K.,Rapp, B.,Maschek, H.,Petry, K. U. and Iftner, T. (1996). "Identification of a differentiation-inducible promoter in the E7 open reading frame of human papillomavirus type 16 (HPV-16) in raft cultures of a new cell line containing high copy numbers of episomal HPV-16 DNA". J Virol **70**(4): 2339-49.

Gu, W.,Putral, L.andMcmillan, N. (2008). "siRNA and shRNA as anticancer agents in a cervical cancer model". Methods Mol Biol **442**: 159-72.

Hafner, N.,Driesch, C.,Gajda, M.,Jansen, L.,Kirchmayr, R.,Runnebaum, I. B. and Durst, M. (2008). "Integration of the HPV16 genome does not invariably result in high levels of viral oncogene transcripts". Oncogene **27**(11): 1610-7.

Harwood, C. A. and Proby, C. M. (2002). "Human papillomaviruses and non-melanoma skin cancer". Curr Opin Infect Dis **15**(2): 101-14.

Heck, D. V.,Yee, C. L.,Howley, P. M. and Munger, K. (1992). "Efficiency of binding the retinoblastoma protein correlates with the transforming capacity of the E7 oncoproteins of the human papillomaviruses". Proc Natl Acad Sci U S A **89**(10): 4442-6.

Helt, A. M.,Funk, J. O. and Galloway, D. A. (2002). "Inactivation of both the retinoblastoma tumor suppressor and p21 by the human papillomavirus type 16 E7 oncoprotein is necessary to inhibit cell cycle arrest in human epithelial cells". J Virol **76**(20): 10559-68.

Hillemanns, P.andWang, X. (2006). "Integration of HPV-16 and HPV-18 DNA in vulvar intraepithelial neoplasia". Gynecol Oncol **100**(2): 276-82.

Ho, L.,Chan, S. Y.,Burk, R. D.,Das, B. C.,Fujinaga, K.,Icenogle, J. P.,Kahn, T.,Kiviat, N.,Lancaster, W.,Mavromara-Nazos, P. and Et Al. (1993). "The genetic drift of human papillomavirus type 16 is a means of reconstructing prehistoric viral spread and the movement of ancient human populations". J Virol **67**(11): 6413-23.

Huelsken, J. and Behrens, J. (2002). "The Wnt signalling pathway". J Cell Sci **115**(Pt 21): 3977-8.

Hughes, F. J. and Romanos, M. A. (1993). "E1 protein of human papillomavirus is a DNA helicase/ATPase". Nucleic Acids Res **21**(25): 5817-23.

Jabbar, S. F.,Abrams, L.,Glick, A. and Lambert, P. F. (2009). "Persistence of high-grade cervical dysplasia and cervical cancer requires the continuous expression of the human papillomavirus type 16 E7 oncogene". Cancer Res **69**(10): 4407-14.

Jeon, S. and Lambert, P. F. (1995). "Integration of human papillomavirus type 16 DNA into the human genome leads to increased stability of E6 and E7 mRNAs: implications for cervical carcinogenesis". Proc Natl Acad Sci U S A **92**(5): 1654-8.

Jia, R.,Liu, X.,Tao, M.,Kruhlak, M.,Guo, M.,Meyers, C.,Baker, C. C. and Zheng, Z. M. (2009). "Control of the papillomavirus early-to-late switch by differentially expressed SRp20". J Virol **83**(1): 167-80.

Klaes, R.,Woerner, S. M.,Ridder, R.,Wentzensen, N.,Duerst, M.,Schneider, A.,Lotz, B.,Melsheimer, P. and Von Knebel Doeberitz, M. (1999). "Detection of high-risk cervical intraepithelial neoplasia and cervical cancer by amplification of transcripts derived from integrated papillomavirus oncogenes". Cancer Res **59**(24): 6132-6.

Klaes, R.,Friedrich, T.,Spitkovsky, D.,Ridder, R.,Rudy, W.,Petry, U.,Dallenbach-Hellweg, G.,Schmidt, D. and Von Knebel Doeberitz, M. (2001). "Overexpression of p16(INK4A) as a specific marker for dysplastic and neoplastic epithelial cells of the cervix uteri". Int J Cancer **92**(2): 276-84.

Klingelhutz, A. J.,Foster, S. A. and Mcdougall, J. K. (1996). "Telomerase activation by the E6 gene product of human papillomavirus type 16". Nature **380**(6569): 79-82.

Koutsky, L. A.,Holmes, K. K.,Critchlow, C. W.,Stevens, C. E.,Paavonen, J.,Beckmann, A. M.,Derouen, T. A.,Galloway, D. A.,Vernon, D. and Kiviat, N. B. (1992). "A cohort study of the risk of cervical intraepithelial neoplasia grade 2 or 3 in relation to papillomavirus infection". N Engl J Med **327**(18): 1272-8.

Kubota, Y.,Fujinami, K.,Uemura, H.,Dobashi, Y.,Miyamoto, H.,Iwasaki, Y.,Kitamura, H. and Shuin, T. (1995). "Retinoblastoma gene mutations in primary human prostate cancer". Prostate **27**(6): 314-20.

Lace, M. J.,Anson, J. R.,Klingelhutz, A. J.,Lee, J. H.,Bossler, A. D.,Haugen, T. H. and Turek, L. P. (2009). "Human Papillomavirus (HPV) Type -18 Induces Extended Growth in Primary Human Cervical, Tonsillar or Foreskin Keratinocytes More Effectively Than Other High-Risk Mucosal HPVs". J Virol.

Lace, M. J.,Yamakawa, Y.,Ushikai, M.,Anson, J. R.,Haugen, T. H. and Turek, L. P. (2009). "Cellular factor YY1 downregulates the human papillomavirus 16 E6/E7 promoter, P97, in vivo and in vitro from a negative element overlapping the transcription-initiation site". J Gen Virol **90**(Pt 10): 2402-12.

Lambert, P. F.,Ozbun, M. A.,Collins, A.,Holmgren, S.,Lee, D. and Nakahara, T. (2005). "Using an immortalized cell line to study the HPV life cycle in organotypic "raft" cultures". Methods Mol Med **119**: 141-55.

Lee, C. and Laimins, L. A. (2004). "Role of the PDZ domain-binding motif of the oncoprotein E6 in the pathogenesis of human papillomavirus type 31". J Virol **78**(22): 12366-77.

Li, Y.,Nichols, M. A.,Shay, J. W. and Xiong, Y. (1994). "Transcriptional repression of the D-type cyclin-dependent kinase inhibitor p16 by the retinoblastoma susceptibility gene product pRb". Cancer Res **54**(23): 6078-82.

Longworth, M. S.,Wilson, R. and Laimins, L. A. (2005). "HPV31 E7 facilitates replication by activating E2F2 transcription through its interaction with HDACs". EMBO J **24**(10): 1821-30.

Maiorano, D.,Lutzmann, M. and Mechali, M. (2006). "MCM proteins and DNA replication". Curr Opin Cell Biol **18**(2): 130-6.

Manabe, M. and O'guin, W. M. (1994). "Existence of trichohyalin-keratohyalin hybrid granules: co-localization of two major intermediate filament-associated proteins in non-follicular epithelia". Differentiation **58**(1): 65-75.

Masterson, P. J.,Stanley, M. A.,Lewis, A. P. and Romanos, M. A. (1998). "A C-terminal helicase domain of the human papillomavirus E1 protein binds E2 and the DNA polymerase alpha-primase p68 subunit". J Virol **72**(9): 7407-19.

Matsumine, A.,Ogai, A.,Senda, T.,Okumura, N.,Satoh, K.,Baeg, G. H.,Kawahara, T.,Kobayashi, S.,Okada, M.,Toyoshima, K. and Akiyama, T. (1996). "Binding of APC to the human homolog of the Drosophila discs large tumor suppressor protein". Science **272**(5264): 1020-3.

Mclaughlin-Drubin, M. E. and Munger, K. (2009). "The human papillomavirus E7 oncoprotein". Virology **384**(2): 335-44.

Meyers, C.,Bromberg-White, J. L.,Zhang, J.,Kaupas, M. E.,Bryan, J. T.,Lowe, R. S. and Jansen, K. U. (2002). "Infectious virions produced from a human papillomavirus type 18/16 genomic DNA chimera". J Virol **76**(10): 4723-33.

Middleton, K.,Peh, W.,Southern, S.,Griffin, H.,Sotlar, K.,Nakahara, T.,El-Sherif, A.,Morris, L.,Seth, R.,Hibma, M.,Jenkins, D.,Lambert, P.,Coleman, N. and Doorbar, J. (2003). "Organization of human papillomavirus productive cycle during neoplastic progression provides a basis for selection of diagnostic markers". J Virol **77**(19): 10186-201.

Milligan, S. G.,Veerapraditsin, T.,Ahamet, B.,Mole, S. and Graham, S. V. (2007). "Analysis of novel human papillomavirus type 16 late mRNAs in differentiated W12 cervical epithelial cells". Virology **360**(1): 172-81.

Miyamoto, H.,Shuin, T.,Torigoe, S.,Iwasaki, Y. and Kubota, Y. (1995). "Retinoblastoma gene mutations in primary human bladder cancer". Br J Cancer **71**(4): 831-5.

Modis, Y.,Trus, B. L. and Harrison, S. C. (2002). "Atomic model of the papillomavirus capsid". EMBO J **21**(18): 4754-62.

Morin, P. J. (1999). "beta-catenin signaling and cancer". Bioessays **21**(12): 1021-30.

Morris, P. J.,Dent, C. L.,Ring, C. J. and Latchman, D. S. (1993). "The octamer binding site in the HPV16 regulatory region produces opposite effects on gene expression in cervical and non-cervical cells". Nucleic Acids Res **21**(4): 1019-23.

Munger, K.,Werness, B. A.,Dyson, N.,Phelps, W. C.,Harlow, E. and Howley, P. M. (1989). "Complex formation of human papillomavirus E7 proteins with the retinoblastoma tumor suppressor gene product". EMBO J **8**(13): 4099-105.

Munoz, N.,Bosch, F. X.,De Sanjose, S.,Herrero, R.,Castellsague, X.,Shah, K. V.,Snijders, P. J. and Meijer, C. J. (2003). "Epidemiologic classification of human papillomavirus types associated with cervical cancer". N Engl J Med **348**(6): 518-27.

Nagasaka, K.,Nakagawa, S.,Yano, T.,Takizawa, S.,Matsumoto, Y.,Tsuruga, T.,Nakagawa, K.,Minaguchi, T.,Oda, K.,Hiraike-Wada, O.,Ooishi, H.,Yasugi, T. and Taketani, Y. (2006). "Human homolog of Drosophila tumor suppressor Scribble negatively regulates cell-cycle progression from G1 to S phase by localizing at the basolateral membrane in epithelial cells". Cancer Sci **97**(11): 1217-25.

Nakagawa, S.,Yano, T.,Nakagawa, K.,Takizawa, S.,Suzuki, Y.,Yasugi, T.,Huibregtse, J. M. and Taketani, Y. (2004). "Analysis of the expression and localisation of a LAP protein, human scribble, in the normal and neoplastic epithelium of uterine cervix". Br J Cancer **90**(1): 194-9.

Nakahara, T.,Peh, W. L.,Doorbar, J.,Lee, D. and Lambert, P. F. (2005). "Human papillomavirus type 16 E1circumflexE4 contributes to multiple facets of the papillomavirus life cycle". J Virol **79**(20): 13150-65.

Nelson, W. G. and Sun, T. T. (1983). "The 50- and 58-kdalton keratin classes as molecular markers for stratified squamous epithelia: cell culture studies". J Cell Biol **97**(1): 244-51

Noya, F.,Chien, W. M.,Broker, T. R. and Chow, L. T. (2001). "p21cip1 Degradation in differentiated keratinocytes is abrogated by costabilization with cyclin E induced by human papillomavirus E7". J Virol **75**(13): 6121-34

Oren, M.,Damalas, A.,Gottlieb, T.,Michael, D.,Taplick, J.,Leal, J. F.,Maya, R.,Moas, M.,Seger, R.,Taya, Y. and Ben-Ze'ev, A. (2002). "Regulation of p53: intricate loops and delicate balances". Biochem Pharmacol **64**(5-6): 865-71.

Paramio, J. M.,Casanova, M. L.,Segrelles, C.,Mittnacht, S.,Lane, E. B. and Jorcano, J. L. (1999). "Modulation of cell proliferation by cytokeratins K10 and K16". Mol Cell Biol **19**(4): 3086-94.

Peh, W. L.,Middleton, K.,Christensen, N.,Nicholls, P.,Egawa, K.,Sotlar, K.,Brandsma, J.,Percival, A.,Lewis, J.,Liu, W. J. and Doorbar, J. (2002). "Life cycle heterogeneity in animal models of human papillomavirus-associated disease". J Virol **76**(20): 10401-16.

Peh, W. L. and Doorbar, J. (2005). "Detection of papillomavirus proteins and DNA in paraffin-embedded tissue sections". Methods Mol Med **119**: 49-59.

Pfister, H. (1992). "Human papillomaviruses and skin cancer". Semin Cancer Biol **3**(5): 263-71.

Pfister, H. (2003). "Chapter 8: Human papillomavirus and skin cancer". J Natl Cancer Inst Monogr(31): 52-6.

Piccini, A.,Storey, A.,Romanos, M. and Banks, L. (1997). "Regulation of human papillomavirus type 16 DNA replication by E2, glucocorticoid hormone and epidermal growth factor". J Gen Virol **78 (Pt 8)**: 1963-70.

Pim, D.,Tomaic, V. and Banks, L. (2009). "The Hpv E6* Proteins from High-Risk, Mucosal Human Papillomaviruses Can Direct the Degradation of Cellular Proteins in the Absence of Full-Length E6 Protein". J Virol.

Plug-Demaggio, A. W. and Mcdougall, J. K. (2002). "The human papillomavirus type 16 E6 oncogene induces premature mitotic chromosome segregation". Oncogene **21**(49): 7507-13.

Presland, R. B.,Kimball, J. R.,Kautsky, M. B.,Lewis, S. P.,Lo, C. Y. and Dale, B. A. (1997). "Evidence for specific proteolytic cleavage of the N-terminal domain of human profilaggrin during epidermal differentiation". J Invest Dermatol **108**(2): 170-8.

Pyeon, D.,Newton, M. A.,Lambert, P. F.,Den Boon, J. A.,Sengupta, S.,Marsit, C. J.,Woodworth, C. D.,Connor, J. P.,Haugen, T. H.,Smith, E. M.,Kelsey, K. T.,Turek, L. P. and Ahlquist, P. (2007). "Fundamental differences in cell cycle deregulation in human papillomavirus-positive and human papillomavirus-negative head/neck and cervical cancers". Cancer Res **67**(10): 4605-19.

Pyeon, D.,Pearce, S. M.,Lank, S. M.,Ahlquist, P. and Lambert, P. F. (2009). "Establishment of human papillomavirus infection requires cell cycle progression". PLoS Pathog **5**(2): e1000318.

Rubin, M. A.,Kleter, B.,Zhou, M.,Ayala, G.,Cubilla, A. L.,Quint, W. G. and Pirog, E. C. (2001). "Detection and typing of human papillomavirus DNA in penile carcinoma: evidence for multiple independent pathways of penile carcinogenesis". Am J Pathol **159**(4): 1211-8.

Scheffner, M.,Huibregtse, J. M.,Vierstra, R. D. and Howley, P. M. (1993). "The HPV-16 E6 and E6-AP complex functions as a ubiquitin-protein ligase in the ubiquitination of p53". Cell **75**(3): 495-505.

Serrano, M.,Hannon, G. J. and Beach, D. (1993). "A new regulatory motif in cell-cycle control causing specific inhibition of cyclin D/CDK4". Nature **366**(6456): 704-7.

Shai, A.,Brake, T.,Somoza, C. and Lambert, P. F. (2007). "The human papillomavirus E6 oncogene dysregulates the cell cycle and contributes to cervical carcinogenesis through two independent activities". Cancer Res **67**(4): 1626-35.

Smotkin, D. and Wettstein, F. O. (1986). "Transcription of human papillomavirus type 16 early genes in a cervical cancer and a cancer-derived cell line and identification of the E7 protein". Proc Natl Acad Sci U S A **83**(13): 4680-4.

Sousa, R.,Dostatni, N. and Yaniv, M. (1990). "Control of papillomavirus gene expression". Biochim Biophys Acta **1032**(1): 19-37.

Stanley, M. (2008). "Immunobiology of HPV and HPV vaccines". Gynecol Oncol **109**(2 Suppl): S15-21.

Stanley, M. A.,Browne, H. M.,Appleby, M. and Minson, A. C. (1989). "Properties of a non-tumorigenic human cervical keratinocyte cell line". Int J Cancer **43**(4): 672-6.

Steger, G. and Corbach, S. (1997). "Dose-dependent regulation of the early promoter of human papillomavirus type 18 by the viral E2 protein". J Virol **71**(1): 50-8.

Strefford, J. C. and Parker, H. (2009). "Array-based comparative genomic hybridization as a tool for analyzing the leukemia genome". Methods Mol Biol **538**: 151-77.

Takizawa, S.,Nagasaka, K.,Nakagawa, S.,Yano, T.,Nakagawa, K.,Yasugi, T.,Takeuchi, T.,Kanda, T.,Huibregtse, J. M.,Akiyama, T. and Taketani, Y. (2006). "Human scribble, a novel tumor suppressor identified as a target of high-risk HPV E6 for ubiquitin-mediated degradation, interacts with adenomatous polyposis coli". Genes Cells **11**(4): 453-64.

Tan, S. H.,Leong, L. E.,Walker, P. A. and Bernard, H. U. (1994). "The human papillomavirus type 16 E2 transcription factor binds with low cooperativity to two flanking sites and represses the E6 promoter through displacement of Sp1 and TFIID". J Virol **68**(10): 6411-20.

Thomas, M.,Narayan, N.,Pim, D.,Tomaic, V.,Massimi, P.,Nagasaka, K.,Kranjec, C.,Gammoh, N. and Banks, L. (2008). "Human papillomaviruses, cervical cancer and cell polarity". Oncogene **27**(55): 7018-30.

Thorland, E. C.,Myers, S. L.,Gostout, B. S. and Smith, D. I. (2003). "Common fragile sites are preferential targets for HPV16 integrations in cervical tumors". Oncogene **22**(8): 1225-37.

Todaro, G. J. and Green, H. (1963). "Quantitative studies of the growth of mouse embryo cells in culture and their development into established lines". J Cell Biol **17**: 299-313.

Vessey, C. J.,Wilding, J.,Folarin, N.,Hirano, S.,Takeichi, M.,Soutter, P.,Stamp, G. W. and Pignatelli, M. (1995). "Altered expression and function of E-cadherin in cervical intraepithelial neoplasia and invasive squamous cell carcinoma". J Pathol **176**(2): 151-9.

Walboomers, J. M.,Jacobs, M. V.,Manos, M. M.,Bosch, F. X.,Kummer, J. A.,Shah, K. V.,Snijders, P. J.,Peto, J.,Meijer, C. J. and Munoz, N. (1999). "Human papillomavirus is a necessary cause of invasive cervical cancer worldwide". J Pathol **189**(1): 12-9.

Wilding, J.,Vousden, K. H.,Soutter, W. P.,Mccrea, P. D.,Del Buono, R. and Pignatelli, M. (1996). "E-cadherin transfection down-regulates the epidermal growth factor receptor and reverses the invasive phenotype of human papilloma virus-transfected keratinocytes". Cancer Res **56**(22): 5285-92.

Williams, G. H.,Romanowski, P.,Morris, L.,Madine, M.,Mills, A. D.,Stoeber, K.,Marr, J.,Laskey, R. A. and Coleman, N. (1998). "Improved cervical smear assessment using antibodies against proteins that regulate DNA replication". Proc Natl Acad Sci U S A **95**(25): 14932-7.

Wilson, R. and Laimins, L. A. (2005). "Differentiation of HPV-containing cells using organotypic "raft" culture or methylcellulose". Methods Mol Med **119**: 157-69.

Woodman, C. B.,Collins, S.,Winter, H.,Bailey, A.,Ellis, J.,Prior, P.,Yates, M.,Rollason, T. P. and Young, L. S. (2001). "Natural history of cervical human papillomavirus infection in young women: a longitudinal cohort study". Lancet **357**(9271): 1831-6.

You, J.,Croyle, J. L.,Nishimura, A.,Ozato, K. and Howley, P. M. (2004). "Interaction of the bovine papillomavirus E2 protein with Brd4 tethers the viral DNA to host mitotic chromosomes". Cell **117**(3): 349-60.

Yuan, H.,Ito, S.,Senga, T.,Hyodo, T.,Kiyono, T.,Kikkawa, F. and Hamaguchi, M. (2009). "Human papillomavirus type 16 oncoprotein E7 suppresses cadherin-mediated cell adhesion via ERK and AP-1 signaling". Int J Oncol **35**(2): 309-14.

Zerfass-Thome, K.,Zwerschke, W.,Mannhardt, B.,Tindle, R.,Botz, J. W. and Jansen-Durr, P. (1996). "Inactivation of the cdk inhibitor p27KIP1 by the human papillomavirus type 16 E7 oncoprotein". Oncogene **13**(11): 2323-30.

Zheng, Z. M. and Baker, C. C. (2006). "Papillomavirus genome structure, expression, and post-transcriptional regulation". Front Biosci **11**: 2286-302.

Ziegert, C.,Wentzensen, N.,Vinokurova, S.,Kisseljov, F.,Einenkel, J.,Hoeckel, M. and Von Knebel Doeberitz, M. (2003). "A comprehensive analysis of HPV integration loci in anogenital lesions combining transcript and genome-based amplification techniques". Oncogene **22**(25): 3977-84.

Zur Hausen, H. (1977). "Human papillomaviruses and their possible role in squamous cell carcinomas". Curr Top Microbiol Immunol **78**: 1-30.